

# Modern Statistical Models and Methods for Estimating Fatigue-Life and Fatigue-Strength Distributions from Experimental Data

William Q. Meeker\*

Luis A. Escobar<sup>†</sup>

Francis G. Pascual<sup>‡</sup>

Yili Hong<sup>§</sup>

Peng Liu <sup>¶</sup>

Wayne M. Falk<sup>||</sup>

Balajee Ananthasayanam <sup>\*\*</sup>

09 April 2024

## Abstract

Engineers and scientists have been collecting and analyzing fatigue data since the 1800s to ensure the reliability of life-critical structures. Applications include (but are not limited to) bridges, building structures, aircraft and spacecraft components, ships, ground-based vehicles, and medical devices. Engineers need to estimate  $S$ - $N$  relationships (Stress versus Number of cycles to failure), typically with a focus on estimating small quantiles of the *fatigue-life* distribution. Estimates from this kind of model are used as input to models (e.g., cumulative damage models) that predict failure-time distributions under varying stress patterns. Also, design engineers need to estimate lower-tail quantiles of the closely related *fatigue-strength* distribution. The history of applying incorrect statistical methods is nearly as long and such practices continue to the present. Examples include treating the applied stress (or strain) as the response and the number of cycles to failure as the explanatory variable in regression analyses (because of the need to estimate fatigue-strength distributions) and ignoring or otherwise mishandling censored observations (known as runouts in the fatigue literature). The first part of the paper reviews the traditional modeling approach where a fatigue-life model is specified. Then we show how this specification induces a corresponding fatigue-strength model. The second part of the paper presents a novel alternative modeling approach where a fatigue-strength model is specified and a corresponding fatigue-life model is induced. We explain and illustrate the important advantages of this new modeling approach.

**Keywords:** Bayesian inference, censored data, failure-time regression, fracture, maximum likelihood, nonlinear regression, reliability,  $S$ - $N$  curves.

---

\*Department of Statistics, Iowa State University

<sup>†</sup>Department of Experimental Statistics, Louisiana State University

<sup>‡</sup>Department of Mathematics and Statistics, Washington State University

<sup>§</sup>Department of Statistics, Virginia Tech

<sup>¶</sup>JMP Statistical Discovery LLC

<sup>||</sup>U.S. Food and Drug Administration

<sup>\*\*</sup>Honda Aero

# Contents

<b>1</b>	<b>Introduction</b>	<b>6</b>
1.1	Motivation	6
1.2	Laboratory Experiments to Obtain $S$ - $N$ Data	6
1.3	Motivating Examples	6
1.4	Fatigue Life, Fatigue Strength, and System Reliability	9
1.4.1	The Relationship Between Fatigue Life and Fatigue Strength	9
1.4.2	Using experimental fatigue-life data to determine the safe life of an aircraft turbine engine disk	11
1.4.3	Using experimental fatigue-life data to assure the reliability of medical devices	11
1.5	History and Literature Review	12
1.6	Contributions	13
1.7	Overview	13
<b>2</b>	<b>Statistical Models for Fatigue <math>S</math>-<math>N</math> Data</b>	<b>14</b>
2.1	A Modular Framework for Modeling Fatigue $S$ - $N$ Data	14
2.2	Log-Location-Scale Probability Distributions	14
2.3	Basic $S$ - $N$ Relationships and Statistical Models for Fatigue Life	15
2.3.1	A statistical model for fatigue-life	15
2.3.2	The Basquin model	15
2.3.3	The Stremeyer relationship	16
2.3.4	Box-Cox (power) transformation model	16
2.3.5	A model component to describe nonconstant $\sigma_N$	16
2.4	Linking Fatigue-Life and Fatigue-Strength Models	17
2.4.1	The induced fatigue-strength model when $\log[g(S; \beta)]$ has neither a vertical nor a horizontal asymptote	18
2.4.2	The induced fatigue-strength model when $\log[g(S; \beta)]$ has a horizontal asymptote	19
2.4.3	The induced fatigue-strength model when $\log[g(S; \beta)]$ has a vertical asymptote	19
2.4.4	Equivalence of fatigue-life and fatigue-strength quantile curves	20
2.5	Choosing a Fatigue-Life Probability Distribution	20
2.6	An Example of Fitting a Fatigue-Life Model	21
2.7	Compatibility Conditions and Characteristics of $S$ - $N$ Models	22
<b>3</b>	<b>Statistical Models for Fatigue-Strength</b>	<b>22</b>
3.1	Estimating a Fatigue-Strength Distribution Using Binary Data	22
3.2	Modeling $S$ - $N$ Data by Specifying a Fatigue-Strength Model	23
3.2.1	The advantages of specifying the fatigue-strength model to describe $S$ - $N$ data	23
3.2.2	A statistical model for fatigue-strength	24
3.2.3	The induced fatigue-life model when $\log[h(N; \beta)]$ has neither a vertical nor a horizontal asymptote	24
3.2.4	The induced fatigue-life model when $\log[h(N; \beta)]$ has a horizontal asymptote	25
3.2.5	The induced fatigue-life model when $\log[h(N; \beta)]$ has a vertical asymptote	25

3.2.6	Visualization of the effect that $S$ - $N$ relationship coordinate asymptotes have on quantile curves and the induced fatigue-life distributions . . . . .	25
<b>4</b>	<b>Estimating <math>S</math>-<math>N</math> Model Parameters, Model-Fitting Diagnostics, and Making Inferences about Fatigue Distributions</b>	<b>26</b>
4.1	Likelihood-Based Methods . . . . .	27
4.1.1	Log-likelihood for an $S$ - $N$ regression model with runouts . . . . .	27
4.1.2	Methods for computing confidence intervals when using likelihood-based inference	27
4.1.3	Equivalence of likelihood pointwise confidence interval bands for cdfs and quantiles	28
4.2	Bayesian Inference Methods . . . . .	28
4.2.1	Specifying the joint prior distribution . . . . .	28
4.2.2	Generating and using draws from the joint posterior distribution . . . . .	28
4.2.3	Numerical methods to obtain starting values and default joint prior distributions	29
4.3	Using Residuals as Model-Checking Diagnostics . . . . .	29
4.4	Tolerance Bounds Versus Credible/Confidence Intervals for Quantiles . . . . .	31
<b>5</b>	<b>Other <math>S</math>-<math>N</math> Regression Relationships and Modeling Examples</b>	<b>31</b>
5.1	Physical Explanation of the Curvature and Nonconstant Spread in $S$ - $N$ Data . . . . .	31
5.2	The Modified Bastenaire $S$ - $N$ Relationship . . . . .	32
5.3	The Nishijima $S$ - $N$ Hyperbola Relationship . . . . .	32
5.4	The Rectangular Hyperbola $S$ - $N$ Relationship . . . . .	34
5.5	The Coffin–Manson Relationship . . . . .	34
5.6	The Random Fatigue-Limit Model . . . . .	36
5.6.1	The RFL fatigue-life model . . . . .	36
5.6.2	The RFL fatigue-strength model . . . . .	36
5.7	The Castillo et al. $S$ - $N$ Model . . . . .	37
5.8	A Comparison and Operational Considerations for Choosing an $S$ - $N$ Model . . . . .	37
5.8.1	Models with no coordinate asymptotes . . . . .	38
5.8.2	Models with a horizontal asymptote . . . . .	39
5.8.3	Models with a vertical asymptote . . . . .	39
<b>6</b>	<b>Concluding Remarks and Areas for Future Research</b>	<b>39</b>
<b>A</b>	<b>Overview of the Materials in Appendices</b>	<b>41</b>
<b>B</b>	<b>Technical Details for <math>S</math>-<math>N</math> Regression Models Where the Fatigue-Life Model is Specified and the Fatigue-Strength Model is Induced</b>	<b>41</b>
B.1	Basic $S$ - $N$ Relationships for $N = g(S; \beta)$ and General Assumptions . . . . .	41
B.2	The Specified Fatigue-Life Model . . . . .	42
B.3	Additional Results for Induced Fatigue-Strength Models . . . . .	42
B.3.1	The induced fatigue-strength cdf for the Basquin model . . . . .	42
B.3.2	The induced fatigue-strength cdf for the Stromeier model . . . . .	43
B.3.3	The induced fatigue-strength cdf for the Box–Cox model . . . . .	43
B.4	Expressions for the Induced Fatigue-Strength Model pdfs . . . . .	44
B.4.1	Expression for the induced fatigue-strength pdf for the Basquin model . . . . .	44

B.4.2	Expression for the induced fatigue-strength pdf for the Stromeyer model . . . .	44
B.4.3	Expression for the induced fatigue-strength pdf for the Box–Cox model . . . .	44
<b>C</b>	<b>Technical Details for <math>S</math>-<math>N</math> Regression Models Where the Fatigue-Strength Model is Specified and the Fatigue-Life Model is Induced</b>	<b>44</b>
C.1	Basic $S$ - $N$ Relationships for $S = h(N; \beta)$ and General Assumptions . . . . .	45
C.2	Additional Motivation for Specifying the Fatigue-Strength Distribution . . . . .	45
C.3	The Specified Fatigue-Strength Distribution . . . . .	47
C.4	Additional Results for Induced Fatigue-Life Models . . . . .	47
C.4.1	The induced fatigue-life distribution for the Stromeyer model . . . . .	47
C.4.2	The induced fatigue-life cdf for the Box–Cox model . . . . .	48
C.5	Expressions for the Induced Fatigue-Life Model pdfs . . . . .	48
C.5.1	Expressions for the induced fatigue-life pdf for the Coffin–Manson model . . .	48
C.5.2	Expressions for the induced fatigue-life pdf for the Nishijima relationship . . .	49
C.5.3	Expression for the induced fatigue-life pdf for the Stromeyer model . . . . .	49
C.5.4	Expression for the induced fatigue-life pdf for the Box–Cox model . . . . .	49
<b>D</b>	<b>Technical Details of Results Stated in the Main Paper</b>	<b>50</b>
D.1	Equivalence of Fatigue-Life and Fatigue-Strength Quantile Curves . . . . .	50
D.1.1	Proof of the equivalence of fatigue-life and fatigue-strength quantile curves when there is neither a horizontal nor a vertical asymptote . . . . .	50
D.1.2	The effect of coordinate asymptotes on the equivalence of fatigue-life and fatigue-strength quantile curves . . . . .	50
D.2	Proof that Concave-up Curvature in the $S$ - $N$ Relationship Induces Fatigue-Life Distributions with Increasing Spread at Lower Stress Levels . . . . .	52
D.3	A Generalization of Relationship between the Specified Fatigue-Strength Model and the Induced Fatigue-Life Model . . . . .	53
D.3.1	A statistical model for fatigue-strength . . . . .	54
D.3.2	The induced fatigue-life model when $\log[h(N; \beta)]$ has neither a vertical nor a horizontal asymptote . . . . .	54
D.3.3	The induced fatigue-life model when $\log[h(N; \beta)]$ has a horizontal asymptote . . .	55
D.3.4	The induced fatigue-life model when $\log[h(N; \beta)]$ has a vertical asymptote . . .	55
D.4	Some History and an Alternative Way to View the Relationship among Fatigue-Strength cdfs, Fatigue-Life cdfs, and their Respective Quantile Functions . . . . .	56
<b>E</b>	<b>A Comparison of <math>S</math>-<math>N</math> Relationship Shapes and How to Choose the Best One</b>	<b>57</b>
<b>F</b>	<b>Examples Comparing Lognormal and Weibull Distributions Fit to <math>S</math>-<math>N</math> Data from Different Materials and Specimen Types</b>	<b>60</b>
<b>G</b>	<b>Further Explanation of the Castillo et al. <math>S</math>-<math>N</math> Model</b>	<b>64</b>
G.1	The Distribution of Fatigue Life . . . . .	64
G.2	Distribution of Fatigue Strength . . . . .	64
G.3	Quantiles of the Fatigue-life and the Fatigue-Strength Distributions . . . . .	65
G.4	Comments . . . . .	65



<b>H</b>	<b>More Details from the Data Analysis/Modeling Examples</b>	<b>67</b>
H.1	More Details for the Box–Cox/Loglinear- $\sigma_N$ $S$ - $N$ Model Fit to the Laminate Panel Data	67
H.1.1	Model and prior distributions . . . . .	67
H.1.2	Posterior draws and parameter estimates . . . . .	68
H.2	More Details for the Nishijima/Lognormal $S$ - $N$ Model Fit to the Ti64 Data . . . . .	69
H.2.1	Comparison of lognormal and Weibull distributions . . . . .	69
H.2.2	Model and prior distributions . . . . .	69
H.2.3	Posterior draws and parameter estimates for the weakly informative prior for qlogisp (Nishijima model) . . . . .	71
H.2.4	Posterior draws and parameter estimates for the informative prior for qlogisp (rectangular hyperbola model) . . . . .	72
H.2.5	Additional residual analyses . . . . .	73
H.3	More Details for the Coffin–Manson/Lognormal $S$ - $N$ Model Fit to the Superelastic Nitinol Data . . . . .	74
H.3.1	Comparison of lognormal and Weibull distributions . . . . .	74
H.3.2	Model and prior distributions . . . . .	74
H.3.3	Posterior draws and parameter estimates . . . . .	75
H.3.4	Additional residual analyses . . . . .	76
	<b>References</b>	<b>76</b>

# 1 Introduction

## 1.1 Motivation

Engineers and scientists have been collecting and analyzing fatigue data since the 1800s to ensure the reliability of life-critical structures. Applications include (but are not limited to) bridges, building structures, aircraft and spacecraft components, ships, ground-based vehicles, and medical devices. Because of its importance, fatigue has been and continues to be the most widely studied failure mechanism. Hundreds of technical papers describing fatigue data are published each year. Even today, many of these papers are not using appropriate statistical methods. *Current* standards and handbooks such as [ISO \(2012\)](#), [ASTM \(2015\)](#), and [MMPDS \(2021\)](#) describe and recommend *archaic statistical methods* developed from the late 1940s to the late 1960s. Modern statistical methods and the availability of computational power allow engineers to fit needed nonlinear regression models and properly handle runouts (right-censored observations). The modern statistical methods that provide improved statistical inference, however, are not presented in engineering standards. While this paper will not immediately remedy the omission of these topics, the information presented in this paper can guide inclusion in future revisions of engineering standards and handbooks.

## 1.2 Laboratory Experiments to Obtain $S$ - $N$ Data

In laboratory testing, under cyclic stress or strain loading (often a sine wave where the amount of stress or strain is usually given in terms of amplitude), test units accumulate damage—crack initiation and subsequent growth. Depending on the material and range of stress to be applied in the test it is sometimes appropriate to control stress (or displacement that causes stress) amplitude and in other applications it is more appropriate to control strain amplitude. Textbooks such as [Dowling \(2013\)](#) provide more details about how fatigue tests are conducted. For consistency, we will generally use the word “stress” except in the numerical examples where strain-control was used.

The damage accumulation rate depends on levels of stress. A representative sample of specimens from some production process (e.g., selected from multiple heats or batches) will be tested. These specimens should be randomly assigned to test conditions and order of testing. The number and location of stress levels, the number of test specimens, and the allocation of the test specimens needs to be specified in a purposeful way (described further in Section 6). Fatigue tests can be conducted to control stress amplitude, displacement (which is proportional to stress), or strain amplitude. Some fatigue testing machines can test only one specimen at a time. Other machines are available to do stressing simultaneously on multiple specimens. Typically units are tested at a fixed stress amplitude until failure or a prespecified censoring point, whichever comes first. Unfailed units are known as runouts or right-censored observations and are an important part of the data.

## 1.3 Motivating Examples

This section presents motivating examples based on fatigue tests with three different materials: a composite material and two metals with different characteristics. As will be shown in subsequent sections, the features of the different data sets will suggest regression models with different characteristics.

**Example 1.1 Fatigue-Life Data from a Test on a Laminate Panel.** Four-point out-of-plane bending tests were run on 25 specimens of carbon eight-harness satin/epoxy laminate panels at each

of five different stress levels. There were ten runouts at the two lowest stress levels. Fatigue life was considered to be the number of cycles until a specimen fractured. These data were previously analyzed (using models different from those presented in this paper) in [Shimokawa and Hamaguchi \(1987\)](#), [Pascual and Meeker \(1999\)](#), and [Meeker et al. \(2022, Chapter 17\)](#).

Figure 1a is a log-log scatterplot of the laminate panel  $S$ - $N$  data with the response (thousands of cycles) on the vertical axis. Figure 1b plots the same data with the response on the horizontal axis. It is common practice to plot a regression response on the vertical axis. In the fatigue literature, however, the response is plotted on the horizontal axis and we will follow that convention here. Although it is partially obscured by the runouts, there is strong statistical evidence of curvature in the data on log-log scales. Such curvature is ubiquitous in  $S$ - $N$  data, especially when there are tests at low stress levels resulting in long failure times (i.e., high-cycle fatigue or HCF).

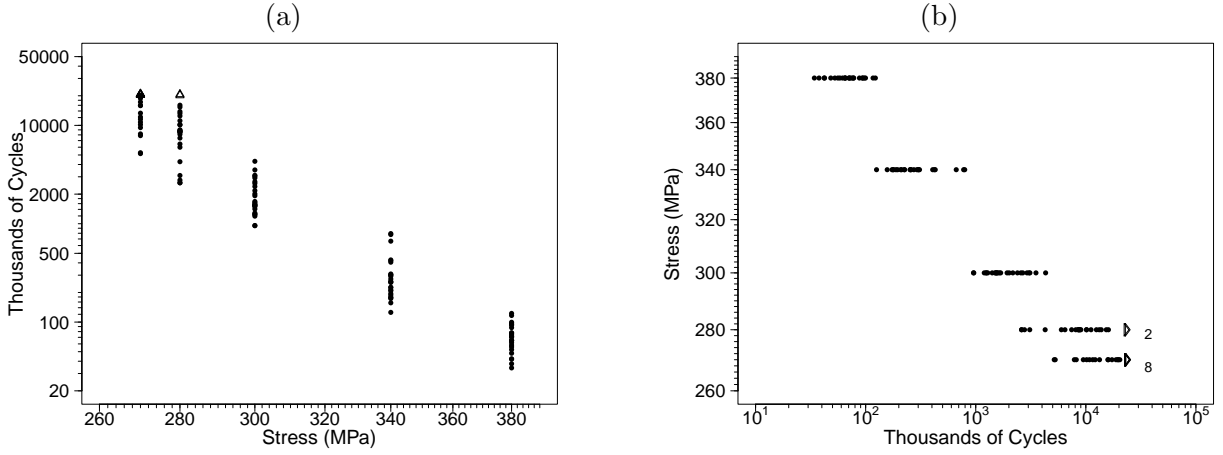


Figure 1: Laminate panel  $S$ - $N$  data with number of cycles on the vertical axis (a) and the horizontal axis (b).

Figure 2 shows Weibull and lognormal probability plots for the laminate panel fatigue-life data with estimates of the cdfs (the lines going through the nonparametric estimate points) at each level of stress. These plots suggest that the lognormal distribution provides a better description of the data.

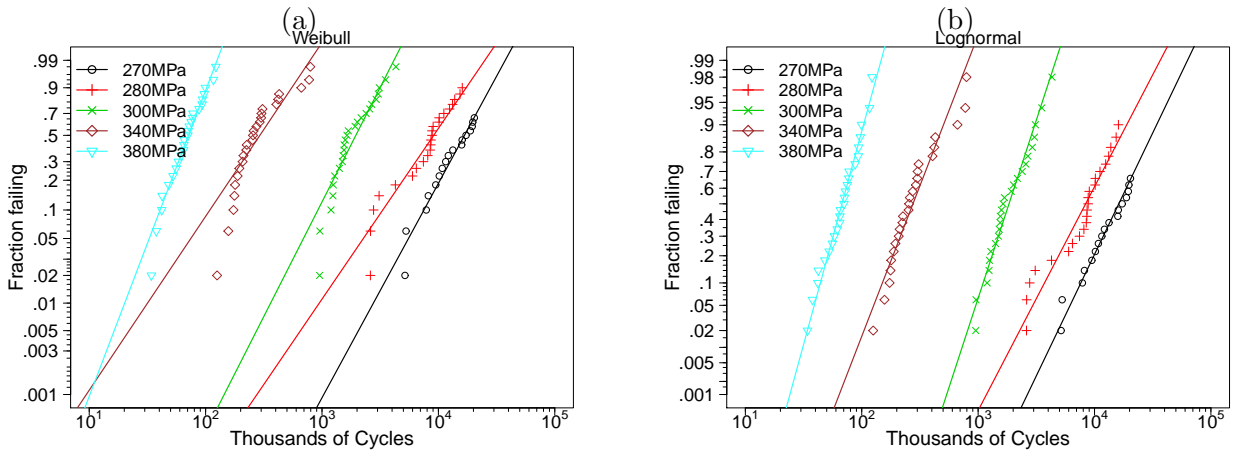


Figure 2: Laminate panel  $S$ - $N$  data Weibull (a) and lognormal (b) probability plots with separate distributions fit to each level of stress.

The slopes of the cdf-estimate lines in Figure 2b tend to decrease from left to right. This implies more

spread in the data at lower stress levels, another common characteristic of  $S$ - $N$  data. Section 2.6 will present an appropriate fatigue-life regression model to describe these data. ■

**Example 1.2 Fatigue-Life Data from a Test on Ti64 Specimens.** Ti-6Al-4V (Ti64) is an alloy of titanium, aluminum, and vanadium that has a high strength-to-weight ratio and corrosion resistance. Because of these properties, Ti64 is used widely in aerospace applications. Data from a fatigue test are shown in Figure 3a. Units were subjected to cyclic loading at a temperature of 350°F with a stress ratio  $R = -1$  (fully reversed loading with a zero-mean stress) with stress amplitudes of 60 (37 specimens), 70 (12 specimens), 80 (11 specimens), and 90 (12 specimens) ksi (thousands of pounds per square inch). More units were tested at 60 ksi because it was expected that a smaller proportion of tested units would fail there. Of the 37 specimens tested at 60 ksi, 28 were runouts that survived between 30,000 and 46,505 thousand cycles (indicated by the triangles pointing to the right in the figure). Figure 3a indicates strong curvature in the  $S$ - $N$  relationship and increasing spread at lower stress levels. Figure 3b is a lognormal probability plot for the Ti64 data. For these data, the lognormal

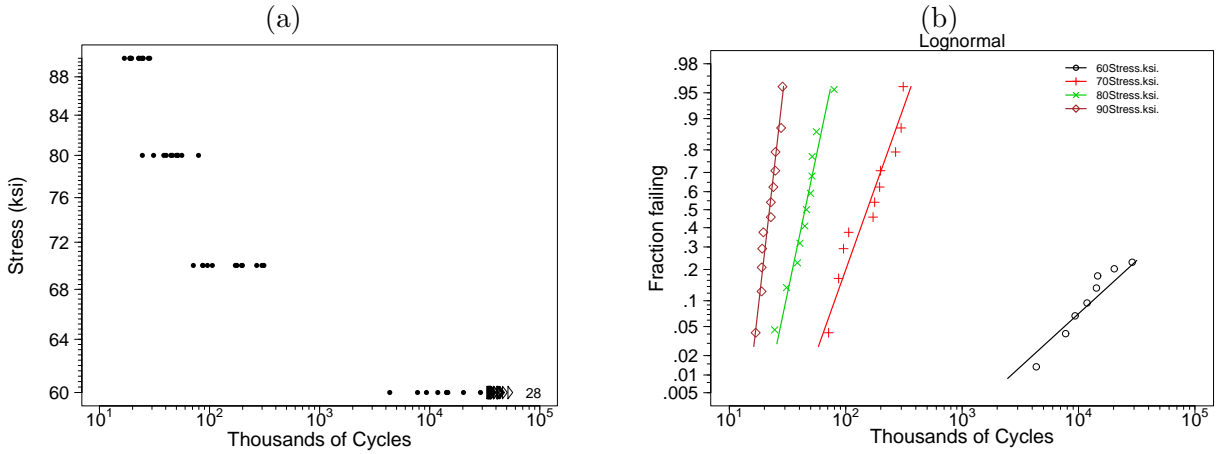


Figure 3: Ti64  $S$ - $N$  Data scatter plot (a) and lognormal probability plot (b) with separate lognormal distributions fit to each level of stress.

distribution provides a better fit than the Weibull distribution (see Figure 23 in the Appendix for a side-by-side comparison). The changes in slopes of the fitted lines (corresponding to estimates of the lognormal shape parameters) indicate the increase in spread at lower stress levels. ■

**Example 1.3 Fatigue-Life Data from a Test on Superelastic Nitinol Specimens.** Nitinol is an alloy of nickel and titanium able to accommodate large recoverable strains via martensitic phase transition, an effect sometimes referred to as super-elasticity. Nitinol has found numerous successful applications in implantable medical devices which are designed to remain durable beyond 100 million cycles. Rotary bend fatigue tests with nitinol straight wire specimens were conducted with target alternating strain ranging from 0.28 to 2.66%. The material specification, sample preparation and test procedure, and interpretation of the results can be found in Weaver et al. (2023). Rotating bend produces inherently fully reversed loading with a zero-mean stress. All tests were conducted in phosphate buffered saline maintained at  $37 \pm 2^\circ\text{C}$  to approximate *in vivo* conditions. Tests were run until fracture or until completion of 1 billion cycles. Surviving units are runouts. The data from tests conducted at one of two laboratories is plotted in Figure 4a, resulting in 46 fractures and 20 runouts. The nitinol data set used in Weaver et al. (2023) also contains a variable “Exact Strain”

that results after applying a small correction to five nominal strain levels. Because the size of the correction varies from unit to unit, this results in a substantial increase in the number of strain levels making it impossible to use some of the diagnostics we want to illustrate.

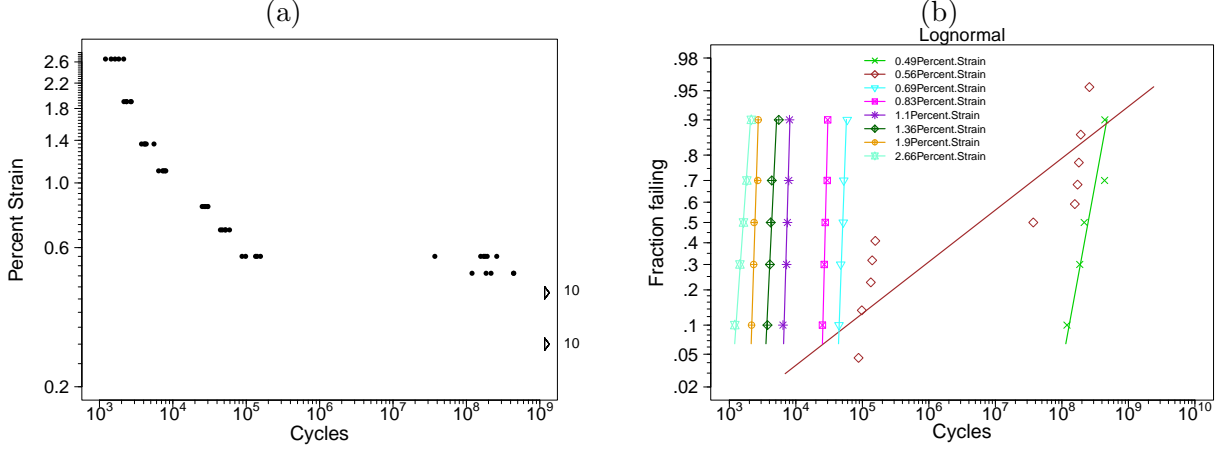


Figure 4: Nitinol  $S$ - $N$  Data scatter plot (a) and lognormal probability plots (b) with separate distributions fit to each level of strain.

Similar to the Ti64 data in Example 1.2, the scatter plot in Figure 4a shows an  $S$ - $N$  relationship with strong curvature and increased spread at low levels of strain. Figure 4b is a lognormal probability plot for the nitinol data. The most striking feature in the plot is at 0.56% strain where there were five early failures and, after a gap, five later failures. This kind of bimodal behavior is often seen in  $S$ - $N$  data of standard metallic materials, especially at intermediate levels of stress or strain where cycling might be either elastic or plastic. In nitinol, however, early fractures predominately initiate at small inclusions. The inclusions initiate propagation sooner under conditions of cyclic martensitic transformation than under conditions of purely elastic cycling. For the other levels of strain, either a lognormal or a Weibull distribution provides an excellent description of the data (see Figure 28 in the Appendix for a side-by-side comparison). ■

## 1.4 Fatigue Life, Fatigue Strength, and System Reliability

This section describes, at a high level, the relationship between fatigue life and fatigue strength—two closely-related random quantities that are of interest when studying the reliability of a system or component that is subject to failure from fatigue caused by cyclic loading. Technical details about this relationship are given in Section 2.4 and 3.2. This description is followed by brief explanations of how laboratory-test results are used to quantify system reliability in two important application areas.

### 1.4.1 The Relationship Between Fatigue Life and Fatigue Strength

Fatigue life  $N$  is defined as the time (number of cycles) when a unit fails from repeated cyclic loading. Failure can be defined in different ways, depending on the application. Examples include time to fracture of a specimen, crack initiation, crack reaching a critical size, or a specimen experiencing irreversible deformation; in a composite-material structure, failure might be defined as time of the beginning of a delamination. A fatigue-life probability model describes the distribution of  $N$  and is generally given as a function of stress amplitude  $S_e$  (although other variables such as stress ratio,

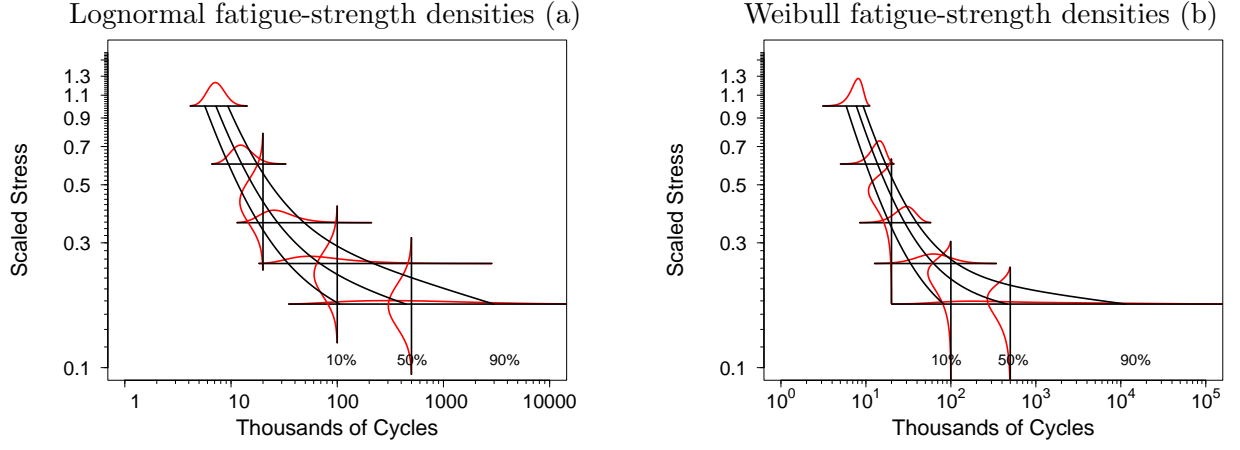


Figure 5: Plot showing lognormal fatigue-strength densities (vertical, constant spread/shape) and corresponding *induced* fatigue-life densities (horizontal) (a); Plot showing Weibull fatigue-strength densities (vertical, constant spread/shape) and corresponding *induced* fatigue-life densities (horizontal) (b).

temperature, and dwell time, are sometimes used as factors in a fatigue experiment and included in a larger regression model). The horizontal densities in Figure 5 are fatigue-life densities.

The fatigue-strength random variable  $X$  is defined as the *level of stress* at which a unit would fail at a given number of cycles,  $N_e$ . Fatigue strength is *not observable* because test-stress levels,  $S$ , are specified experimental factors and the number of cycles at failure,  $N$ , is random. It is possible, however, to estimate the distribution of  $X$  by using fatigue-life data (if failures are observed at more than one level of stress). The vertical densities in Figure 5a are lognormal fatigue-strength densities and those in Figure 5b are Weibull fatigue-strength densities (lognormal and Weibull are the most commonly used probability distributions for modeling fatigue-life data). For the examples in Figure 5, the scale parameters of the fatigue-strength distributions depend on the given number of cycles,  $N_e$ , and the shape parameters are constant.

There are two ways to view the relationship between the fatigue-life model and the fatigue-strength model. Specification of a fatigue-life (fatigue-strength) implies a corresponding fatigue-strength (fatigue-life) model. Relatedly, the models generally have the same quantile lines, as illustrated in Figure 5. The relationship between the models can also be expressed in a mathematically precise manner, as it is in Sections 2.4 (specified fatigue-life model and induced fatigue-strength model) and 3.2 (specified fatigue-strength model and induced fatigue-life model).

Correspondingly, there are two different approaches for modeling fatigue-life data. The traditional approach is to specify a model for the observable fatigue-life random variable  $N$ . Then there is an induced model for the fatigue-strength random variable  $X$ . Alternatively (as illustrated in Figure 5), one can specify a fatigue-strength model which then induces the fatigue-life model that is used as a basis for defining a likelihood in terms of the observable  $N$ . These approaches are equivalent (and the distributions of  $N$  and  $X$  have the same form) *if and only if* the  $S$ - $N$  relationship is linear on log-log scales (unlike Figure 5). The important advantages of using the new specify-the-fatigue-strength-model approach when the  $S$ - $N$  relationship is *nonlinear* are described in Section 3.2.1.

#### 1.4.2 Using experimental fatigue-life data to determine the safe life of an aircraft turbine engine disk

The primary threat for an aircraft engine turbine disk failure is the initiation and growth of a fatigue crack. Such failures could endanger the continued safe operation of the aircraft and, in the worst-case scenario, could lead to loss of the aircraft. To avoid catastrophic disk failures, the design life (also known as safe life and approved life) of the disks in commercially operated jet engines are required to be computed by the engine manufacturer and disclosed to the FAA (FAA, 2009a). Similar policies are used in Europe (EASA, 2018) and in other places around the world. When a part reaches its safe life, it must be retired from service.

The safe life is specified in terms of the number of flight take-off-landing cycles. Turbine disk lifetimes are affected by many factors including engine design, flight mission, and the materials used. The FAA (FAA, 2009a) dictates that the acceptable part risk level (i.e., safe life) be the lower 95% confidence bound for the 0.001 quantile (also known as B0.1 life) of the turbine disk failure-time distribution.

Fatigue tests at various levels of stress, temperature, and dwell time, are conducted using simple material coupons (titanium alloys are typically used in the cool parts of an engine, and nickel alloys are used in the hot parts of the engine). Statistical methods are used with the experimental data to estimate lower-tail  $S$ - $N$  curves (also known as quantile curves) and to compute corresponding lower confidence bounds. Based on a given flight mission, the operating conditions of the engine are specified in terms of variables such as engine rotating speed, metal temperature and their gradients across the part, and duration of the maximum load. Using these operating conditions, detailed finite-element stress analyses are conducted to quantify the stress at various critical locations in the complex geometry of the part (e.g. Mattingly et al., 2002, Appendix N). Using the stress values and the lower confidence bounds of the lower tail  $S$ - $N$  quantile curves, the safe-life limit for the disk is determined. This is known as the safe-life method and a general outline of the procedure is given in FAA (2009a, Figure 1) and Mattingly et al. (2002, Figure N.1). Additional safety margins and methods are added to make the safe-life limit more conservative and reduce the risk of part failure. One such method, known as the Damage Tolerance approach, is applied by adding required periodic inspections of critical parts using nondestructive evaluation (NDE) methods. For this method, fatigue-test results are also an important input for determining the inspection schedule, as described in FAA (2009b).

#### 1.4.3 Using experimental fatigue-life data to assure the reliability of medical devices

Implantable medical devices must safely survive fatigue loading, often for more than a decade. In the case of cardiovascular devices, such as stents and heart valves, the design life is 10 or 15 years, corresponding to 400 or 600 million cardiac cycles (FDA, 2010; ISO, 2017). Medical device manufacturers establish safety by comparing the stress analysis of the in-vivo cycle to the component's fatigue strength. Typically, the regulatory requirement is that the component must be shown to have greater than 0.90 reliability with 95% confidence at the design life  $N_e$ .

The component's fatigue-strength distribution at the design life is estimated by collecting experimental fatigue data on representative test units over a range of test amplitudes. For each unit, cycles to fracture is recorded, or the unit is right censored if it survives until the design life. Appropriate statistical methods are used to compute lower confidence bounds for quantiles of the fatigue-strength



distribution at the design life  $N_e$ .

In its simplest form, the estimation of a fatigue-strength distribution is used to calculate a factor of safety. In this case, a lower 95% confidence bound for the 0.1 quantile of the fatigue-strength distribution at the design life  $N_e$  (corresponding to 0.9 reliability) is computed. The factor of safety is calculated by dividing this bound by the highest cyclic stress determined in the stress analysis of the in-vivo cycle. If this factor of safety is greater than one, then the component is considered acceptable (ASTM, 2017).

Alternatively, estimation of the fatigue-strength distribution can be used as input to the classical stress-strength interference model to predict a probability of failure. Shanmugam et al. (2019) illustrate this approach (see Section 23.2 of Meeker et al., 2022, for technical details of the stress-strength interference model). In addition, Haddad et al. (2014) developed a Bayesian approach which uses  $S$ - $N$  regression analysis to estimate the probability of failure of a medical device, in the case of a complicated in-vivo cycle.

## 1.5 History and Literature Review

Scientific and engineering focus on understanding and managing fatigue as a failure mechanism accelerated in the 1950s after there were several fatigue-related failures in the rapidly growing area of aerospace applications. These and some other earlier fatigue-related reliability disasters are described in Woo (2020, Chapter 2). Engineers collecting fatigue data in the 1950s through the 1970s generally did not know how to properly handle censored data and other complications that arise in  $S$ - $N$  data. Stress was sometimes treated as the response variable (due to the desire to estimate fatigue-strength distributions) and runouts were either ignored or treated as failures (practices that unfortunately still, in some places, continue today).

Examples of early development of statistical theory for the analysis of fatigue data include Freudenthal and Gumbel (1953, 1954); Weibull (1956); Freudenthal and Gumbel (1956); Bastenaire et al. (1961). Wayne Nelson (while working at GE Corporate Research and Development) did pioneering work in developing appropriate statistical methods for modeling and making inferences from complicated *censored*  $S$ - $N$  data. Nelson (1984, 2004) illustrates these methods which include maximum likelihood estimation, model-checking diagnostics, and confidence intervals for fatigue-life distribution quantiles. He illustrated the methods on data from a strain-controlled experiment on a nickel-base super alloy used in high-temperature components of an aircraft engine. Log-life was modeled as a quadratic function of log pseudo-stress (strain multiplied by Young’s modulus, a covariate) to describe the characteristic curvature of most HCF  $S$ - $N$  data when plotted on log-log scales. He also employed a log-linear relationship for the lognormal shape parameter (also used in Section 2.3) to describe the often-seen increase in spread at lower stress levels.

As mentioned in Section 1.1, thousands of papers have been published in the engineering literature describing methods for modeling fatigue data, often for specific applications. Dozens of statistical models for fatigue data have been suggested in these papers. Castillo and Fernández-Canteli (2009) review and describe many of these models. We review several of the most commonly used  $S$ - $N$  models in Section 2. More complicated  $S$ - $N$  models are described and applied to the Ti64 and nitinol data in Section 5.

The publication of early papers using maximum likelihood methods, such as Spindel and Haibach (1979) and Nelson (1984), began a trend that continues today, of more analysts using ap-



appropriate methods for handling  $S$ - $N$  data with runouts. More recently, papers like [Babuška et al. \(2016\)](#) and [Castillo et al. \(2019\)](#) illustrate the use of Bayesian methods to fit and compare models fit to fatigue data. Bayesian methods can also properly handle runouts and correctly quantify statistical uncertainty.

## 1.6 Contributions

In addition to some review, this paper contains many new and important technical results.

1. A general, flexible, modular framework for statistical modeling  $S$ - $N$  data for which most of the models that have been used in the thousands of published papers in the engineering literature, can be viewed as special cases.
2. Engineers (and some statisticians) have, conceptually, known about the closely connected distributions of fatigue life and fatigue strength (e.g., [Freudenthal and Gumbel, 1956](#); [Weibull, 1956](#); [Bastenaire et al., 1961](#); [Castillo and Galambos, 1987](#)). Because fatigue life is observable and fatigue strength is not, there has not been a unified and flexible estimation method for these distributions. We present a unified flexible model that connects these two important distributions and allows for the efficient use of  $S$ - $N$  data to estimate both fatigue-life and fatigue-strength distributions. These connected distributions are at the heart of the framework in Contribution 1.
3. Perhaps most importantly, and building on Contribution 2, insights from [Weibull \(1956\)](#) and [Bastenaire et al. \(1961\)](#), and an important contribution by [Falk \(2019\)](#), we show how one can usefully specify a relatively simple fatigue-strength model that will then induce an appropriate fatigue-life model. We demonstrate and illustrate the important advantages of specifying the fatigue model for  $S$ - $N$  data in this manner.
4. We describe the physical explanation for the curvature in the  $S$ - $N$  relationship and show how this curvature induces fatigue-life distributions with an increased spread at lower levels of stress.

## 1.7 Overview

The remainder of this paper is organized as follows. Section 2 outlines our general approach for modeling  $S$ - $N$  data and illustrates it on an example where a fatigue-life model is specified and the corresponding *fatigue-strength model is induced*. Section 3 describes fatigue-strength models and shows how a specified fatigue-strength model *induces a corresponding fatigue-life model*. Section 4 briefly reviews likelihood and Bayesian methods for statistical inference, including residual analysis for censored data and general methods for estimating lower-tail quantiles of fatigue-life and fatigue-strength distributions that engineers need. Section 5 describes and compares additional widely-used nonlinear regression relationships for  $S$ - $N$  data, describes the important advantages of specifying a fatigue-strength model that induces a fatigue-life model, and illustrates the approach with two additional HCF applications. Section 6 provides concluding remarks and outlines areas for future research. To save space and improve readability, proofs, various technical details, additional plots, and more detailed numerical results have been relegated to appendices.

## 2 Statistical Models for Fatigue $S$ - $N$ Data

As mentioned in Section 1.5, dozens of different statistical models have been suggested to describe  $S$ - $N$  data. This section introduces a modular framework that includes most of these models as special cases. For a given  $S$ - $N$  data set, appropriate model components are chosen to comprise a specific model or to describe the data. We encourage fitting and comparing alternative statistical models.

### 2.1 A Modular Framework for Modeling Fatigue $S$ - $N$ Data

As described in Section 1.4.1, a statistical model for fatigue  $S$ - $N$  experimental data has two closely related random variables—fatigue life  $N$  and fatigue strength  $X$ .

There are two different ways to specify a statistical model for  $S$ - $N$  data:

1. Specify a model  $F_N(t; S_e, \theta)$  for fatigue life  $N$  as a function of a given stress amplitude  $S_e$  which will induce (imply) a corresponding fatigue-strength model (Section 2.4).
2. Specify a model  $F_X(x; N_e, \theta)$  for the fatigue-strength random variable  $X$  as a function of a given number of cycles  $N_e$ . This model will induce a corresponding fatigue-life model (Section 3.2).

Here  $\theta$  is a vector of unknown parameters (the nature of which depends on the particular model components) to be estimated from the  $S$ - $N$  data. To simplify notation, we will usually suppress the dependency of  $F_N(t; S_e)$ ,  $F_X(x; N_e)$ , or their corresponding density and quantile functions on  $\theta$ .

Because  $N$  is *observable* (and  $X$  is not), the first approach for  $S$ - $N$  model specification has been used most commonly in practice and will be described and illustrated in the rest of this section. The second approach is new, has important advantages, and will be described in detail in Section 3.2 and illustrated in Examples 5.1 and 5.2. After deciding whether to specify the model for  $N$  or  $X$ , two model components need to be specified:

- A functional  $S$ - $N$  regression relationship (decreasing, usually nonlinear, continuous, and differentiable) describing how the distribution of the observable fatigue life  $N$  depends on the experimental factor stress amplitude  $S_e$  (or how the distribution of the not-observable fatigue strength  $X$  depends on the given number of cycles  $N_e$ ). Although it is possible to have explanatory/experimental variables other than Stress in a fatigue-life test, and such extensions are straightforward, we will focus on a model with just this one experimental factor and describe the extensions in our concluding remarks.
- A probability model to describe spread in the  $S$ - $N$  data. In this paper we use the log-location-scale family of distributions because they include the lognormal and Weibull distributions that are used almost exclusively for fatigue modeling. Extensions to other, more general, families of distributions are possible, as described in Section D.3 of the Appendix.

### 2.2 Log-Location-Scale Probability Distributions

If  $Y$  has a location-scale distribution, then  $T = \exp(Y)$  has a log-location-scale distribution with cdf

$$F(t; \mu, \sigma) = \Phi \left[ \frac{\log(t) - \mu}{\sigma} \right] = \Phi \left[ \log \left( \left[ \frac{t}{\exp(\mu)} \right]^{(1/\sigma)} \right) \right], \quad t > 0 \quad (1)$$

where  $\Phi(z)$  is the cdf for the particular standard location-scale distribution,  $\exp(\mu)$  is a scale parameter and  $\sigma$  is the shape parameter. The most well-known log-location-scale distributions are the lognormal ( $\Phi(z) = \Phi_{\text{norm}}(z)$  is the standard normal cdf), and Weibull ( $\Phi(z) = \Phi_{\text{sev}}(z) = 1 - \exp[-\exp(z)]$  is the standard smallest extreme value cdf) distributions. See Chapter 4 of [Meeker et al. \(2022\)](#) for more information about these and other log-location-scale distributions.

## 2.3 Basic $S$ - $N$ Relationships and Statistical Models for Fatigue Life

This section describes simple  $S$ - $N$  relationships that are useful for specifying a fatigue-life model for  $S$ - $N$  data. More complicated  $S$ - $N$  relationships that are better suited when a fatigue-strength model is specified are given in Section 5.

### 2.3.1 A statistical model for fatigue-life

Suppose that the logarithm of the fatigue-life random variable  $N$  at a *given* stress level  $S_e$  is

$$\log(N) = \log[g(S_e; \boldsymbol{\beta})] + \sigma_N \epsilon, \quad (2)$$

where  $N = g(S; \boldsymbol{\beta})$  is a positive monotonically decreasing  $S$ - $N$  regression relationship of known form,  $\boldsymbol{\beta}$  is a vector of regression parameters,  $\sigma_N \epsilon$  is a random-error term and  $\epsilon$  has a location-scale distribution with  $\mu = 0$  and  $\sigma = 1$ . Then for any given stress level  $S_e$ ,  $N$  has a log-location-scale distribution with cdf

$$F_N(t; S_e) = \Pr(N \leq t; S_e) = \Phi\left(\frac{\log(t) - \log[g(S_e; \boldsymbol{\beta})]}{\sigma_N}\right), \quad t > 0, S_e > 0, \quad (3)$$

where  $g(S_e; \boldsymbol{\beta})$  is a scale parameter and  $\sigma_N$  is the shape parameter of the distribution of  $N$ . The fatigue-life  $p$  quantile is obtained by solving  $p = F_N(t_p(S_e); S_e)$  for  $t_p(S_e)$ , giving

$$t_p(S_e) = \exp(\log[g(S_e; \boldsymbol{\beta})] + \Phi^{-1}(p)\sigma_N), \quad 0 < p < 1, S_e > 0. \quad (4)$$

### 2.3.2 The Basquin model

The [Basquin \(1910\)](#)  $S$ - $N$  relationship (sometimes referred to as the *inverse-power rule*) is

$$N = A \times S^{-B},$$

where  $A$  and  $B$  are parameters. As usually presented in the engineering literature, there is no random-error term in the relationship, which is generally taken to represent the relationship between a particular failure-time distribution quantile (e.g., the median) and stress  $S$ . Taking logs, changing parameter names and a sign, and adding a random-error term gives the statistical model for fatigue life  $N$

$$\log(N) = \beta_0 + \beta_1 \log(S) + \sigma_N \epsilon. \quad (5)$$

For any given level of stress  $S_e$ ,  $N$  has a log-location-scale distribution with constant  $\sigma_N$  with cdf and quantile functions given by (3) and (4), respectively, where  $\log[g(S_e; \boldsymbol{\beta})] = \beta_0 + \beta_1 \log(S_e)$ . Basquin is the simplest and most widely used model for fatigue life.

### 2.3.3 The Stromeyer relationship

Stromeyer (1914) introduced the *fatigue-limit*  $S$ - $N$  model

$$\log(N) = \beta_0 + \beta_1 \log(S - \gamma) + \sigma_N \epsilon, \quad S > \gamma, \quad (6)$$

which is a generalization to the Basquin relationship in (5). The Stromeyer relationship describes (for  $\gamma > 0$ ) the concave-up curvature commonly seen in  $S$ - $N$  data when plotted on log-log scales. For any given level of stress  $S_e$ ,  $N$  has a log-location-scale distribution with cdf and quantile functions given by (3) and (4), respectively, where  $\log[g(S_e; \beta)] = \beta_0 + \beta_1 \log(S_e - \gamma)$ . In this model, if  $S_e$  is less than the fatigue-limit  $\gamma$  (also known as an endurance-limit), lifetime is infinite—stress is low enough that cycling does not cause permanent damage. Although there are dissenters, (e.g., Bathias, 1999), it is widely believed that fatigue-limits exist in hard metals like steel and some titanium alloys but not in soft metals like aluminum or copper. Even if fatigue-limits exist, it is unreasonable to assume that  $\gamma$  would be constant in a process/population because there are many additional sources of variability that would affect such fatigue-limits (e.g., surface finish, residual stresses, other manufacturing variabilities, and environmental variables). This motivates the random fatigue-limit (RFL) model described in Section 5.6.

### 2.3.4 Box–Cox (power) transformation model

Nelson (2004, page 96) mentions the use of a power transformation of stress instead of a log transformation. Although the Box–Cox transformation is widely used to transform the response in statistical modeling, it can also be used to transform explanatory variables (e.g., Carroll and Ruppert, 1988). Meeker et al. (2003) and Meeker et al. (2022, Section 18.5.5) use a Box–Cox transformation  $S$ - $N$  model

$$\log(N) = \beta_0 + \beta_1 \nu(S, \lambda) + \sigma_N \epsilon = \begin{cases} \beta_0 + \beta_1 \left( \frac{S^\lambda - 1}{\lambda} \right) + \sigma_N \epsilon & \text{if } \lambda \neq 0 \\ \beta_0 + \beta_1 \log(S) + \sigma_N \epsilon & \text{if } \lambda = 0 \end{cases} \quad (7)$$

instead. Here  $\nu(S_e, \lambda)$  is the Box–Cox power transformation of stress. This transformation is preferred because  $\nu(S_e, \lambda)$  is continuous in the power parameter  $\lambda$  and the special case  $\lambda = 0$  corresponds to the Basquin relationship. For any given level of stress  $S_e$ ,  $N$  has a log-location-scale distribution with cdf and quantile functions given by (3) and (4), respectively, where  $\log[g(S_e; \beta)] = \beta_0 + \beta_1 \nu(S_e, \lambda)$ .

For  $\lambda < 0$  and  $\beta_1 < 0$  (values expected in  $S$ - $N$  applications) the Box–Cox relationship has a concave-up shape. In contrast to the Stromeyer relationship, as shown in Figure 6a, there is vertical asymptote in the  $S$ - $N$  relationship at  $B = \beta_0 + \beta_1(-1/\lambda)$ . As described in Sections 2.4.3 and 3.2.5, this asymptotic behavior can lead to physically unreasonable model features. When, however, the steep asymptotic behavior is outside the range where the model would be used (e.g., Example 2.2), there are no practical problems. For example, the Box–Cox model nicely describes the laminate panel data in Example 1.1, as will be shown in Example 2.2.

### 2.3.5 A model component to describe nonconstant $\sigma_N$

The models described earlier in this section do not account for nonconstant  $\sigma_N$  that is often seen in  $S$ - $N$  data (e.g., the data introduced in Examples 1.2 and 1.3). Thus, for some data sets, it is necessary

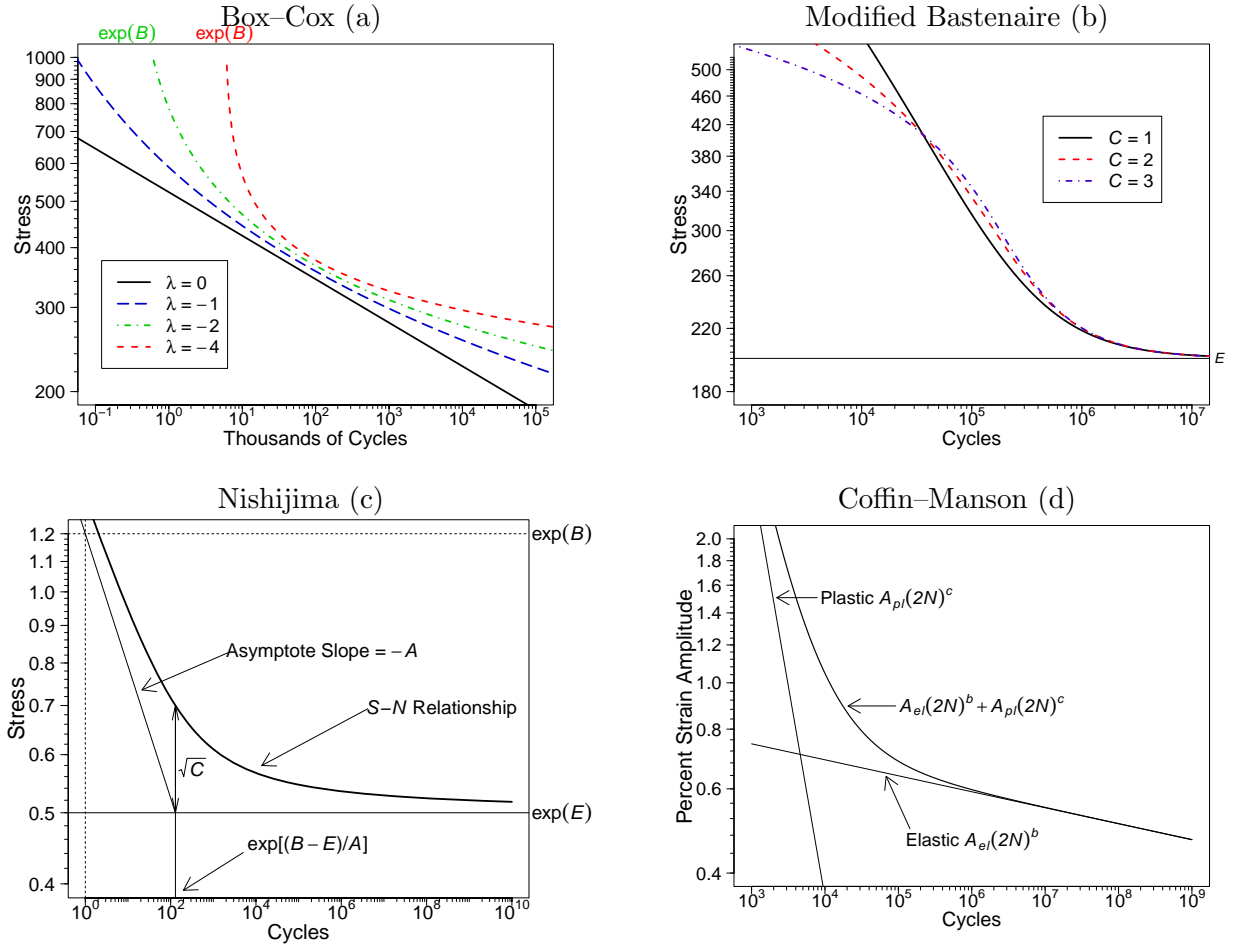


Figure 6:  $S-N$  relationships: Box-Cox (Section 2.3.4) (a), modified Bastenaire (Section 5.2) (b), Nishijima (Section 5.3) (c), and Coffin-Manson (Section 5.5) (d).

to add an additional model component such as

$$\sigma_N = \exp\left[\beta_0^{[\sigma_N]} + \beta_1^{[\sigma_N]} \log(S_e)\right]. \quad (8)$$

Nelson (1984) used a quadratic  $S-N$  relationship and (8) to estimate  $S-N$  curves for a nickel-based superalloy. Pascual and Meeker (1997) used a Stromeyer  $S-N$  relationship (Section 2.3.3) and (8) to describe the same data. Section 2.6, uses a Box-Cox relationship with (8) to describe the increase in spread at the lower stress levels seen in Figure 2. Although this loglinear- $\sigma_N$  model component has been useful in applications we want to note that its use will cause violations of certain compatibility conditions, described further in Section 2.7.

## 2.4 Linking Fatigue-Life and Fatigue-Strength Models

This section describes the relationship between a specified fatigue-life model and the corresponding induced fatigue-strength model.

### 2.4.1 The induced fatigue-strength model when $\log[g(S; \beta)]$ has neither a vertical nor a horizontal asymptote

Section 2.1 defined the unobservable *fatigue-strength* random variable  $X$  as the level of applied stress that would result in a failure at a given number of cycles  $N_e$ . This definition describes the close relationship to the observable fatigue-life random variable  $N$ . In this model, the distributions of  $X$  and  $N$  share the same random-error term. For the moment, suppose that  $\log[g(S_e; \beta)]$  has neither a horizontal nor a vertical asymptote. To derive the distribution of  $X$ , replace  $N$  with  $N_e$  and  $S_e$  with  $X$  in (2) giving

$$\log(N_e) = \log[g(X; \beta)] + \sigma_N \epsilon. \quad (9)$$

This shows that the common random-error term  $\sigma_N \epsilon$  drives the random variable  $X$  at fixed  $N_e$  as well as the random variable  $N$  at fixed  $S_e$ . Also, (9) implies that  $(\log(N_e) - \log[g(X; \beta)])/\sigma_N = \epsilon$  has a location-scale distribution with  $\mu = 0$  and  $\sigma = 1$ . Then using (9) and the fact that  $g(S; \beta)$  is monotonically decreasing in  $S$ , the cdf of  $X$  is

$$\begin{aligned} F_X(x; N_e) &= \Pr(X \leq x; N_e) = \Pr[g(X; \beta) > g(x; \beta)] \\ &= \Pr(\log[g(X; \beta)] > \log[g(x; \beta)]) = \Pr(-\log[g(X; \beta)] < -\log[g(x; \beta)]) \\ &= \Pr(\log(N_e) - \log[g(X; \beta)] < \log(N_e) - \log[g(x; \beta)]) \\ &= \Phi \left[ \frac{\log(N_e) - \log[g(x; \beta)]}{\sigma_N} \right], \quad x > 0, N_e > 0. \end{aligned} \quad (10)$$

Note that (10) is a log-location-scale distribution if and only if the  $S$ - $N$  relationship  $\log[g(x; \beta)]$  is a linear function of  $\log(x)$  (i.e., the Basquin relationship in (5)). For nonlinear  $S$ - $N$  relationships, the induced distribution for  $X$  provides a theoretically justified method for making inferences about fatigue-strength distributions as a function of the given number of cycles  $N_e$  and the fatigue-life model parameters  $(\beta, \sigma_N)$ .

Expressions for the corresponding pdf of  $X$  are given in Section B.4. The  $p$  quantile of the fatigue-strength distribution is obtained by solving  $F_X(x_p; N_e) = p$  in (10) for  $x_p$  giving

$$x_p(N_e) = g^{-1}(\exp[\log(N_e) - \Phi^{-1}(p)\sigma_N]; \beta), \quad 0 < p < 1, N_e > 0. \quad (11)$$

**Example 2.1 The Induced Fatigue-Strength Model for the Basquin Relationship.** This example provides details for the special-case induced fatigue-strength model for the Basquin relationship, illustrated in Figure 7 for the lognormal and Weibull distributions. Substituting  $\log[g(x; \beta)] = \beta_0 + \beta_1 \log(x)$  into (10), with  $\beta_1 < 0$  (because the  $S$ - $N$  relationship is strictly decreasing), gives

$$\begin{aligned} F_X(x; N_e) &= \Phi \left[ \frac{\log(N_e) - [\beta_0 + \beta_1 \log(x)]}{\sigma_N} \right], \quad x > 0, N_e > 0 \\ &= \Phi \left[ \frac{\log(x) - [\beta_0 - \log(N_e)]/|\beta_1|}{\sigma_N/|\beta_1|} \right] = \Phi \left[ \frac{\log(x) - [\beta_0^\dagger + \beta_1^\dagger \log(N_e)]}{\sigma_X} \right], \end{aligned}$$

where  $\beta_0^\dagger = \beta_0/|\beta_1|$ ,  $\beta_1^\dagger = -1/|\beta_1|$ , with  $\beta_1^\dagger < 0$ , and  $\sigma_X = \sigma_N/|\beta_1|$ . This shows that the induced fatigue-strength model has the same log-location-scale form with different parameters. Grove and

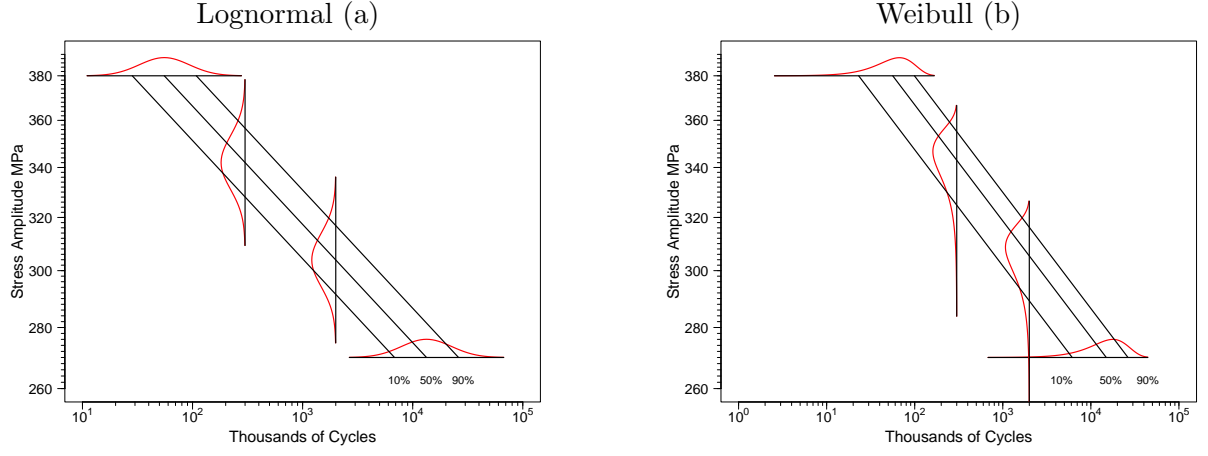


Figure 7: Lognormal (a) and Weibull (b) fatigue-life (horizontal) and fatigue-strength (vertical) distributions for the Basquin  $S$ - $N$  relationship.

Campean (2008) give a similar result. ■

#### 2.4.2 The induced fatigue-strength model when $\log[g(S; \beta)]$ has a horizontal asymptote

When  $\log[g(x; \beta)]$  has a horizontal asymptote at  $\log(S) = E$ ,  $\lim_{x \downarrow \exp(E)} \log[g(x; \beta)] = \infty$  as illustrated in Figure 6b and c. Because  $(\log(N_e) - \log[g(x; \beta)])/\sigma_N$  is unbounded, the derivation of the cdf for  $X$  is the same as (10) but because of the asymptote, for given  $N_e$ ,

$$\lim_{x \downarrow \exp(E)} F_X(x; N_e) = \Phi\left(\frac{\log(N_e) - \infty}{\sigma_N}\right) = 0,$$

and thus

$$F_X(x; N_e) = \Phi\left(\frac{\log(N_e) - \log[g(x; \beta)]}{\sigma_N}\right), \quad x > \exp(E), \quad N_e > 0.$$

The range of  $X$  depends on the unknown threshold parameter  $\exp(E)$ , so the model is not regular (e.g., Smith, 1985). The horizontal asymptote also implies that fatigue strength  $X$  will never be less than  $\exp(E)$ . The pdf of  $X$  is the same as (45) in Section B.4, except that it is positive only when  $x > \exp(E)$ . The quantiles of  $X$  are the same as (11) but as  $p \rightarrow 0$ ,  $x_p(N_e) \rightarrow \exp(E)$ .

#### 2.4.3 The induced fatigue-strength model when $\log[g(S; \beta)]$ has a vertical asymptote

If  $\log[g(x; \beta)]$  has a vertical asymptote (e.g., the Box-Cox relationship in Section 2.3.4 and see Figure 6a with  $\lambda < 0$ ), then  $\lim_{x \rightarrow \infty} \log[g(x; \beta)] = B$  and thus  $B$  is a lower bound for  $\log[g(x; \beta)]$ . Consequently,  $[\log(N_e) - B]/\sigma_N$  is an upper bound for  $\epsilon$ , but the range of  $\epsilon$  is  $(-\infty, \infty)$ . To resolve this inconsistency, we modify (9) and use

$$\log(N_e) = \log[g(X; \beta)] + \sigma_N \epsilon I[-\infty < \epsilon < (\log(N_e) - B)/\sigma_N],$$



where  $I[\cdot]$  is the indicator function. The derivation of the cdf for  $X$  is the same as (10) but because of the asymptote, for given  $N_e$ ,

$$\lim_{x \rightarrow \infty} F_X(x; N_e) = \Phi\left(\frac{\log(N_e) - B}{\sigma_N}\right) < 1.$$

This implies that the distribution of  $X$  has a discrete atom of probability at  $\infty$ . The size of the discrete atom is

$$1 - \Phi\left(\frac{\log(N_e) - B}{\sigma_N}\right). \quad (12)$$

This discrete atom corresponds to the limiting proportion of units for which  $N > N_e$  as  $x \rightarrow \infty$ . This can be interpreted as the (physically questionable) proportion of units that would survive  $N_e$  cycles, even as stress approaches  $\infty$ . The pdf of  $X$  is the same as (45) in Section B.4 but it does not integrate to 1 because of the discrete atom of probability at  $\infty$ . The quantiles of  $X$  are the same as (11) but, because of the discrete atom at  $\infty$ ,  $x_p(N_e)$  is finite only for  $0 \leq p < \Phi[(\log(N_e) - B)/\sigma_N]$ . As an example, Section B.3.3 in the Appendix gives details for the Box-Cox  $S$ - $N$  model.

#### 2.4.4 Equivalence of fatigue-life and fatigue-strength quantile curves

For  $S$ - $N$  relationships that have neither a horizontal nor a vertical asymptote, the fatigue-life and fatigue-strength models have the same quantile curves and thus when estimating a fatigue-life model, one is simultaneously estimating the fatigue-strength model. For  $S$ - $N$  relationships that have either a horizontal or a vertical asymptote the fatigue-life and fatigue-strength quantile curves are still equivalent except that quantile lines for certain values of  $p$  do not exist because of the discrete atom of probability at  $\infty$ , as described in Sections 2.4.3, 3.2.4, and 3.2.6. Section D.1 provides a proof of this result and more explanation about the exceptions.

### 2.5 Choosing a Fatigue-Life Probability Distribution

The lognormal and Weibull distributions are the most commonly used distributions in fatigue data analysis. This is because one or the other often fits well and because there is physical motivation for using them. Meeker et al. (2022, Section 4.6.2) give physics-of-failure arguments (based on cumulative damage mechanisms like fatigue) for using the lognormal distribution to describe time to fracture from fatigue in ductile materials like metals, when there is a single crack growing toward fracture. Mathematical justification for this physical/chemical motivation is given in Gnedenko et al. (1969, pages 36–37) and Mann et al. (1974, pages 133–134). Crowder et al. (Section 4.6 1994), Castillo and Fernández-Canteli (2009), and Meeker et al. (2022, Section 4.8.4) describe extreme-value-theory arguments for using the Weibull distribution to describe time to fracture from fatigue in brittle materials like ceramics or metals if there are potentially many cracks competing to be the first to cause fracture (e.g., in a wire, chain, gear, or bearing).

Although this kind of physical guidance is useful in deciding which distribution to use, it is important to use probability plots like those in Figures 2, 3b, and 4b to help make a decision. It is also important to use sensitivity analysis to assess the effect of alternative choices in the distribution (especially when the data do not result in a definitive conclusion or when extrapolating into the lower tail of a fatigue-life or fatigue-strength distribution). For additional illustrations of this, Section F



provides a side-by-side comparison of lognormal and Weibull distributions fit to nine different  $S$ - $N$  data sets. For the four data sets where tests were on wire specimens, the Weibull distribution fits well (as predicted by extreme-value theory). For the others (e.g., notched or hour-glass shaped metal specimens), the data show that the lognormal distribution is a more appropriate distribution (as predicted by the cumulative damage theory).

## 2.6 An Example of Fitting a Fatigue-Life Model

This section provides an example to illustrate the key ideas presented earlier in this section and to set the stage for the remainder of the paper.

### Example 2.2 Fitting the Box–Cox/Loglinear- $\sigma_N$ $S$ - $N$ Model to the Laminate Panel Data.

This example is a continuation of Example 1.1. A description of the noninformative joint prior distribution that was used, and other details are in Section H.1. Figure 8a is a lognormal probability plot showing Bayesian cdf estimates. The estimates were computed by taking the median of the empirical distribution of the draws from the marginal posterior distributions of  $F_N(t; S_e)$  for a large number of values of  $t$  for each of the five levels of  $S_e$  used in the experiment. The Bayesian estimates agree well with the nonparametric estimates at all levels of  $S_e$ . For estimation at  $S_e = 270$  MPa, corresponding 95% credible intervals are also plotted. These were obtained from the 0.025 and 0.975 quantiles of the empirical distribution of the draws from the marginal posterior distribution  $F_N(t; 270)$  for the same values of  $t$  used to compute the cdf estimates. The credible intervals are narrow because of the large number of tested specimens with few runouts.

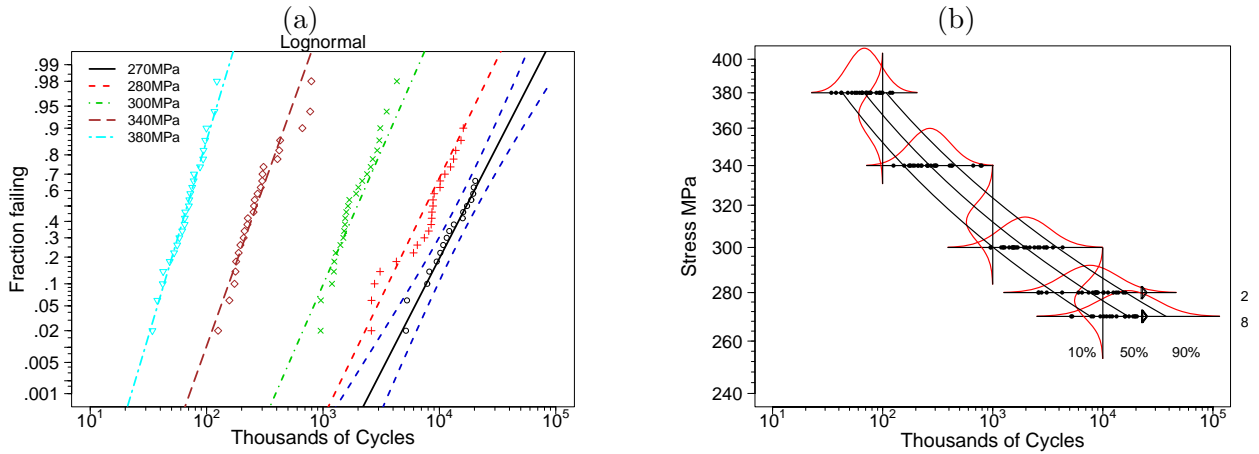


Figure 8: Lognormal probability plot showing the cdf estimates from the Box–Cox/loglinear- $\sigma_N$  model fit to the laminate panel  $S$ - $N$  Data (a) and the corresponding model plot showing the (shared) quantile curves and density estimates for fatigue life (horizontal) and fatigue strength (vertical) (b).

Figure 8b is a fitted *model plot* showing the estimates of the 0.10, 0.50, and 0.9 quantile curves, along with estimates of the fatigue-life and fatigue-strength densities superimposed on top of the  $S$ - $N$  data that we first saw in Figure 1b. The increase in spread in the fatigue-life (horizontal) densities (due to the loglinear- $\sigma_N$  component in the model) is evident. Interestingly, the spread in the *induced* fatigue-strength (vertical) densities appears to be approximately constant. ■

## 2.7 Compatibility Conditions and Characteristics of $S$ - $N$ Models

Bastenaire (1972) and Castillo and Fernández-Canteli (2009, Chapter 2) describe various characteristics or “compatibility conditions” that are required for statistical models for fatigue to be sensible both physically and probabilistically. This section reviews some of these characteristics.

Perhaps the most important model characteristic is that the  $S$ - $N$  relationship (e.g.,  $N = g(S)$ , corresponding to a particular quantile curve) should be positive and monotonically decreasing—higher stress implies shorter life. Additionally, the fatigue-life model cdf  $F_N(t; S_e, \theta)$  should be

- Monotonically increasing in  $t$  for fixed  $S_e$  and
- Monotonically increasing in  $S_e$  for fixed  $t$ .

The first condition is generally met for any of the continuous cdfs typically used in fatigue-life models and used in this paper. Whether the second condition holds or not will depend on the nature of the regression model. Generally, the condition will hold if cdfs for different stress levels like those in Figure 8a do not cross. Equivalently, the condition will hold if quantile curves like those in Figure 8b do not cross. Although desirable, it is not essential that these not-cross conditions hold over the entire range of  $t$  and  $S_e$ . It is, however, essential that the conditions hold over the range of  $t$  and  $S_e$  where the model is used. Bastenaire (1972, page 10) makes a similar point.

For example, with the fitted quadratic model used in Nelson (1984) (mentioned in Section 1.5), the quantile curves are decreasing in pseudo-stress over the range of the data but begin to increase for larger values of the pseudo-stress used there—but this happens only outside of the range of pseudo-stress where the model would be used. The model used for the laminate panel data in Section 2.6 allows  $\sigma_N$  to be a loglinear function of stress. This causes the slopes of the estimates of the lognormal cdfs in a lognormal probability plot (see Figure 8a) to depend on stress, implying that the cdfs will cross. The crossing behavior, however, is far away from the region where the model would be used.

Similar conditions can be stated for the fatigue-strength model  $F_X(x; N_e)$ . Recognizing that the fatigue-life and fatigue-strength models have the same quantile curves (Section 2.4.4) shows that if the conditions hold for the fatigue-life model, they also hold for the fatigue-strength model and vice versa. This crossing behavior can be avoided by specifying a fatigue-strength model with constant  $\sigma_X$  which, if there is curvature in the  $S$ - $N$  relationship, will result in a change in spread for the induced fatigue-life model for  $N$ . This illuminates an important advantage in specifying the  $S$ - $N$  model in terms of the fatigue-strength distribution. This modeling approach is described in detail in Section 3.2.

## 3 Statistical Models for Fatigue-Strength

### 3.1 Estimating a Fatigue-Strength Distribution Using Binary Data

Because fatigue strength is not directly observable, the traditional way to estimate a fatigue-strength distribution at a given level  $N_e$  (e.g., Little and Jebe, 1975; Nelson, 2004; Awad et al., 2004; Grove and Campean, 2008) has been to

- Test a sample of  $n$  units at different fixed stress levels  $S_i$ ,  $i = 1, \dots, n$ . The units are tested until failure or the given value of  $N_e$  cycles (whichever comes first).

- Dichotomize the data to consist of only the runouts (right-censored at  $S_i$  because  $X > S_i$ ) and failures (left-censored at  $S_i$  because  $X < S_i$ ). The actual failure times are ignored.
- Use binary regression methods (e.g., logit or probit regression, possibly on  $\log(S)$ ) to estimate the fatigue-strength distribution at  $N_e$  cycles.

Data from the well-known and commonly used staircase method (e.g., Pollak et al., 2006; Müller et al., 2017) provide useful estimates of the *median* of the fatigue-strength distribution, but not small quantiles that are needed in high-reliability applications. This is because the method concentrates observations near the center of the fatigue-strength distribution. Wu and Tian (2014) review and suggest an alternative sequential method when the goal is to estimate a particular quantile of a distribution based on binary data.

Dichotomizing  $S$ - $N$  data to estimate fatigue-strength distributions has serious disadvantages. Such methods are statistically inefficient and limit the range of  $N_e$  for which fatigue-strength distributions can be estimated. Sections 2.4 and 2.6 showed how fitting a specified fatigue-life model can be used to estimate characteristics of fatigue-strength distributions, using all of the available  $S$ - $N$  data (i.e., not ignoring the failure times). Section 3.2 shows how to use a *specified fatigue-strength model* that also uses all of the available  $S$ - $N$  data to make inferences for either fatigue-strength or fatigue-life distributions.

### 3.2 Modeling $S$ - $N$ Data by Specifying a Fatigue-Strength Model

The relationship between  $F_N(t; S_e)$  and  $F_X(x; N_e)$  described in Sections 1.4.1 and 2.4 suggests an alternative path for specifying a statistical model for  $S$ - $N$  data. Similar to Falk (2019), one can specify the form of the fatigue-strength distribution and use a specified  $S$ - $N$  relationship to *induce* a fatigue-life model that can be fit to the  $S$ - $N$  data using statistical methods (e.g., maximum likelihood or Bayesian estimation) that can accommodate censored data.

#### 3.2.1 The advantages of specifying the fatigue-strength model to describe $S$ - $N$ data

Specifying a fatigue-strength model and having it induce the corresponding fatigue-life model has important advantages. Weibull (1956) recognized these advantages but his ideas were, unfortunately, lost over time, perhaps because fatigue-strength cannot be observed directly. The most important advantage is that fatigue-strength distributions generally have a simpler form than fatigue life distributions. In particular,  $F_X(x; N_e)$  tends to have constant shape/spread for different values of  $N_e$  whereas the fatigue-life distributions  $F_N(t; S_e)$  often have increased spread and a different shape at lower levels of stress. This was also noted by Hanaki et al. (2003, 2010). Empirically, Figure 15 in Section C.2 provides six HCF examples where the vertical spread in the data is relatively constant but the spread in the fatigue-life distributions is larger at lower levels of stress. Thus a model component to describe increasing spread in fatigue life  $N$  will usually *not* be needed (further physical explanation is given in Section 5.1). As described in Section 2.7, this implies that the compatibility conditions will hold (e.g., quantile lines will not cross). More generally, when there is curvature in the  $S$ - $N$  relationship, the induced fatigue-life distributions have features that agree better with the physical nature of fatigue data—increased spread at lower levels of stress.

### 3.2.2 A statistical model for fatigue-strength

Suppose that the logarithm of the fatigue-strength random variable  $X$  at a *given* number of cycles  $N_e$  is

$$\log(X) = \log[h(N_e; \boldsymbol{\beta})] + \sigma_X \epsilon, \quad (13)$$

where  $S = h(N; \boldsymbol{\beta})$  is a positive monotonically decreasing  $S$ - $N$  regression relationship of known form,  $\boldsymbol{\beta}$  is a vector of regression parameters,  $\sigma_X \epsilon$  is a random-error term, and  $\epsilon$  has a location-scale distribution with  $\mu = 0$  and  $\sigma = 1$ . Then for any given number of cycles  $N_e$ ,  $X$  has a log-location-scale distribution with cdf

$$F_X(x; N_e) = \Pr(X \leq x; N_e) = \Phi \left[ \frac{\log(x) - \log[h(N_e; \boldsymbol{\beta})]}{\sigma_X} \right], \quad x > 0, N_e > 0, \quad (14)$$

where  $h(N_e; \boldsymbol{\beta})$  is a scale parameter and  $\sigma_X$  is the shape parameter of the distribution of  $X$ . The fatigue-strength  $p$  quantile is obtained by solving  $p = F_X(x_p(N_e); N_e)$  for  $x_p(N_e)$ , giving

$$x_p(N_e) = \exp(\log[h(N_e; \boldsymbol{\beta})] + \Phi^{-1}(p)\sigma_X), \quad 0 < p < 1, N_e > 0. \quad (15)$$

### 3.2.3 The induced fatigue-life model when $\log[h(N; \boldsymbol{\beta})]$ has neither a vertical nor a horizontal asymptote

For the moment, suppose that the positive monotonically decreasing  $S$ - $N$  relationship  $S = h(N; \boldsymbol{\beta})$  has neither a vertical nor a horizontal asymptote. Replacing  $N_e$  with  $N$  and  $X$  with  $S_e$  in (13) gives

$$\log(S_e) - \log[h(N; \boldsymbol{\beta})] = \sigma_X \epsilon. \quad (16)$$

In this role switching,  $N$  at given  $S_e$  replaces  $X$  at fixed  $N_e$ , but the random variables  $X$  and  $N$  have the same  $\sigma_X \epsilon$  random-error term. Equation (16) implies that  $(\log(S_e) - \log[h(N; \boldsymbol{\beta})])/\sigma_X = \epsilon$  has a location-scale distribution with  $\mu = 0$  and  $\sigma = 1$ . Thus the induced cdf of  $N$  is

$$\begin{aligned} F_N(t; S_e) &= \Pr(N \leq t; S_e) = \Pr[h(N; \boldsymbol{\beta}) > h(t; \boldsymbol{\beta})] \\ &= \Pr(\log[h(N; \boldsymbol{\beta})] > \log[h(t; \boldsymbol{\beta})]) = \Pr(-\log[h(N; \boldsymbol{\beta})] < -\log[h(t; \boldsymbol{\beta})]) \\ &= \Pr(\log(S_e) - \log[h(N; \boldsymbol{\beta})] < \log(S_e) - \log[h(t; \boldsymbol{\beta})]) \\ &= \Phi \left[ \frac{\log(S_e) - \log[h(t; \boldsymbol{\beta})]}{\sigma_X} \right], \quad t > 0, S_e > 0. \end{aligned} \quad (17)$$

Expressions for the corresponding pdf of  $N$  (needed to compute a likelihood function) are given in (45) in Section C.5. Note that (17) is a log-location-scale distribution if and only if  $\log[h(t; \boldsymbol{\beta})]$  is a linear function of  $\log(t)$  (i.e., the Basquin relationship in (5)). For linear or nonlinear  $S$ - $N$  relationships, the induced distribution for  $N$  provides a theoretically justified method for making inferences about fatigue-life distributions as a function of the fatigue-strength model parameters  $(\boldsymbol{\beta}, \sigma_X)$ . The  $p$  quantile of  $N$  is obtained by solving  $F_N(t_p; S_e) = p$  for  $t_p$  giving

$$t_p(S_e) = h^{-1}(\exp[\log(S_e) - \Phi^{-1}(p)\sigma_X]; \boldsymbol{\beta}), \quad 0 < p < 1, S_e > 0. \quad (18)$$

### 3.2.4 The induced fatigue-life model when $\log[h(N; \beta)]$ has a horizontal asymptote

When  $\lim_{t \rightarrow \infty} \log[h(t; \beta)] = E > -\infty$ ,  $\log[h(N; \beta)]$  has a horizontal asymptote, as illustrated in Figure 6b and c. Note that both axes in these plots are logarithmic so  $\exp(E) = 0.5$  in Figure 6c. Because  $E$  is a lower bound for  $\log[h(N; \beta)]$ ,  $[\log(S_e) - E]/\sigma_X$  is an upper bound for  $\epsilon$ , but the range of  $\epsilon$  in (16) is  $(-\infty, \infty)$ . To resolve this inconsistency, we modify (16) and use

$$\log(S_e) = \log[h(N; \beta)] + \sigma_X \epsilon I[-\infty < \epsilon < (\log(S_e) - E)/\sigma_X],$$

where  $I[\cdot]$  is the indicator function. The cdf for  $N$  is still (17) but because  $\lim_{t \rightarrow \infty} \log[h(t; \beta)] = E$ ,

$$\lim_{t \rightarrow \infty} F_N(t; S_e) = \Phi\left(\frac{\log(S_e) - E}{\sigma_X}\right) < 1, \quad (19)$$

which implies that the cdf  $F_N(t; S_e)$  has a discrete atom of probability at  $\infty$ . The size of the discrete atom is

$$1 - \Phi\left(\frac{\log(S_e) - E}{\sigma_X}\right). \quad (20)$$

This discrete atom corresponds to the limiting proportion of units for which fatigue strength  $X > S_e$ , as  $t \rightarrow \infty$ . This can be interpreted as the proportion of units that, if tested at stress  $S_e$ , would not fail because  $X > \exp(E)$ , where  $\exp(E)$  can be interpreted as a fatigue limit. The quantiles  $t_p(S_e)$  are the same as in (18), but because of the discrete atom of probability at  $\infty$ ,  $t_p(S_e)$  is only finite for  $0 < p < \Phi[(\log(S_e) - E)/\sigma_X]$ .

### 3.2.5 The induced fatigue-life model when $\log[h(N; \beta)]$ has a vertical asymptote

Consider, for example, the Box–Cox  $S$ - $N$  curves in Figure 6a which, for  $\lambda < 0$ , have vertical asymptotes at  $B = \log(N)$ . When  $t$  decreases to  $\exp(B)$ ,  $\log[h(t; \beta)]$  is unbounded. That is,  $\lim_{t \downarrow \exp(B)} \log[h(t; \beta)] = \infty$ . The cdf is obtained as in (17) except that  $\exp(B)$  is a threshold parameter (i.e.,  $\Pr[N \leq \exp(B)] = 0$ ) and thus

$$F_N(t; S_e) = \Phi\left(\frac{\log(S_e) - \log[h(t; \beta)]}{\sigma_X}\right), \quad t > \exp(B), \quad S_e > 0. \quad (21)$$

The quantiles  $t_p(S_e)$  of  $F_N(t; S_e)$  are the same as (18) but as  $p \rightarrow 0$ ,  $t_p(S_e) \rightarrow \exp(B)$ .

The interpretation of this threshold parameter is similar to that described in Section 2.3.4. For models with a vertical asymptote, even as stress increases to high levels, there is a positive value of  $N$  that a unit could survive. Of course that positive value could be a small fraction of a cycle. Even so, it could be argued that  $S$ - $N$  relationships with a vertical asymptote are inconsistent with what happens physically. As mentioned in Section 2.3.4, however, when the asymptotic behavior occurs far outside the range where the model would be used, any inconsistency is not of practical concern.

### 3.2.6 Visualization of the effect that $S$ - $N$ relationship coordinate asymptotes have on quantile curves and the induced fatigue-life distributions

Figure 9 is a plot of a fitted rectangular hyperbola model that has a vertical asymptote at  $\exp(B)$  and a horizontal asymptote at  $\exp(E)$ . The plot provides a visualization of the effects described in

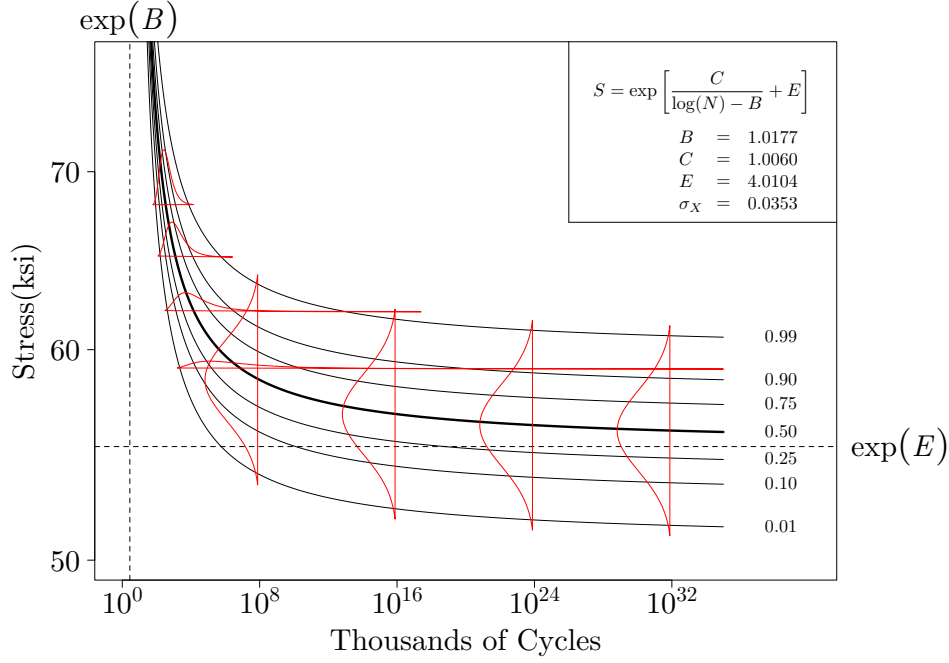


Figure 9: A fitted rectangular-hyperbola  $S$ - $N$  regression model.

Sections 3.2.4 and 3.2.5. The plot shows quantiles curves for  $p = 0.01, 0.1, 0.25, 0.5, 0.75, 0.9$ , and  $0.99$ . The vertical densities at  $N_e = 10^8, 10^{16}, 10^{24}$ , and  $10^{32}$  thousand cycles correspond to lognormal fatigue-strength distributions with a constant  $\sigma_X$  shape parameter. These densities look like normal densities because the vertical axis is a log axis. Also shown are the horizontal densities corresponding to the *induced* fatigue-life distributions at  $S_e = 59, 62, 65$ , and  $68$  ksi. The curves are quantile curves for both the fatigue-strength and the fatigue-life models.

The effect of the vertical asymptote at  $\exp(B)$  is that the induced fatigue-life distributions have a threshold parameter at  $\exp(B)$  and thus  $\Pr[N < \exp(B)] = 0$  for any value of  $S_e$ . It is also interesting to see the relatively small amount of spread in the induced fatigue-life distributions at high levels of stress.

The effect of the horizontal asymptote at  $\exp(E)$  is more subtle. As suggested by the exaggerated time range in Figure 9, each quantile curve has its own horizontal asymptote. Imagine the fatigue-life distribution at a level of stress  $S_e^*$  that is infinitesimally below the asymptote for the  $0.99$  (top) quantile curve in Figure 9. That fatigue-life distribution does not have a finite  $0.99$  quantile and has an atom of probability at infinity that is infinitesimally larger than  $0.01$ . Another way to explain the atom at infinity is that even as  $N_e \rightarrow \infty$ ,  $\Pr(X > S_e^*) \approx 0.01$  (the probability that fatigue strength is greater than  $S_e^*$ —and failure will never occur—has a positive limit).

## 4 Estimating $S$ - $N$ Model Parameters, Model-Fitting Diagnostics, and Making Inferences about Fatigue Distributions

This section briefly describes maximum likelihood and Bayesian methods for fitting  $S$ - $N$  models, estimating tail probabilities and quantiles, and computing confidence or credible intervals for quantifying statistical uncertainty (i.e., uncertainty due to limited data). Both methods are well suited to handle runouts that appear in many fatigue tests. Ordinary least squares should not be used for estimation

when there are runouts.

## 4.1 Likelihood-Based Methods

Likelihood is the primary tool for making non-Bayesian inferences when using advanced statistical models. The method is general, versatile, and has been widely implemented in readily available software for many different kinds of statistical models. Under mild conditions (met in the applications in this paper), likelihood methods have desirable statistical properties in large samples and are generally difficult or impossible to beat even with small samples. Among others, [Severini \(2000\)](#) and [Pawitan \(2013\)](#) provide likelihood theory and methods.

### 4.1.1 Log-likelihood for an $S$ - $N$ regression model with runouts

Typical  $S$ - $N$  data are  $(S_i, N_i, \delta_i), i = 1, \dots, n$  giving stress level  $S_i$ , number of cycles  $N_i$ , and a censoring indicator  $\delta_i$  for each of  $n$  observations. The log-likelihood for these data is

$$\mathcal{L}(\boldsymbol{\theta}) = \sum_{i=1}^n \{ \delta_i \log[f_N(N_i; S_i, \boldsymbol{\theta})] + (1 - \delta_i) \log[1 - F_N(N_i; S_i, \boldsymbol{\theta})] \}, \quad (22)$$

where

$$\delta_i = \begin{cases} 1 & \text{if } N_i \text{ is a failure time} \\ 0 & \text{if } N_i \text{ is a runout time.} \end{cases}$$

Here,  $F_N(N_i; S_i, \boldsymbol{\theta})$  is the fatigue-life cdf in (3) when the fatigue-life model is specified and (17) when the fatigue-strength model is specified (and the fatigue-life model is induced). Then  $f_N(t; S_i, \boldsymbol{\theta}) = dF_N(N_i; S_i, \boldsymbol{\theta})/dt$  is the corresponding pdf. Sections B.2 and C.5 give expressions for the pdfs. Standard optimization algorithms can be used to maximize  $\mathcal{L}(\boldsymbol{\theta})$ . [Liu and Meeker \(2024\)](#) provide implementation suggestions for the nonlinear models used in this paper.

### 4.1.2 Methods for computing confidence intervals when using likelihood-based inference

In engineering applications, inferences are generally needed for distribution tail probabilities and distribution quantiles. For non-Bayesian inference, basing confidence intervals for these quantities on the distribution of the likelihood-ratio statistic is perhaps the most natural method to use. Coverage probabilities tend to be close to the specified nominal confidence level. The method is computationally complicated but not hard to implement with modern computing capabilities. [Pascual and Meeker \(1999\)](#) illustrate this approach for the RFL model. [Liu et al. \(2024\)](#) outline algorithms to compute likelihood-based confidence intervals for the fatigue-life and fatigue-strength models described in this paper.

Wald confidence intervals are based on a quadratic approximation to the profile log-likelihood function ([Meeker and Escobar, 1995](#)) and are generally much easier to compute. Wald intervals, however, tend to have actual coverage probabilities that are smaller than the specified nominal confidence level. Bootstrap methods (e.g., [Efron and Tibshirani, 1993](#)) provide another method of potentially improving on the Wald approximation.



### 4.1.3 Equivalence of likelihood pointwise confidence interval bands for cdfs and quantiles

Hong et al. (2008) showed that a band of pointwise confidence intervals for a cdf (e.g., the 270 MPa cdf estimate in Figure 8a) are exactly the same as the band of pointwise confidence intervals for quantiles if the confidence intervals are computed using the likelihood ratio method (and approximately the same for Wald intervals). There are similar results relating bands of confidence intervals for cdfs and quantiles for both fatigue-life and fatigue-strength distributions for the models used in this paper. Technical details are given in Liu et al. (2024).

Similarly, one can use confidence intervals for fatigue-life model quantiles to obtain confidence intervals for quantiles of the corresponding fatigue-strength model. For example, the value of stress  $S_e$  for which the likelihood-based lower confidence bound  $\underline{t}_p(S_e) = N_e$  is then equivalent to  $\underline{x}_p(N_e)$ , the likelihood-based lower confidence bound for the fatigue-strength distribution at  $N_e$ . Again, technical details are given in Liu et al. (2024). The importance of these results is that one can use existing software that computes confidence intervals for fatigue-life quantiles (or probabilities) to obtain confidence intervals for *fatigue-strength* quantiles (or probabilities).

## 4.2 Bayesian Inference Methods

Over the past thirty years, there has been an increasing trend in the proportion of applications where Bayesian methods are used. We use Bayesian inference methods for fitting  $S$ - $N$  regression models because engineers may have informative prior information for some of the model parameters and because we have found that extensions to models using random parameters (e.g., random batch effects) are easier to implement using Bayesian methods.

### 4.2.1 Specifying the joint prior distribution

Bayesian inference requires the specification of a joint prior distribution for the model parameters. For most applications and certainly those considered here, there is usually a desire to use noninformative or other minimally informative priors. Johnson et al. (1999) describe how they developed a partially informative prior (while trying to be minimally informative) to fit the RFL model. Gelman et al. (2017) outline a general strategy for specifying weakly informative priors. Tian et al. (2024) describe methods for specifying prior distributions in reliability applications for a single distribution. The ideas can be extended to regression models and approximately to nonlinear regression models like those used in our paper. Liu and Meeker (2024) outline a general strategy for nonlinear regression based on a stable parameterization and describe how noninformative or minimally informative prior distributions can be specified for models like those used in this paper.

### 4.2.2 Generating and using draws from the joint posterior distribution

For the examples in this paper (with additional details in the Appendix), we use Bayesian methods to fit the  $S$ - $N$  model and to compute credible intervals for quantities of interest like lower-tail quantiles of the fatigue-life and fatigue-strength distributions. For each of the  $S$ - $N$  models that we used in our examples, a stable parameterization was specified (details are provided in Liu and Meeker, 2024) and a Stan (Stan Development Team, 2022b) model was written and run using the RStan (Stan Development Team, 2022a) interface to R (R Core Team, 2022). For each model fit, 20,000 draws from the joint posterior distribution were computed and saved. Then R functions were used to post-process these



draws to compute estimates and credible intervals for quantities interest (e.g., the results in Figure 8) and residuals used for diagnostic checking (e.g., the results in Figure 10).

#### 4.2.3 Numerical methods to obtain starting values and default joint prior distributions

Robust algorithms for estimating the parameters of nonlinear regression models (using either maximum likelihood or Bayesian estimation) require careful attention to parameterization and methods for finding starting values. Satisfactory starting values can often be obtained by using simple moment estimates (e.g., sample means, variances, and linear regression). Our approach is to define a parameterization where all parameters are unrestricted without any ordering relationships. Optimizers tend to perform best with such a parameterization and flat priors provide a natural default joint prior distribution. In some applications, it is necessary to replace the flat prior with an approximately flat normal (Gaussian) distribution with an extremely large standard deviation (e.g., 10 times the standard error obtained from maximum likelihood estimation). Exactly how these ideas are implemented depends on the particular model. [Liu and Meeker \(2024\)](#) give details for the models used in our examples.

### 4.3 Using Residuals as Model-Checking Diagnostics

Although probability plots like those in Figures 2, 3b, 4b, and 8b are useful for detecting departures from the assumed model, such plots are available only when experiments result in data with many observations at each of some number of stress levels. Frequently  $S$ - $N$  data have many stress levels with few repeats. In such cases, residuals can be computed and these can be displayed in various ways to see if they depart from what is expected under the assumed model. [Nelson \(1973\)](#) describes regression analysis methods for censored data. The key idea is that the residual for a censored observation is correspondingly censored.

Here, residuals are defined as estimates of the  $\epsilon$  error variable in models such as (2) and (13). Such residuals are generally known as *standardized residuals* and should behave approximately like independent identically distributed (iid) observations with constant spread from the assumed distribution.

Scatter plots of the residuals versus other variables, such as the fitted values, stress, or other explanatory variables, and potential explanatory variables (e.g., test order and heat or batch) are useful. Systematic dependence of the residuals on any such variable or systematic change in spread versus such variables indicates a departure from the assumed model. Special symbols (e.g., an upward-pointing triangle) should be used to plot censored residuals. Heavy censoring can make residual scatter plots difficult to interpret ([Nelson, 1973](#)). For  $S$ - $N$  data, most censoring occurs at the lowest stress levels so scatter plots can detect model departures. Suppose no serious departures are detected in such scatter plots. In that case, probability plots of the residuals can be used to check the adequacy of the assumed distribution of the  $\epsilon$  error variable. In addition to checking the model fit for individual fitted models, we have found that comparing residual plots for across different fitted models for the same data to be particularly useful. Section E gives a particular example.

Based on the *specified fatigue-life* regression model in (2), the standardized residuals (estimates of the  $\epsilon_i$  error for observation  $i$ ) are

$$\hat{\epsilon}_i = \frac{\log(N_i) - \log[g(S_i; \hat{\beta})]}{\hat{\sigma}_N}, \quad i = 1, \dots, n.$$

When there is a loglinear model for  $\sigma_N$ , as described in Section 2.3.5, the standardized residuals are

$$\hat{\epsilon}_i = \frac{\log(N_i) - \log[g(S_i; \hat{\beta})]}{\exp[\hat{\beta}_0^{[\sigma_N]} + \hat{\beta}_1^{[\sigma_N]} \log(S_i)]}, \quad i = 1, \dots, n. \quad (23)$$

Based on the *specified fatigue-strength* regression model in (13), the standardized residuals are computed from

$$\hat{\epsilon}_i = \frac{\log(S_i) - \log[h(N_i; \hat{\beta})]}{\hat{\sigma}_X}, \quad i = 1, \dots, n.$$

Then the  $\exp(\hat{\epsilon}_i)$  values should, if the assumed model is adequate, behave approximately like an iid sample from the assumed log-location-scale distribution.

Fatigue-life fitted values, a function of stress  $S_e$ , are defined as estimates of the median lifetime  $t_{0.50}(S_e)$ . Fatigue-strength fitted values, a function of the number of cycles  $N_e$ , are defined as estimates of the median strength  $x_{0.50}(N_e)$ . Because of the equivalence of fatigue-life and fatigue-strength quantile curves (as shown in Sections D.1 and D.4 of the Appendix), the functions  $t_{0.50}(S_e)$  and  $x_{0.50}(N_e)$  map out the same curve. For reasons described in Section H.2.5, it is better to plot residuals versus fatigue-life fitted values rather than fatigue-strength fitted values.

**Example 4.1 Residual Analysis for the Laminate Panel Box–Cox/Loglinear- $\sigma_N$   $S$ - $N$  Model.**

This is a continuation of Example 2.2 where the Box–Cox/loglinear- $\sigma_N$   $S$ - $N$  model was fit to the laminate panel data. Figure 10a is a plot of the lifetime residuals versus stress, showing one column of

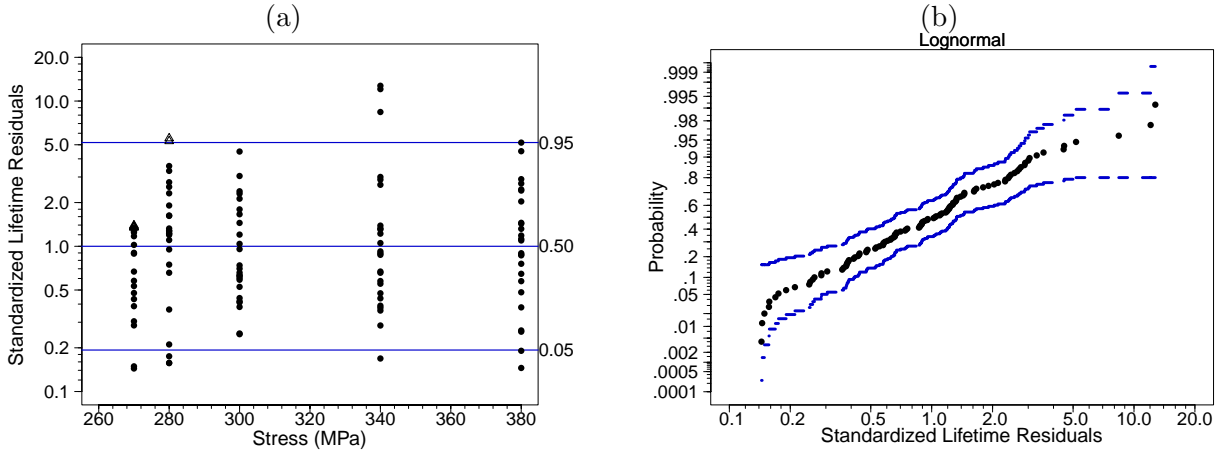


Figure 10: Fatigue-life residuals from the Box–Cox/Loglinear- $\sigma_N$   $S$ - $N$  model fit to the laminate panel data versus stress (a) and lognormal probability plot (b).

residuals for each of the five stress levels. The horizontal lines are estimates of the 0.05, 0.50, and 0.95 quantiles of the distribution of the standardized fatigue-life residuals on the antilog scale. The residuals for stress levels between 280 and 380 have similar distributions, indicating that there is no evidence of model inadequacy. There were eight runouts at  $S = 270$  MPa and this is the reason that column is so short. ■

## 4.4 Tolerance Bounds Versus Credible/Confidence Intervals for Quantiles

After an  $S$ - $N$  model has been chosen and fit to the available data, the results are used by engineers in different ways. For many applications, estimates and confidence intervals for lower-tail quantiles of the fatigue-life distribution (at given  $S_e$ ) and/or the fatigue-strength distribution (at given  $N_e$ ) are of particular interest.

In some parts of the  $S$ - $N$  data modeling literature, there is discussion of lower one-sided tolerance bounds of the fatigue-life and/or the fatigue-strength distributions, which are sometimes called one-sided tolerance intervals (intervals, by definition, have two endpoints and having an infinite endpoint does not help explanation or understanding). As described in [Meeker et al. \(2017, Section 2.4.2\)](#), a one-sided lower  $100(1 - \alpha)\%$  confidence bound on the  $p$  quantile of a distribution is equivalent to a one-sided lower tolerance bound that one can claim, with  $100(1 - \alpha)\%$  confidence, is exceeded by at least a proportion  $1 - p$  of that distribution. In our pedagogical experience, engineers and other practitioners often confuse the  $100(1 - \alpha)\%$  confidence level with the  $1 - p$  exceedance probability of a tolerance bound but that the concept of a small- $p$  lower-tail quantile is easier to separate from the confidence level.

It is common to report (and most statistical software packages only provide) two-sided confidence intervals for specified quantiles. Note that the lower endpoint of a two-sided  $100(1 - \alpha)\%$  confidence interval can be interpreted as a one-sided lower  $100(1 - \alpha/2)\%$  confidence bound (e.g., the endpoints of a two-sided 90% confidence interval are one-sided 95% confidence bounds). A two-sided interval on a quantile, relative to a one-sided bound, provides more information. For a quantile in the lower tail of a fatigue-life or a fatigue-strength distribution, the lower bound tells how bad things might be; the upper bound tells *how good things might be*.

The relationship between one-sided confidence (credible) bounds and two-sided intervals presumes that the procedures provide, at least approximately, equal error probabilities for each tail and this is the reason that percentile credible intervals are recommended (as opposed to highest posterior density) and that simulation-based confidence intervals (e.g., Chapters 13 and 14 in [Meeker et al., 2017](#)) should calibrate each endpoint separately.

## 5 Other $S$ - $N$ Regression Relationships and Modeling Examples

Section 2 introduced three, relatively simple,  $S$ - $N$  regression relationships. Many other such relationships have been suggested. This section, while not exhaustive, describes several other  $S$ - $N$  relationships, illustrates how they fit within our modular framework, and illustrates the use of two of these relationships with the Ti64 and nitinol data that were introduced in Section 1.3.

### 5.1 Physical Explanation of the Curvature and Nonconstant Spread in $S$ - $N$ Data

Figures 3a and 4a are examples of  $S$ - $N$  data with strong curvature when plotted on log-log axes. Materials will exhibit this curvature differently depending on the damage accumulation mechanisms that are activated by cyclic loading. Curvature in the  $S$ - $N$  curve demonstrates that the rate of damage accumulated per cycle has a strong dependence on the magnitude of the load amplitude. Curvature will be greatest at load levels where the material transitions between micro-mechanical deformation regimes. A well documented example of this phenomena is the transition between elasto-plastic and

purely elastic deformation in high-strength metallic materials. The  $S$ - $N$  relationship tends to be approximately linear (on log-log scales) when cycling is causing cyclic elasto-plastic deformation, but as one moves to lower stress levels, the deformation becomes purely elastic leading to much longer life and this results in the concave-up curvature.

As noted in Section 3.2.3 (also see Example 2.1 and Figure 7) when the  $S$ - $N$  relationship is linear on log-log axes (i.e., the Basquin relationship) with  $\sigma_X$  not depending on  $N_e$ , the induced fatigue-life distribution will belong to the same family as the fatigue-strength distribution and will have constant spread. When, however, the  $S$ - $N$  relationship has the usual concave-up curvature described in the previous paragraph, the induced fatigue-life distribution will have increasing spread as stress decreases. Technical details for this result are given in Section D.2. This behavior will be illustrated in Examples 5.1 and 5.2 (and corresponding Figures 11 and 13).

## 5.2 The Modified Bastenaire $S$ - $N$ Relationship

The original Bastenaire (1972) relationship is

$$N = g(S; \beta) = \frac{A \exp[-C(S - E)]}{S - E}, \quad S > E.$$

As illustrated in Figure 6b, this model has been modified (e.g., in ISO, 2012; Hauteville et al., 2022) to have more flexibility by adding a fourth parameter giving

$$N = g(S; \beta) = \frac{A \exp\left(-\left[\frac{S - E}{B}\right]^C\right)}{S - E}, \quad S > E.$$

## 5.3 The Nishijima $S$ - $N$ Hyperbola Relationship

The Nishijima  $S$ - $N$  relationship (Nishijima, 1980, 1985), illustrated in Figure 6c, is

$$[\log(S) - E][\log(S) + A \log(N) - B] = C.$$

where the regression parameters are  $\beta = (A, B, C, E)$ . The parameters  $A$  and  $B$  are, respectively, the negative of the slope and the  $\log(N) = 0$  intercept of the large- $S$  oblique asymptote (sometimes called the plastic-zone asymptote);  $E$  is the horizontal asymptote;  $\sqrt{C}$  is the vertical distance between the  $S$ - $N$  curve and the point where the two asymptotes intersect (all on the log-log scales of the Figure 6c plot). For purposes of specifying a fatigue-strength model that can be used to induce a fatigue-life model, the relationship can be expressed as

$$S = h(N; \beta) = \exp\left(\frac{-A \log(N) + B + E + \sqrt{[A \log(N) - (B - E)]^2 + 4C}}{2}\right). \quad (24)$$

**Example 5.1 Fitting the Nishijima/Lognormal Model to the Ti64  $S$ - $N$  Data.** This example is a continuation of Example 1.2. A description of the noninformative/weakly informative joint prior distribution that was used, additional residual plots, and other details are in Section H.2. The Nishijima  $S$ - $N$  relationship (24) was fit to the data under the assumption that fatigue strength has a lognormal distribution with a constant shape parameter  $\sigma_X$ . The induced fatigue-life model

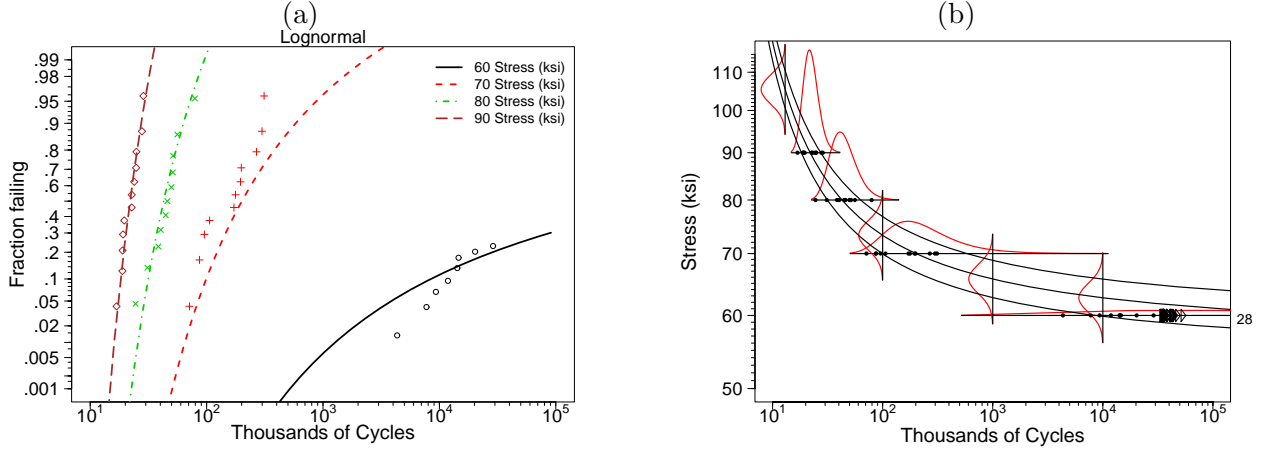


Figure 11: Lognormal probability plot showing the fatigue-life cdf estimates from the Nishijima model fit to the Ti64  $S$ - $N$  Data (a) and the corresponding model plot showing 0.10, 0.50, and 0.90 quantile curves and densities for fatigue strength (vertical) and fatigue life (horizontal) (b).

(Section 3.2.4) was used to define the log-likelihood in (22). Figure 11a is a lognormal probability plot showing, as symbols, the nonparametric estimate of fraction failing as a function of cycles and the corresponding regression-model estimates. The agreement is good. The early failures at 60 ksi deviate from the regression-model estimate but given the large amount of variability in small order statistics, this kind of deviation is consistent with the fitted model. As described in Section 3.2.4, the induced fatigue-life cdf (18) will level off to  $\Phi_{\text{norm}}([\log(S_e) - \hat{E}]/\hat{\sigma}_X)$  for large values of  $t$ . The marginal posterior distribution of this probability at 60 ksi has a median of 0.9754 and results in a 95% credible interval [0.708, 0.9997]. Figure 11b shows the fitted model superimposed on the same data in Figure 3a. Note the vertical fatigue-strength densities with constant  $\hat{\sigma}_X = 0.0362$  and the horizontal induced fatigue-life densities with increasing spread at lower stress levels. Figure 14a plots

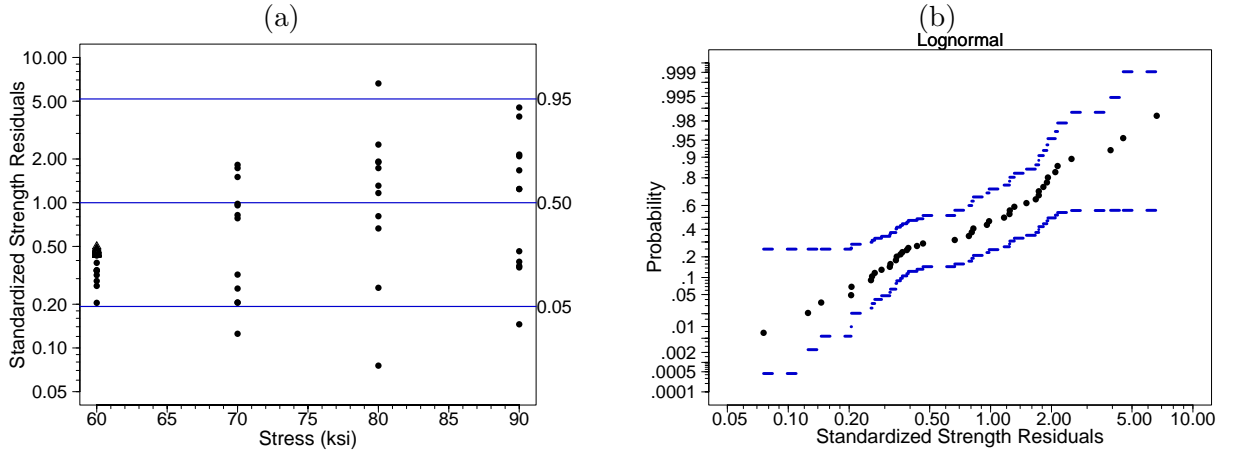


Figure 12: Fatigue-strength residuals from the Nishijima  $S$ - $N$  model fit to the Ti64 data versus stress (a) and lognormal probability plot (b).

the standardized residuals of the fatigue-strength distribution computed from (23) versus Stress. The horizontal lines are estimates of the 0.05, 0.50, and 0.95 quantiles of the distribution of the standardized fatigue-strength residuals on the antilog scale. Figure 12b is a lognormal probability plot of the same residuals. Figure 12 does not suggest departures from the assumed model (note that there are

## 5.4 The Rectangular Hyperbola $S$ - $N$ Relationship

The rectangular hyperbola (RH)  $S$ - $N$  relationship can be written as

$$[\log(N) - B][\log(S) - E] = C,$$

where  $B$  is a vertical asymptote,  $E$  is a horizontal asymptote, and  $C$  controls how fast the  $S$ - $N$  curve approaches the respective asymptotes. All of these parameters are defined on the log-log scales that are used in this paper to display  $S$ - $N$  relationships. Figures 9 and 16d illustrates this relationship. For purposes of specifying a fatigue-strength model that can be used to induce a fatigue-life model and likelihood, the relationship can be expressed as

$$S = h(N; \beta) = \exp \left[ \frac{C}{\log(N) - B} + E \right].$$

The RH model is a limiting case of the Nishijima model that arises as the plastic-zone slope approaches being vertical, as described in Liu and Meeker (2024, Section 5.6). Model features that arise from the asymptotes depend on whether the fatigue-life model is specified (see Sections 2.4.2 and 2.4.3) or the fatigue-strength model is specified (see Sections 3.2.4 and 3.2.5).

## 5.5 The Coffin–Manson Relationship

The Coffin–Manson relationship (e.g., pages 748–754 in Dowling, 2013) (also known as the generalized strain-life relationship) is widely used to model fatigue-life data in strain-controlled experiments (but can also be used to describe  $S$ - $N$  data from stress-controlled experiments). For this model, fatigue life  $N$  and applied stress  $S$  are related through the relationship

$$S = h(N; \beta) = A_{\text{el}}(2N)^b + A_{\text{pl}}(2N)^c. \quad (25)$$

This relationship is illustrated in Figure 6d. The terms  $A_{\text{el}}(2N)^b$  and  $A_{\text{pl}}(2N)^c$  represent separate Basquin relationships for the elastic and the plastic regimes. Here  $A_{\text{el}}$ ,  $A_{\text{pl}}$ ,  $b$ , and  $c$  are material-property parameters to be estimated from  $S$ - $N$  data. In particular,  $A_{\text{el}}$  and  $A_{\text{pl}}$  are the intercepts of the lines  $A_{\text{el}}(2N)^b$  and  $A_{\text{pl}}(2N)^c$ , respectively, when they are plotted on log-log axes;  $b$  and  $c$  are the corresponding slopes (note that the intercepts are defined as the value of stress at one half of a cycle when the response is in units of cycles). The sum of these lines provides a relationship with concave-up curvature commonly seen in  $S$ - $N$  data plotted on log-log scales.

**Example 5.2 Fitting the Coffin–Manson/Lognormal Model to the Superelastic Nitinol  $S$ - $N$  Data.** This example is a continuation of Example 1.3. A description of the noninformative joint prior distribution that was used, additional residual plots, and other details are in the Section H.3. The model fitting and likelihood construction and resulting plots are similar to those described in Example 5.1, except that the Coffin–Manson  $S$ - $N$  relationship  $S = h(N; \beta)$  is defined by (25) and, because there is neither a horizontal nor a vertical asymptote, the induced fatigue-life model is given by (17) in Section 3.2.3. Figure 13a is a lognormal probability plot similar to Figure 4b but with the

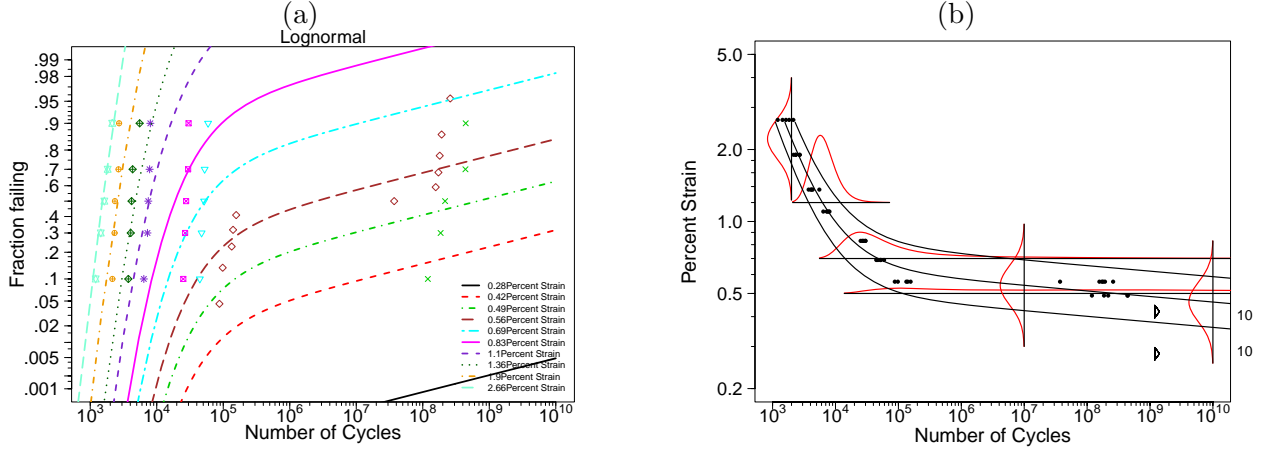


Figure 13: Lognormal probability plot showing the cdf estimates from the Coffin–Manson model fit to the nitinol  $S$ - $N$  Data (a) and the corresponding model plot showing 0.10, 0.50, and 0.90 quantile curves and densities for fatigue life (horizontal) and fatigue strength (vertical) (b).

Coffin–Manson/lognormal regression model cdf estimates plotted for the eight levels of strain. Interestingly, the upper tails of the plotted cdfs are linear, implying that the upper tail of the distributions behave like a lognormal distribution, in contrast to the horizontal asymptote in the Nishijima model illustrated in Figure 11a.

The bimodality at 0.56% strain stands out again and is highly influential, inflating the estimate of spread in the induced fatigue-life distributions at the lower levels of strain and leading to lack of fit at the lower levels of strain (i.e., below 0.56% strain). Weaver et al. (2023) fit a mixture model to these nitinol data to accommodate the bimodality. Consideration of such a model is beyond the scope of this paper but is mentioned as an area for future research in Section 6.

Figure 13b shows the same data as Figure 4a but now has the 0.10, 0.50, and 0.90 quantile lines and estimated densities superimposed. Engineers demonstrating the reliability of an artificial heart valve would typically be interested in the 0.10 quantile of the fatigue-strength distribution at 600 million cycles (15 years). For the nitinol data, the marginal posterior draws of the 0.10 quantile of the lognormal strength distribution at  $N_e = 600,000,000$  cycles is computed using (15) and these provide the point estimate 0.10223 and a 95% credible interval [0.0794, 0.128] in percent strain.

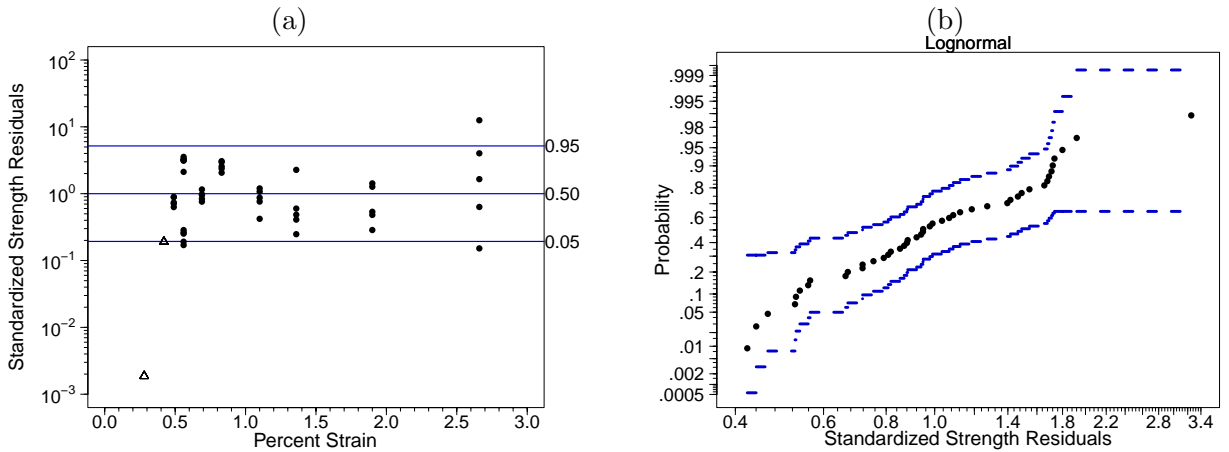


Figure 14: Fatigue-strength residuals from the Coffin–Manson  $S$ - $N$  model fit to the nitinol data versus strain (a) and lognormal probability plot (b).



Figure 14a plots the standardized residuals of the fatigue-strength distribution computed from (23) versus % strain. The bimodality can be seen in the two clusters of residuals at 0.56% strain. Other single clusters can be seen at 0.49, 0.69, and 0.83% strain. The small spread within these clusters suggests, in comparison with the overall spread in the residuals, that the residuals are not an iid sample. Such dependence could be due to lack of randomization with respect to factors like batch, test-machine effects, or the location of specimen wires cut from the spools. Figure 14b is a lognormal probability plot of the same residuals showing that the lognormal distribution fits well. ■

## 5.6 The Random Fatigue-Limit Model

Pascual and Meeker (1999) extended the Stromeyer model (Section 2.3.3) by allowing the fatigue-limit  $\gamma$  to vary from unit to unit. The Random Fatigue-Limit (RFL) model describes both the curvature and the increased variability at lower stress levels when plotting  $S$ - $N$  data on log-log scales.

### 5.6.1 The RFL fatigue-life model

For stress  $S_e$  conditional on a fixed value of  $\gamma > 0$ ,

$$F_{N|\gamma}(t; S_e|\gamma) = \Pr(N \leq t; S_e|\gamma) = \Phi\left(\frac{\log(t) - \mu(S_e, \gamma)}{\sigma_\epsilon}\right), \quad t > 0, S_e > 0,$$

where  $\Phi$  is the standard location-scale distribution cdf corresponding to the conditional log-location-scale distribution for  $N$  (i.e.,  $N|\gamma$ ) and  $\mu(S_e, \gamma) = \beta_0 + \beta_1 \log(S_e - \gamma)$ . Then the unconditional distribution of  $N$  is obtained by averaging over the distribution of  $\log(\gamma)$

$$F_N(t; S_e) = \Pr(N \leq t; S_e) = \int_{-\infty}^{\log(S_e)} \frac{1}{\sigma_{\log(\gamma)}} \Phi\left(\frac{\log(t) - \mu(S_e, \nu)}{\sigma_\epsilon}\right) \phi_\gamma\left(\frac{\nu - \mu_{\log(\gamma)}}{\sigma_{\log(\gamma)}}\right) d\nu, \quad t > 0, S_e > 0, \quad (26)$$

where  $\phi_\gamma$  is the standard location-scale distribution pdf corresponding to the log-location-scale distribution of  $\gamma$ , and the parameters of the model are  $\theta = (\beta_0, \beta_1, \sigma_\epsilon, \mu_{\log(\gamma)}, \sigma_{\log(\gamma)})$ . Pascual and Meeker (1999) illustrated the fitting of the RFL model for several data sets using all combinations of Weibull and lognormal distributions for  $N|\gamma$  and  $\gamma$ .

### 5.6.2 The RFL fatigue-strength model

As with other fatigue-life models for  $S$ - $N$  data, the RFL model can be used to define a distribution of fatigue strength  $X$  for a given value of  $N_e$ . Similar to what was done in Sections 2.4 and 3.2, replacing  $t$  with  $N_e$  and  $S_e$  with  $x$  in the integral of (26) gives

$$F_X(x; N_e) = \Pr(X \leq x; N_e) = \int_{-\infty}^{\log(x)} \frac{1}{\sigma_{\log(\gamma)}} \Phi\left(\frac{\log(N_e) - \mu(x, \nu)}{\sigma_\epsilon}\right) \phi_\gamma\left(\frac{\nu - \mu_{\log(\gamma)}}{\sigma_{\log(\gamma)}}\right) d\nu. \quad (27)$$

Interestingly, as  $N_e \rightarrow \infty$  in (27), the cdf in the integrand approaches one and the cdf of fatigue strength  $X$  approaches the cdf of the random fatigue-limit  $\gamma$ . There are no closed-form expressions for the quantiles of the RFL model fatigue-life or fatigue-strength distributions but they can be readily computed by numerically inverting the cdfs.



## 5.7 The Castillo et al. $S$ - $N$ Model

Castillo et al. (e.g., in [Castillo et al., 1985](#), [Castillo and Galambos, 1987](#), [Castillo et al., 2008](#), [Castillo and Fernández-Canteli, 2009](#), and Equation (2) of [Castillo et al., 2019](#)) suggest an  $S$ - $N$  model based on the rectangular hyperbola  $S$ - $N$  relationship and a three-parameter Weibull distribution given by

$$F(t, x) = 1 - \exp \left\{ - \left[ \frac{[\log(t) - B][\log(x) - E] - \gamma}{\eta} \right]^\beta \right\} \quad (28)$$

with parameters  $\theta = (B, E, \gamma, \eta, \beta)$  where  $B$  is a vertical asymptote for log fatigue life (i.e., minimum value for  $\log(N)$ ),  $E$  is a horizontal asymptote for log fatigue strength (i.e., a fatigue-limit and minimum value for  $\log(X)$ ), and  $\gamma$ ,  $\eta$ , and  $\beta$  are related to the Weibull distribution parameters. Their model derives from a compatibility condition implying that the fatigue-life and the fatigue-strength quantile curves coincide, as described for our (different) models in Section 2.4.4.

Replacing  $x$  with  $S_e$ , (28) can be interpreted as the cdf for fatigue life  $N$  at a given level of stress  $S_e$ . That is,

$$\begin{aligned} F_N(t; S_e) &= \Pr(N \leq t; S_e) = F(t, S_e) \\ &= 1 - \exp \left\{ - \left[ \frac{[\log(t) - B][\log(S_e) - E] - \gamma}{\eta} \right]^\beta \right\}, \end{aligned}$$

where  $t > \exp(B + \gamma/[\log(S_e) - E])$  and  $S_e > \exp(E)$ . Similarly, replacing  $t$  with  $N_e$ , (28) can be interpreted as the cdf for fatigue strength  $X$  at a given number of cycles  $N_e$ . That is,

$$\begin{aligned} F_X(x; N_e) &= \Pr(X \leq x; N_e) = F(N_e, x) \\ &= 1 - \exp \left\{ - \left[ \frac{[\log(N_e) - B][\log(x) - E] - \gamma}{\eta} \right]^\beta \right\}, \end{aligned}$$

where  $x > \exp(E + \gamma/[\log(N_e) - B])$  and  $N_e > \exp(B)$ . Expressions for the Weibull parameters, quantile functions for  $N$  and  $X$ , and a plot of the quantile curves are given in Section G.

## 5.8 A Comparison and Operational Considerations for Choosing an $S$ - $N$ Model

Table 1 provides a summary of several  $S$ - $N$  models that fit within our modular framework and that we have either used in our examples or that are commonly used in the fatigue literature. The table is not meant to be an exhaustive list, but a sample of the alternative models that are available. Broadly, there are two categories of models, depending on whether the fatigue-life or the fatigue-strength model is specified. Technically, any suitable  $S$ - $N$  relationship (such as those given in Sections 2.4, 2.3, and 5.2–5.5) could be used by specifying either the fatigue-life or the fatigue-strength model (and having the other be induced). The specification of Life or Strength given in the third column of Table 1 corresponds to the specification that we expect would be most useful given the properties of the resulting  $S$ - $N$  models and our experience with analyzing various  $S$ - $N$  data sets.

As part of our research, beyond the three examples presented in the paper, we fit the Basquin, Box–Cox/loglinear- $\sigma_N$ , Nishijima, Coffin–Manson, and RFL models to 18 different  $S$ - $N$  data sets (and other models to a smaller number of data sets) covering a wide range of materials, specimen types, and sample sizes. Based on those experiences and our knowledge of the nature of the different models,

Table 1: Summary of Selected Models for  $S$ - $N$  Data

Model	# Params	Model Specified for Fatigue	Vertical Asymptote for Large $S$	Horizontal Asymptote for Large $N$	Curvature and Nonconstant Spread
Basquin (inverse-power)	2+1=3	Life	No	No	No
Box–Cox/loglinear- $\sigma_N$	3+2=5	Life	Yes	No	Yes
Stromeyer/loglinear- $\sigma_N$	3+2=5	Life	No	Yes	Yes
Box–Cox	3+1=4	Strength	Yes	No	Yes
Stromeyer	3+1=4	Strength	No	Yes	Yes
Nishijima	4+1=5	Strength	No	Yes	Yes
Coffin–Manson	4+1=5	Strength	No	No	Yes
Bastenaire	3+1=4	Strength	No	Yes	Yes
Modified Bastenaire	4+1=5	Strength	No	Yes	Yes
Rectangular hyperbola	3+1=4	Strength	Yes	Yes	Yes
Castillo et al.	3+2=5	Both	Yes	Yes	Yes
Random fatigue-limit	3+2=5	Life	No	Yes	Yes

The number of parameters in the # Params column is the sum of the number of parameters in the  $S$ - $N$  relationship and those that describe variability in the statistical model.

the remainder of this section provides recommendations on how to choose which model or models to use in a particular situation (as in most statistical modeling applications, it is generally important to fit and compare different models).

Key features of the various models are the existence (or not) of coordinate (i.e., vertical or horizontal) asymptotes in the  $S$ - $N$  relationship and the way that variability (including changes in variability as a function of stress) is described. Figure 16 illustrates the fitting of four  $S$ - $N$  models, with different combinations of the existence of asymptotes or not, to a version of the nitinol data. Figure 17 provides corresponding plots of the residuals versus strain. Plots like these, for the many data sets, helped inform the following discussion.

### 5.8.1 Models with no coordinate asymptotes

Because of its simplicity, the Basquin (inverse-power rule) statistical model (Section 2.3.2 and Figure 7) is the most common model fit to  $S$ - $N$  data and it is appropriate when testing is done at relatively high stress levels (plastic range) where the relationship between log-life and log-stress is approximately linear with constant spread. Such tests are frequently conducted to compare fatigue-life distributions for factors such as different treatments, test conditions like temperature or frequency, formulations of product materials, or different mechanical designs. When units are tested at high stress levels to estimate fatigue-life at lower stress levels (accelerated testing), the Basquin model will provide conservative estimates of low-stress fatigue-life quantiles, relative to models that describe the concave-up curvature typically seen at low stress levels (e.g., Examples 19.11–19.14 in Meeker et al., 2022).

The Coffin–Manson relationship (Section 5.5 and Figure 6c) is appropriate when there is curvature in the  $S$ - $N$  data plotted on log-log axes but no evidence for the existence of a fatigue limit. When used with a specified fatigue-strength distribution with constant  $\sigma_X$  (as suggested in Falk (2019) and as we recommend), the model describes the increase in spread at lower stress levels.

### 5.8.2 Models with a horizontal asymptote

The Stromeier (Section 2.3.3), Bastenaire (Section 5.2 and Figure 6b), Nishijima (Section 5.3 and Figure 6d), and the Random fatigue-limit (Section 5.6)  $S$ - $N$  models all have a horizontal asymptote that suggests the possible existence of a fatigue limit. A fatigue limit does not have to exist to use these models, as long as the model fits well and there is no extrapolation in stress. In such cases, the model provides valid inferences for lower-tail quantiles of the fatigue-life and fatigue-strength distributions. For  $S$ - $N$  data with the common concave-up shape when plotted on log-log axes, we found the properties of the induced fatigue-life model (for a specified fatigue-strength model with constant  $\sigma_X$ ) have better agreement with physical reality (also see Section 3.2.4) when compared to a specified fatigue-life model.

### 5.8.3 Models with a vertical asymptote

The Box–Cox model (Section 2.3.4 and Figure 6a) has a vertical asymptote. The rectangular hyperbola model (Section 5.4 and Figure 16d) and the Castillo et al. model (Section 5.7 and Figure 21) have both vertical and horizontal asymptotes. The vertical asymptote is related to some interesting features of these models. First, the asymptote is related to the smallest number of cycles where a failure could occur, even as stress amplitude approaches infinity. Second (as noted, for example, in Section 4 of [Toasa Caiza and Ummenhofer, 2018](#)), the shape of the  $S$ - $N$  relationship does not agree with the most commonly seen behavior of  $S$ - $N$  data at higher stress levels. Finally, as shown in Figure 21, for small values of  $N_e$ , the spread in the induced distribution of fatigue strength  $X$  can increase dramatically. As described in Section 2.3.4, these issues are not of concern if this asymptotic behavior occurs outside the range where the model would be used (e.g., Figure 8b).

## 6 Concluding Remarks and Areas for Future Research

This paper outlines a modular framework for specifying, fitting, checking statistical models for  $S$ - $N$  fatigue data. The framework includes most of the  $S$ - $N$  relationships previously suggested in the fatigue literature. We illustrated the use of flexible Bayesian methods with noninformative or weakly informative prior distributions to estimate fatigue-life and fatigue-strength models. We illustrated the methods using  $S$ - $N$  data from three different materials and specimen types and described our experiences with many other data sets and types of materials.

When modeling  $S$ - $N$  data, how should one choose whether to specify the fatigue-life model (resulting in an induced fatigue-strength model) or specify a fatigue-strength model (resulting in an induced fatigue-life model)? When there is curvature in the  $S$ - $N$  relationship (which is common in HCF applications), given the manner in which it naturally describes increasing spread at lower stress levels (as explained in Section 5.1), and other reasons given in Section 3.2.1, we strongly favor the approach that specifies the fatigue-strength model (Examples 5.1 and 5.2). What reasons are there to continue to use the approach that specifies the fatigue-life model (Example 2.2)? It is traditional, widely known, and software is readily available. We see no other advantages.

The following are areas where further research is needed.

- There is a need to develop practical methods for designing statistically efficient experiments to obtain  $S$ - $N$ / $e$ - $N$  data (how many and which levels of stress, number of specimens, and how to

allocate them to stress levels). Although existing results for planning accelerated life tests (e.g., Chapter 6 in [Nelson, 2004](#)) may provide insight, there are important differences. Often there is no need to extrapolate in stress (although there may be extrapolation into the lower tails of both the fatigue-life and the fatigue-strength distributions). Depending on the application, inferences are generally needed for fatigue life over a range of stress values or fatigue-strength quantiles at particular points in time. Tools to quantify estimation precision for these quantities for proposed experimental designs are needed. [King et al. \(2016\)](#) describe such work for estimating fatigue-life distributions for a particular fatigue-life model. Their methods could be extended to focus on fatigue-strength distributions and other models.

- Our modeling has focused on experiments in which stress *amplitude* is the experimental variable. Mean stress (or equivalently, the min/max stress ratio), temperature, cycling frequency, and surface condition/treatments are additional factors that are often studied in fatigue experiments. For example, [Pascual \(2003\)](#) and [King et al. \(2016\)](#) illustrate the use of such multiple explanatory variable fatigue modeling. The models and methods presented in this paper can be readily extended to allow for such additional explanatory variables.
- In experimental studies, it is important to understand and take account of important sources of variability. In fatigue testing, batch-to-batch (also called heat-to-heat or blend-to-blend) variability can be importantly large. Traditionally, careful experimenters would test the same number of specimens from each heat at each stress level. This equally represents the heats across the stress levels. [Nelson \(1984\)](#) provides an example and shows how to assess, graphically, whether there is heat-to-heat variability. A more quantitative approach would be needed to assess statistical significance of suspected batch-to-batch variability and assess whether efforts to reduce variability are successful. The methods presented in this paper could be readily extended to model batch-to-batch variability, in a manner similar to that used in [Meeker et al. \(2022, Section 23.4\)](#) to describe batch-to-batch variability in an accelerated life test.
- We have seen numerous examples of  $S$ - $N$ / $e$ - $N$  data where there is a bimodal distribution of lifetimes (e.g., in the nitinol example presented here), usually at an intermediate level of stress. Various explanations have been suggested for this phenomenon. These include material defects (similar to multiple failure modes) and batch-to-batch variability. Appropriate models to describe such behavior need to be developed. [Weaver et al. \(2023\)](#) give an example of such a model.
- There is extensive existing knowledge of material properties. For example, [Dowling \(2013, page 751\)](#) provides a table containing nominal values for the parameters of the Coffin–Manson model for different materials. [MMPDS \(2021\)](#) contains a large amount of information about materials properties for different alloys that used in aerospace applications. This kind of information, combined with general engineering principles, could be used to help inform prior distributions for estimating the parameters of  $S$ - $N$  models.
- Statisticians (e.g., [Koenker, 2005](#)) have developed quantile regression methods that might be useful for the analysis of fatigue data. These methods do not require specification of a particular failure-time distribution and have been used effectively to model regression data with noncon-

stant spread. However, such methods require much larger sample sizes than the fully parametric modes that are traditionally used in fatigue data modeling.

## Acknowledgments

We would like to thank Charles Annis, Necip Doganaksoy, Woong Kim, Larry Leemis, Lu Lu, Wayne B. Nelson, Peter Parker, and an anonymous referee for providing helpful comments on an earlier version of our paper. We would also like to thank Professors Enrique Castillo and Alfonso Fernández-Canteli for helping us to understand some aspects of their approach to modeling fatigue data. Elena García-Sánchez provided much useful information and references to us explaining how manufacturers and regulators interact to assure aircraft safety.

## A Overview of the Materials in Appendices

The purpose of the appendix is to provide additional technical details including derivations, additional examples, simulation results, and other technical details. This appendix is organized as follows. Section B provides additional technical details (i.e., beyond what is in the main paper) for  $S$ - $N$  regression models where the fatigue-life model is specified and the fatigue-strength model is induced. Similarly, Section C provides additional technical details for  $S$ - $N$  regression models where the fatigue-strength model is specified and the fatigue-life model is induced. Section D provides proofs of some of the technical results stated in the main paper. Section E compares the different basic  $S$ - $N$  model shapes and illustrates the importance of using residual analysis to help compare and choose such an  $S$ - $N$  relationship. Section F compares lognormal and Weibull probability plots for nine  $S$ - $N$  data sets based on fatigue tests for nine different materials and specimen types. Section G provides, for the Castillo et al.  $S$ - $N$  model (described in Section 5.7), additional technical details and characteristics. Section H gives the prior distributions, numerical results and other details for the three data analysis/modeling examples in the paper.

## B Technical Details for $S$ - $N$ Regression Models Where the Fatigue-Life Model is Specified and the Fatigue-Strength Model is Induced

This section outlines additional technical details of specifying a fatigue-life model and using it to induce a fatigue-strength model.

### B.1 Basic $S$ - $N$ Relationships for $N = g(S; \beta)$ and General Assumptions

Here we consider  $S$ - $N$  relationships of the type

$$N = g(S; \beta), \tag{29}$$

where  $\beta$  is a vector of regression model parameters and  $g(x; \beta)$  satisfies the following general conditions:

- $g(x; \beta)$  is positive; that is  $g(x; \beta) > 0$  for  $0 < x < \infty$ .

- $g(x; \beta)$  is strictly decreasing in  $x$ .
- $g(x; \beta)$  is differentiable for all  $x$ .

There are potentially two asymptotes for  $\log[g(S; \beta)]$ : A horizontal asymptote at  $E = \log(S)$  and a vertical asymptote at  $B = \log(N)$ , as illustrated in Figure 21 for the case  $\exp(B) = \exp(E) = 1$ .

## B.2 The Specified Fatigue-Life Model

The random variable  $N$  is the observed number of cycles for a unit at stress amplitude  $S_e$ . Based on the  $S$ - $N$  relationship (29), taking logs, replacing  $S$  with  $S_e$  and adding an error term  $\epsilon$  gives

$$\log(N) = \log[g(S_e; \beta)] + \sigma_N \epsilon, \quad (30)$$

where  $\epsilon$  has a location-scale distribution with  $\mu = 0$  and  $\sigma = 1$ , and  $\sigma_N$  is constant. Thus the log-location-scale cdf  $F_N(t; S_e)$  for fatigue life  $N$  is

$$\begin{aligned} F_N(t; S_e) &= \Pr(N \leq t) = \Pr[\log(N) \leq \log(t)] \\ &= \Phi \left[ \frac{\log(t) - \log[g(S_e; \beta)]}{\sigma_N} \right], \quad t > 0, S_e > 0. \end{aligned} \quad (31)$$

This cdf has the standard properties of a cdf for a positive random variable. In particular,  $\lim_{t \downarrow 0} F_N(t; S_e) = 0$  and  $\lim_{t \rightarrow \infty} F_N(t; S_e) = 1$ .

Then the pdf of  $N$  is

$$\begin{aligned} f_N(t; S_e) &= \frac{d}{dt} F_N(t; S_e) \\ &= \frac{1}{t \sigma_N} \phi \left[ \frac{\log(t) - \log[g(S_e; \beta)]}{\sigma_N} \right], \quad t > 0. \end{aligned} \quad (32)$$

The quantiles of  $F_N(t; S_e)$  are the solution to  $F_N(t_p) = p$ . Using (31),

$$t_p = \exp[\log[g(S_e; \beta)] + \Phi^{-1}(p) \sigma_N], \quad 0 < p < 1, S_e > 0. \quad (33)$$

## B.3 Additional Results for Induced Fatigue-Strength Models

The induced fatigue-strength cdfs (and corresponding quantile functions) are described, in general terms, depending on whether the  $S$ - $N$  relationship has asymptotes or not, in Sections 2.4.1, 2.4.2, and 2.4.3 of the main paper. This section provides some additional, potentially useful, results not given there.

### B.3.1 The induced fatigue-strength cdf for the Basquin model

Example 2.1 in Section 2.4.1 of the main paper provides details on the induced fatigue-strength cdf for the Basquin model.

### B.3.2 The induced fatigue-strength cdf for the Stromeyer model

For the Stromeyer model (Section 2.3.3 of the main paper), the induced fatigue-strength cdf  $F_X(x; N_e)$  is obtained from (10) by using

$$\log[g(x; \boldsymbol{\beta})] = \beta_0 + \beta_1 \log(x - \gamma), \quad x > \gamma.$$

Note that (with  $\beta_1 < 0$ ) there is a horizontal asymptote at  $E = \log(\gamma)$  and thus  $\lim_{x \downarrow \gamma} [\beta_0 + \beta_1 \log(x - \gamma)] = \infty$ . This implies  $\lim_{x \downarrow \gamma} F_X(x; N_e) = 0$ , and thus  $\gamma$  is a threshold parameter for the fatigue-strength distribution, implying that fatigue strength  $X$  will never be less than  $\gamma$ .

To obtain the quantile function  $x_p(N_e)$  for  $N_e$ , use (11) in the main paper with

$$g^{-1}(w; \boldsymbol{\beta}) = \gamma + \exp\left[\frac{\log(w) - \beta_0}{\beta_1}\right]. \quad (34)$$

Because of the horizontal asymptote, as  $p \rightarrow 0$ ,  $x_p(N_e) \rightarrow \exp(E) = \gamma$  is a lower bound on the fatigue-life quantile.

### B.3.3 The induced fatigue-strength cdf for the Box–Cox model

For the Box–Cox model (Section 2.3.4), the induced fatigue-strength cdf  $F_X(x; N_e)$  is obtained from (10) by using

$$\log[g(x; \boldsymbol{\beta})] = \beta_0 + \beta_1 \nu(x; \lambda) = \begin{cases} \beta_0 + \beta_1 \left( \frac{x^\lambda - 1}{\lambda} \right) & \text{if } \lambda \neq 0 \\ \beta_0 + \beta_1 \log(x) & \text{if } \lambda = 0. \end{cases} \quad (35)$$

Because  $\lambda < 0$ ,  $-1/\lambda$  is an upper bound for  $\nu(X; \lambda)$  and thus

$$B = \lim_{x \rightarrow \infty} \log[g(x; \boldsymbol{\beta})] = \lim_{x \rightarrow \infty} \log[\beta_0 + \beta_1 \nu(x; \lambda)] = \beta_0 - \frac{\beta_1}{\lambda}$$

is a vertical asymptote. As described in Section 2.4.3, this vertical asymptote results in a discrete atom of probability of size

$$1 - \Phi\left(\frac{\log(N_e) - (\beta_0 - \beta_1/\lambda)}{\sigma_N}\right)$$

at  $\infty$ . This discrete atom corresponds to the limiting proportion of units for which  $N > N_e$  as  $x \rightarrow \infty$ . This can be interpreted as the (physically questionable) proportion of units that would survive  $N_e$  cycles, even as stress approaches  $\infty$ .

To obtain the quantile function  $x_p(N_e)$  at  $N_e$ , use (11) in the main paper with

$$g^{-1}(t; \boldsymbol{\beta}) = \left\{ 1 + \lambda \left[ \frac{\log(t) - \beta_0}{\beta_1} \right] \right\}^{1/\lambda}.$$

The quantiles are finite for  $0 < p < \Phi([\log(N_e) - (\beta_0 - \beta_1/\lambda)]/\sigma_N)$ .



## B.4 Expressions for the Induced Fatigue-Strength Model pdfs

The pdf corresponding to the fatigue-strength cdf (10) in the main paper for the random variable  $X$  (induced from a specified fatigue-life distribution in Section 2.4.1) is

$$f_X(x; N_e) = \frac{dF_X(x; N_e)}{dx} = \frac{1}{\sigma_N} \left| \frac{d}{dx} \log[g(x; \beta)] \right| \phi \left[ \frac{\log(N_e) - \log[g(x; \beta)]}{\sigma_N} \right]. \quad (36)$$

The expression for  $d \log[g(x; \beta)]/dx$  depends on the particular model being used. The following sections give  $g(x; \beta)$  for some models.

### B.4.1 Expression for the induced fatigue-strength pdf for the Basquin model

For the Basquin model, the fatigue-strength pdf can be obtained by substituting

$$\frac{d}{dx} \log[g(x; \beta)] = \frac{\beta_1}{x}, \quad x > 0,$$

into (36).

### B.4.2 Expression for the induced fatigue-strength pdf for the Stromeyer model

For the Stromeyer model (Section B.3.2), the fatigue-strength pdf can be obtained by substituting

$$\frac{d}{dx} \log[g(x; \beta)] = \frac{\beta_1}{x - \gamma}, \quad x > \gamma,$$

into (36). Because  $\gamma$  is a threshold parameter, the pdf is positive only when  $x > \gamma$ .

### B.4.3 Expression for the induced fatigue-strength pdf for the Box–Cox model

For the Box–Cox model (Section B.3.3), the fatigue-strength pdf can be obtained by substituting

$$\frac{d}{dx} \log[g(x; \beta)] = \frac{g'(x; \beta)}{g(x; \beta)} = \beta_1 x^{\lambda-1}, \quad x > 0,$$

into (36). Because of the discrete atom of probability at  $\infty$  (see Section 2.3.4 in the main paper), (36) will, in this case, integrate to

$$\Phi \left( \frac{\log(N_e) - (\beta_0 - \beta_1/\lambda)}{\sigma_N} \right).$$

## C Technical Details for $S$ - $N$ Regression Models Where the Fatigue-Strength Model is Specified and the Fatigue-Life Model is Induced

This section outlines additional technical details of specifying the fatigue-strength model and using it to induce a fatigue-life model.

## C.1 Basic $S$ - $N$ Relationships for $S = h(N; \beta)$ and General Assumptions

Here we consider  $S$ - $N$  relationships of the type

$$S = h(N; \beta), \quad (37)$$

where  $\beta$  is a vector of regression model parameters and  $h(t; \beta)$  satisfies the following general conditions:

- $h(t; \beta)$  is positive; that is  $h(t; \beta) > 0$  for  $0 < t < \infty$ .
- $h(t; \beta)$  is strictly decreasing in  $t$ .
- $h(t; \beta)$  is differentiable for all  $t$ .

There are potentially two asymptotes for  $\log[h(N; \beta)]$ : A horizontal asymptote at  $E = \log(S)$  and a vertical asymptote at  $B = \log(N)$ , as illustrated in Figure 21.

## C.2 Additional Motivation for Specifying the Fatigue-Strength Distribution

Section 3.2 of the main paper outlined the important advantages of specifying the fatigue-strength distribution in  $S$ - $N$  modeling. Because the variability in fatigue-strength  $X$  tends not to depend strongly on the number of cycles  $N_e$  one can, if there is curvature in the  $S$ - $N$  relationship, avoid having to include an additional model component to describe nonconstant  $\sigma_N$  as was done in Section 2.6 of the main paper. Figure 15 shows scatter plots for six high-cycle-fatigue (HCF) data sets. The data sets in Figure 15 were chosen because cycling was done at a large number of levels of stress/strain (in contrast to the three examples in the main paper). Having so many stress/strain levels allows us to see, empirically, the relatively constant variability in fatigue-strength as a function of cycles. This approximate constancy in the fatigue-strength distribution spread is in contrast to the often sizable increase in spread in fatigue-life distribution at lower stress/strain levels. Thus, model specification is simplified. Also, for the reasons given Section 5.1 of the main paper, we have observed, in many of the data sets that we have analyzed, that the *induced* fatigue-life model tends to nicely describe fatigue-life data.

An important advantage of specifying a fatigue-strength model in which the fatigue-strength distributions have

- a scale parameter that depends on the number of cycles  $N_e$  but
- a constant shape (i.e., shape and spread do not depend on the number of cycles  $N_e$ )

is that the fatigue-strength distributions and the induced fatigue life distributions meet compatibility condition (cdfs are non-decreasing and quantile lines for different levels of  $p$  are monotone decreasing and do not cross). Note that these compatibility conditions do not hold in all cases when one used a model component that allows the distribution shape to depend on stress, as in the loglinear- $\sigma_N$  model component described in Section 2.3.5 of the main paper and used in Example 2.2 with the laminate panel data.

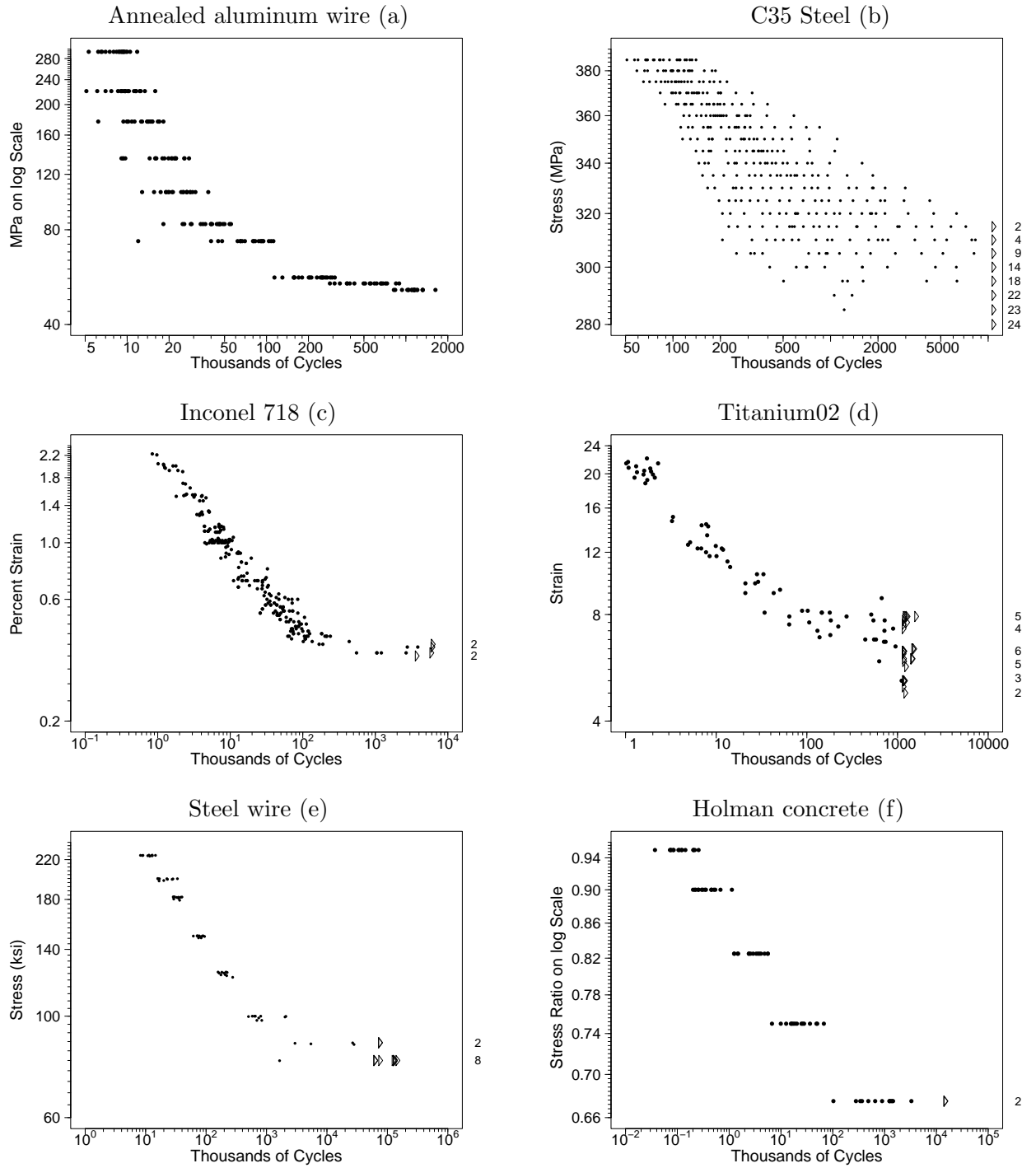


Figure 15: Scatterplots for the annealed aluminum wire (a), C35 steel (b), Inconel 718 (c), Titanium02 (d), steel wire (e), and Holman concrete (f)  $S-N$  data.

### C.3 The Specified Fatigue-Strength Distribution

The fatigue-strength random variable  $X$  is the (unobservable) lowest level of applied stress that would result in a failure at a given number of cycles  $N_e$  cycles. Based on the  $S$ - $N$  relationship (37), taking logs, replacing  $S$  with  $X$  and replacing  $N$  with  $N_e$ , and adding an error term  $\epsilon$  gives

$$\log(X) = \log[h(N_e; \boldsymbol{\beta})] + \sigma_X \epsilon, \quad (38)$$

where  $\epsilon$  has a location-scale distribution with  $\mu = 0$  and  $\sigma = 1$ , and  $\sigma_X$  is constant. Thus the log-location-scale cdf  $F_X(x; N_e)$  for strength  $X$  is

$$\begin{aligned} F_X(x; N_e) &= \Pr(X \leq x) = \Pr[\log(X) \leq \log(x)] \\ &= \Phi\left[\frac{\log(x) - \log[h(N_e; \boldsymbol{\beta})]}{\sigma_X}\right], \quad x > 0, \quad N_e > 0. \end{aligned} \quad (39)$$

This cdf has the standard properties of a cdf for a non-negative random variable. In particular,  $\lim_{x \downarrow 0} F_X(x; S_e) = 0$  and  $\lim_{x \rightarrow \infty} F_X(x; S_e) = 1$ .

### C.4 Additional Results for Induced Fatigue-Life Models

The induced fatigue-life cdfs (and corresponding quantile functions) are described, depending on whether the  $S$ - $N$  relationship has asymptotes or not, in Sections 3.2.3, 3.2.4, and 3.2.5 of the main paper. In this section we provide some additional results not given there.

#### C.4.1 The induced fatigue-life distribution for the Stromeyer model

The Stromeyer (Section 2.3.3)  $S$ - $N$  relationship is

$$N = \exp[\beta_0 + \beta_1 \log(S - \exp(E))]. \quad (40)$$

Solving for  $S$  gives

$$S = h(N; \boldsymbol{\beta}) = \exp(\gamma) + \exp\left(\frac{\log(N) - \beta_0}{\beta_1}\right), \quad (41)$$

where  $N > 0$  and  $\beta_1 < 0$ . Then the induced fatigue-life cdf  $F_N(t; S_e)$  is given by (17) in the main paper. The Stromeyer model has a horizontal asymptote at  $E = \log(\gamma) = \log(S)$  because with  $\beta_1 < 0$ ,

$$\lim_{t \rightarrow \infty} \log[h(t; \boldsymbol{\beta})] = \log\left[\gamma + \exp\left(\frac{t - \beta_0}{\beta_1}\right)\right] = \log(\gamma).$$

Thus, as noted in Section 3.2.4 of the main paper,  $F_N(t; S_e)$  has a discrete atom of probability at  $\infty$  equal to the value in (20).

To obtain the quantile function  $t_p(S_e)$  for  $N$ , use

$$h^{-1}(S) = \exp[\beta_0 + \beta_1 \log(S - \gamma)] \quad (42)$$

in (18) of the main paper but, as noted in Section 3.2.4, because of the discrete atom of probability at  $\infty$ ,  $t_p(S_e)$  is only finite for  $0 \leq p < \Phi[(\log(S_e) - \log(\gamma))/\sigma_X]$  and thus there is a limit, depending

on  $S_e$ , for the largest finite quantile.

#### C.4.2 The induced fatigue-life cdf for the Box–Cox model

The Box–Cox  $S$ - $N$  relationship is  $N = \exp[\beta_0 + \beta_1 \nu(S; \lambda)]$ , where

$$\nu(S; \lambda) = \begin{cases} \frac{S^\lambda - 1}{\lambda} & \text{if } \lambda \neq 0 \\ \log(S) & \text{if } \lambda = 0. \end{cases} \quad (43)$$

In fatigue applications,  $\beta_1 < 0$  and  $\lambda \leq 0$ . For  $\lambda < 0$ , solving for  $S$  in (43),

$$S = h(N; \beta) = \left[ 1 + \frac{\lambda}{\beta_1} [\log(N) - \beta_0] \right]^{1/\lambda}. \quad (44)$$

As described in Section 3.2.5 of the main paper, the induced fatigue-life cdf is given by (21). The Box–Cox model has a vertical asymptote at  $B = \beta_0 - \beta_1/\lambda$ , and this implies that  $N > \exp(\beta_0 - \beta_1/\lambda)$  and thus the cdf has a threshold parameter.

To obtain the quantile function  $t_p(S_e)$  for  $N$ , use

$$h^{-1}(S) = N = \exp[\beta_0 + \beta_1 \nu(S; \lambda)]$$

in (18) of the main paper. As noted in Section 3.2.5, because of the threshold parameter, the quantiles  $t_p(S_e)$  of  $F_N(t; S_e)$  are the same as (18) but as  $p \rightarrow 0$ ,  $t_p(S_e) \rightarrow \exp(\beta_0 - \beta_1/\lambda)$ . Thus the lower bound on the fatigue-life quantile is  $\exp(\beta_0 - \beta_1/\lambda)$ .

### C.5 Expressions for the Induced Fatigue-Life Model pdfs

The pdf of an induced fatigue-life random variable  $N$  is

$$f_N(t; S_e) = \frac{dF_N(t; S_e)}{dt} = \frac{1}{\sigma_X} \left| \frac{d}{dt} \log[h(t; \beta)] \right| \phi \left[ \frac{\log(S_e) - \log[h(t; \beta)]}{\sigma_X} \right]. \quad (45)$$

Expressions for  $d \log[h(t; \beta)]/dt$  depend on the particular  $h(t; \beta)$  relationship and are given for some models in the following subsections.

#### C.5.1 Expressions for the induced fatigue-life pdf for the Coffin–Manson model

For the Coffin–Manson model, following from (25) in the main paper and replacing  $N$  with  $t$  gives

$$S = h(t; \beta) = A_{el}(2t)^b + A_{pl}(2t)^c$$

and thus

$$h'(t; \beta) = d h(t; \beta)/dt = 2b A_{el}(2t)^{b-1} + 2c A_{pl}(2t)^{c-1}.$$

Then

$$\frac{d}{dt} \log[h(t; \beta)] = \frac{h'(t; \beta)}{h(t; \beta)} = \frac{2bA_{el}(2t)^{b-1} + 2cA_{pl}(2t)^{c-1}}{A_{el}(2t)^b + A_{pl}(2t)^c}.$$

This can be substituted into (45) to give the needed expression for the Coffin–Manson model pdf.

### C.5.2 Expressions for the induced fatigue-life pdf for the Nishijima relationship

For the Nishijima relationship, following from (24) replacing  $N$  with  $t$ , gives

$$S = h(t; \beta) = \exp\left(\frac{-A \log(t) + B + E + \sqrt{[A \log(t) - (B - E)]^2 + 4C}}{2}\right).$$

and thus

$$\begin{aligned} \frac{d \log[h(t; \beta)]}{dt} &= \frac{1}{2} \frac{d}{dt} \left[ -A \log(t) + B + E + \sqrt{[A \log(t) - (B - E)]^2 + 4C} \right] \\ &= \frac{A}{2t} \left[ -1 + \frac{A \log(t) - (B - E)}{\sqrt{[A \log(t) - (B - E)]^2 + 4C}} \right]. \end{aligned}$$

This can be substituted into (45) to give the needed expression for the Nishijima model pdf. Note that this pdf does not integrate to 1 due to the discrete atom of probability at  $t = \infty$  (see Section 3.2.4) given in (20).

### C.5.3 Expression for the induced fatigue-life pdf for the Stromeyer model

For the Stromeyer model,

$$\frac{d \log[h(t; \beta)]}{dt} = \left( \frac{1}{t \beta_1} \right) \frac{\exp\left(\frac{\log(t) - \beta_0}{\beta_1}\right)}{\gamma + \exp\left(\frac{\log(t) - \beta_0}{\beta_1}\right)}.$$

This can be substituted into (45) to give the needed expression for the Stromeyer fatigue-life pdf. Due to the discrete atom of probability at  $\infty$  (see Sections 3.2.4 and C.4.1), this pdf integrates to  $\Phi[(\log(S_e) - E)/\sigma_X] < 1$ .

### C.5.4 Expression for the induced fatigue-life pdf for the Box–Cox model

For the Box–Cox model,

$$\frac{d \log[h(t; \beta)]}{dt} = \left( \frac{1}{t \beta_1} \right) \frac{1}{1 + \frac{\lambda}{\beta_1} (\log(t) - \beta_0)}.$$

This can be substituted into (45) to give the needed expression for the pdf. Because of the threshold parameter, caused by the vertical asymptote in the  $S$ – $N$  relationship, noted in Sections 3.2.5 and B.3.3, this pdf is positive only when  $t > \exp(B) = \exp(\beta_0 - \beta_1/\lambda)$ .

## D Technical Details of Results Stated in the Main Paper

### D.1 Equivalence of Fatigue-Life and Fatigue-Strength Quantile Curves

Section 2.4.4 stated that, for  $S$ - $N$  relationships that have neither a horizontal nor a vertical asymptote, the fatigue-life and fatigue-strength models have the same quantile curves. Section D.1.1 proves that result and Section D.1.2 describes the behavior of the exceptional cases, for extreme values of  $p$ , when the  $S$ - $N$  relationship has one or two coordinate asymptotes.

#### D.1.1 Proof of the equivalence of fatigue-life and fatigue-strength quantile curves when there is neither a horizontal nor a vertical asymptote

Consider the quantile function for the specified fatigue-strength distribution in (15). Changing variable names  $x_p(N_e)$  to  $S_e$  and  $N_e$  to  $t_p(S_e)$  gives

$$S_e = \exp(\log[h(t_p(S_e); \beta)] + \Phi^{-1}(p)\sigma_X). \quad (46)$$

Solving (46) for  $t_p(S_e)$  gives

$$t_p(S_e) = h^{-1}(\exp[\log(S_e) - \Phi^{-1}(p)\sigma_X]; \beta),$$

which agrees with the quantile function for the induced fatigue-life model in (18), giving the needed result. There is a similar and parallel result showing the equivalence of the quantiles curves for a specified fatigue-life model and an induced fatigue-strength model.

#### D.1.2 The effect of coordinate asymptotes on the equivalence of fatigue-life and fatigue-strength quantile curves

This section describes the effect that coordinate asymptotes, when they exist, have on the behavior of quantile curves and the equivalence of fatigue-life and fatigue-strength quantile curves. For the *specified* fatigue-life and fatigue-strength distributions, the quantiles functions are defined for all values of  $0 < p < 1$ . This can be seen for a *specified* fatigue-life distribution by comparing (2) and (4) in Section 2.4 and for a *specified* fatigue-strength distribution by comparing (14) and (15) in Section 3.2.2 and noting that there are no restrictions on the error  $\epsilon$ .

If the  $S$ - $N$  relationship has a coordinate asymptote (horizontal or vertical or both), the behavior of the *induced* fatigue-strength and fatigue-life models have special characteristics. For situation where the fatigue-life model is specified, the top row of Table 2 summarizes detailed information given in Sections 2.4.2, 2.4.3, about the effect that coordinate asymptotes have on the *induced* fatigue-strength cdfs  $F_X(x; N_e)$  and the quantile functions  $x_p(N_e)$ . Similarly, for situation where the fatigue-strength model is specified, the bottom row of Table 2 summarizes detailed information given in 3.2.4, and 3.2.5 about the effect that coordinate asymptotes have on the *induced* fatigue-life cdfs  $F_N(t; S_e)$  and corresponding quantile functions  $t_p(S_e)$ .

The table illustrates an interesting duality. The following describes each of the four special cases outlined in Table 2.

- Following the development in Section 2.4.3 for an induced fatigue-strength model, because of the discrete atom of probability at infinity, for a given  $p$ , the quantile will be at infinity until



Table 2: Description of Quantile Function Behavior for Extreme Values of  $p$  for the Induced Fatigue Distributions when the  $S$ - $N$  Relationship Has One or Two Coordinate Asymptotes

Induced Distribution	Horizontal Asymptote $E$	Vertical Asymptote $B$
Fatigue Strength $X$ cdf $F_X(x; N_e)$ Quantile Function $x_p(N_e)$	Section 2.4.2 $\exp(E)$ is a threshold parameter for the induced fatigue-strength cdf $F_X(x; N_e)$ . Fatigue strength $X$ cannot be less than $\exp(E) > 0$ . As $p \rightarrow 0$ , $x_p(N_e) \rightarrow \exp(E)$ .	Section 2.4.3 The induced fatigue-strength cdf $F_X(x; N_e)$ has a discrete atom of probability of size $1 - \Phi\left(\frac{\log(N_e) - B}{\sigma_N}\right)$ at $\infty$ corresponding to the limiting probability that fatigue life $N$ is greater than $N_e$ when $x$ is large. Finite fatigue-strength quantiles exist only for $0 < p < \Phi\left(\frac{\log(N_e) - B}{\sigma_N}\right)$ .
Fatigue Life $N$ cdf $F_N(t; S_e)$ Quantile Function $t_p(S_e)$	Section 3.2.4 The induced fatigue-life cdf $F_N(x; S_e)$ has a discrete atom of probability of size $1 - \Phi\left(\frac{\log(S_e) - E}{\sigma_X}\right)$ at $\infty$ corresponding to the limiting probability that fatigue strength $X$ is greater than applied stress $S_e$ when $t$ is large. Finite fatigue-life quantiles exist only for $0 < p < \Phi\left(\frac{\log(S_e) - E}{\sigma_X}\right)$ .	Section 3.2.5 $\exp(B)$ is a threshold parameter for the induced fatigue-life cdf $F_N(t; S_e)$ . Fatigue life $N$ cannot be less than $\exp(B) > 0$ . As $p \rightarrow 0$ , $t_p(S_e) \rightarrow \exp(B)$ .

cycles level  $N_e = \exp[B + \Phi^{-1}(p)\sigma_N]$  after which it will follow (11) and the fatigue-life and fatigue-strength quantile curves will agree.

- Following the development in Section 3.2.4, for an induced fatigue-life model, because of the discrete atom of probability at infinity, for a given  $p$ , the quantile will be at infinity until stress level  $S_e = \exp[E + \Phi^{-1}(p)\sigma_X]$  after which it will follow (4) and the fatigue-life and fatigue-strength quantile curves will agree.
- Following the development in Sections 2.4.2 and 3.2.5 the induced cdfs have a threshold parameter. In either case, however, the quantile functions  $t_p(S_e)$  and  $x_p(N_e)$  map out the same curve (because one is the inverse function of the other, as shown by the proof in Section D.1.1) even though one of the quantile functions approaches the threshold parameter as  $p \rightarrow 0$ .

## D.2 Proof that Concave-up Curvature in the $S$ - $N$ Relationship Induces Fatigue-Life Distributions with Increasing Spread at Lower Stress Levels

Suppose that a fatigue-stress model with constant  $\sigma_X$  is specified and the induced fatigue-life model is as given in Section 3.2.3 of the main paper, resulting in a quantile function

$$\begin{aligned} t_p(S_e) &= h^{-1}(\exp[\log(S_e) - \Phi^{-1}(p)\sigma_X]) \\ &= g(\exp[\log(S_e) - \Phi^{-1}(p)\sigma_X]), \end{aligned} \quad (47)$$

which is the same as (18) in the main paper except here we suppress the dependency on the parameter vector  $\beta$  and introduce  $g(x)$  to simplify notation. Suppose  $t_p(S_e)$  is differentiable, decreasing, and strictly concave-up in  $\log(S_e)$ , the latter implying

$$\frac{\partial^2 \log[t_p(S_e)]}{\partial [\log(S_e)]^2} > 0. \quad (48)$$

Consider  $t_p(S_e) = g(w_p)$  where  $w_p = \exp[\log(S_e) - \Phi^{-1}(p)\sigma_X]$  can be interpreted as the *pseudo reverse* fatigue-strength  $p$  quantile (pseudo reverse because of the minus sign and that the center of the fatigue-strength distribution is taken to be  $S_e$ ), which then, according to (47), gets mapped, through the  $S$ - $N$  relationship  $g(x)$ , to the fatigue-life quantile  $t_p(S_e)$  at stress  $S_e$ .

First note that  $\partial w_p / \partial \log(S_e) = w_p$ . Using the chain rule, the first partial derivative with respect to  $\log(S_e)$ , is

$$\frac{\partial \log[t_p(S_e)]}{\partial \log(S_e)} = \frac{\partial \log[g(w_p)]}{\partial \log(S_e)} = \frac{\partial \log[g(w_p)]}{\partial w_p} \frac{\partial w_p}{\partial \log(S_e)} = \frac{g'(w_p) w_p}{g(w_p)}, \quad (49)$$

where  $g'(w_p) = dg(w_p)/dw_p$ . Using the result in (49) and the chain rule again, the second partial derivative with respect to  $\log(S_e)$  is

$$\begin{aligned} \frac{\partial^2 \log[t_p(S_e)]}{\partial [\log(S_e)]^2} &= \frac{\partial}{\partial \log(S_e)} \left[ \frac{g'(w_p) w_p}{g(w_p)} \right] = \frac{\partial}{\partial w_p} \left[ \frac{g'(w_p) w_p}{g(w_p)} \right] \frac{\partial w_p}{\partial \log(S_e)} \\ &= \frac{\partial}{\partial w_p} \left[ \frac{g'(w_p) w_p}{g(w_p)} \right] w_p = w_p \frac{\partial}{\partial w_p} \left[ \frac{g'(w_p) w_p}{g(w_p)} \right] \end{aligned} \quad (50)$$

which, from the concave-up property in (48), is positive. Then, because  $w_p$  is positive

$$\frac{\partial}{\partial w_p} \left[ \frac{g'(w_p) w_p}{g(w_p)} \right] > 0. \quad (51)$$

Using the result in (49) and the chain rule again, the second mixed partial derivative with respect to  $p$  is

$$\begin{aligned} \frac{\partial^2 \log[t_p(S_e)]}{\partial p \partial \log(S_e)} &= \frac{\partial}{\partial p} \left[ \frac{g'(w_p) w_p}{g(w_p)} \right] = \frac{\partial}{\partial w_p} \left[ \frac{g'(w_p) w_p}{g(w_p)} \right] \frac{\partial w_p}{\partial p} \\ &= \frac{\partial}{\partial w_p} \left[ \frac{g'(w_p) w_p}{g(w_p)} \right] \left[ -\frac{\sigma_X}{\phi[\Phi^{-1}(p)]} \right] w_p, \end{aligned} \quad (52)$$

where

$$\frac{\partial w_p}{\partial p} = \left[ -\frac{\sigma_X}{\phi[\Phi^{-1}(p)]} \right] w_p$$

and  $\phi(z) = d\Phi(z)/dz$ . Then, because  $\partial w_p/\partial p$  is negative and (51),

$$\frac{\partial^2 \log[t_p(S_e)]}{\partial p \partial \log(S_e)} < 0. \quad (53)$$

Now we show that the difference between two fatigue-life quantiles decreases when  $\log(S_e)$  increases. Consider  $0 < p_L < p_U < 1$ . The sign of the derivative in (53) implies that

$$\frac{\partial \log[t_{p_U}(S_e)]}{\partial \log(S_e)} < \frac{\partial \log[t_{p_L}(S_e)]}{\partial \log(S_e)}.$$

Equivalently,

$$\frac{\partial \log[t_{p_U}(S_e)]}{\partial \log(S_e)} - \frac{\partial \log[t_{p_L}(S_e)]}{\partial \log(S_e)} < 0. \quad (54)$$

Let  $\Delta[\log(t_p)] = \log[t_{p_U}(S_e)] - \log[t_{p_L}(S_e)]$  be the difference between the two fatigue-life quantiles on the log scale. Using (54), the derivative of the difference of the log-quantiles is

$$\begin{aligned} \frac{\partial \Delta[\log(t_p)]}{\partial \log(S_e)} &= \frac{\partial}{\partial \log(S_e)} (\log[t_{p_U}(S_e)] - \log[t_{p_L}(S_e)]) \\ &= \frac{\partial \log[t_{p_U}(S_e)]}{\partial \log(S_e)} - \frac{\partial \log[t_{p_L}(S_e)]}{\partial \log(S_e)} < 0. \end{aligned}$$

Consequently, the difference between the fatigue-life quantiles decreases when the stress increases which implies that the spread in the fatigue-life distribution increases when the stress decreases.

### D.3 A Generalization of Relationship between the Specified Fatigue-Strength Model and the Induced Fatigue-Life Model

This section generalizes the specify-fatigue-strength-model approach that we introduce in Section 3.2 of the main paper. Here we use a scale-shape parameter distribution as a basis for the specified fatigue-strength model. The scale parameter is controlled by the specified monotone decreasing  $S$ - $N$  relationship and the shape parameter(s) are constant. This model has the log-location-scale-based

model Section 3.2 as a special case but still satisfies compatibility conditions. For example, fatigue-strength and fatigue-life quantile curves are decreasing and do not cross or bend back; fatigue-strength and fatigue-life cdfs are non-decreasing.

### D.3.1 A statistical model for fatigue-strength

Suppose that the logarithm of the fatigue-strength random variable  $X$  at a *given* number of cycles  $N_e$  is

$$\log(X) = \log[h(N_e; \boldsymbol{\beta})] + \epsilon, \quad (55)$$

where  $S = h(N; \boldsymbol{\beta})$  is a positive monotonically decreasing  $S$ - $N$  regression relationship of known form,  $\boldsymbol{\beta}$  is a vector of regression parameters, and  $\epsilon$  is a random error such that the distribution of  $Z = \exp(\epsilon)$  is a standard cdf (i.e., a distribution with a scale parameter equal to 1) denoted by  $\Psi(z; \boldsymbol{\kappa})$  having one or more constant shape parameters in  $\boldsymbol{\kappa}$ .

Then for any given number of cycles  $N_e$ , fatigue strength  $X$  has the cdf

$$F_X(x; N_e) = \Pr(X \leq x; N_e) = \Pr[\log(X) \leq \log(x)] \quad (56)$$

$$= \Pr[(\log[h(N_e; \boldsymbol{\beta})] + \epsilon) \leq \log(x)] \quad (57)$$

$$= \Pr(\epsilon \leq \log(x) - \log[h(N_e; \boldsymbol{\beta})]) \quad (58)$$

$$= \Pr\left[\exp(\epsilon) \leq \frac{x}{h(N_e; \boldsymbol{\beta})}\right] \quad (59)$$

$$= \Psi\left(\frac{x}{h(N_e; \boldsymbol{\beta})}; \boldsymbol{\kappa}\right), \quad x > 0, N_e > 0, \quad (60)$$

where  $h(N_e; \boldsymbol{\beta})$  is a scale parameter and  $\boldsymbol{\kappa}$  contains one or more shape parameters of the distribution of  $X$ . Besides distributions in the log-location-scale family, this formulation allows distributions such as the Birnbaum-Saunders, gamma, and generalized gamma distributions (described, e.g., in Chapter 4 of Meeker et al., 2022).

The  $p$  quantile of the fatigue-strength random variable  $X$  is obtained by solving  $p = F_X[x_p(N_e); N_e]$  for  $x_p(N_e)$ , giving

$$x_p(N_e) = h(N_e; \boldsymbol{\beta}) \Psi^{-1}(p; \boldsymbol{\kappa}), \quad 0 < p < 1, N_e > 0. \quad (61)$$

### D.3.2 The induced fatigue-life model when $\log[h(N; \boldsymbol{\beta})]$ has neither a vertical nor a horizontal asymptote

For the moment, suppose that the positive monotonically decreasing  $S$ - $N$  relationship  $S = h(N; \boldsymbol{\beta})$  has neither a vertical nor a horizontal asymptote (e.g., the Basquin or Coffin–Manson  $S$ - $N$  relationship). In our model, based on the definitions of fatigue strength and fatigue life (described in Section 1.4.1), the random variables  $X$  and  $N$  share the same random-error term. Replacing  $N_e$  with  $N$  and  $X$  with  $S_e$  in (55) gives

$$\log(S_e) - \log[h(N; \boldsymbol{\beta})] = \epsilon. \quad (62)$$

In this role switching, fatigue life  $N$  at given  $S_e$  replaces fatigue strength  $X$  at given  $N_e$ , but the random variables  $X$  and  $N$  have the same  $\epsilon$  error term. Equation (62) implies that  $(\log(S_e) - \log[h(N; \beta)])$  has the same distribution as  $\epsilon$ . Thus the induced cdf of fatigue life  $N$  is

$$\begin{aligned}
F_N(t; S_e) &= \Pr(N \leq t; S_e) = \Pr[h(N; \beta) > h(t; \beta)] \\
&= \Pr(\log[h(N; \beta)] > \log[h(t; \beta)]) = \Pr(-\log[h(N; \beta)] < -\log[h(t; \beta)]) \\
&= \Pr((\log(S_e) - \log[h(N; \beta)]) < \log(S_e) - \log[h(t; \beta)]) \\
&= \Psi\left[\frac{S_e}{h(t; \beta)}; \kappa\right], \quad t > 0, S_e > 0.
\end{aligned} \tag{63}$$

The  $p$  quantile of the fatigue-life random variable  $N$  is obtained by solving  $p = F_N[t_p(S_e); S_e]$  for  $t_p(S_e)$ , giving

$$t_p(S_e) = h^{-1}\left(\frac{S_e}{\Psi^{-1}(p; \kappa)}; \beta\right), \quad 0 < p < 1, S_e > 0. \tag{64}$$

The fatigue-life density is  $f_N(t; S_e) = dF_N(t; S_e)/dt$  which can be computed from

$$\begin{aligned}
f_N(t; S_e) &= \frac{dF_N(t; S_e)}{dt} = \frac{\partial}{\partial t} \Psi\left[\frac{S_e}{h(t; \beta)}; \kappa\right] \\
&= \psi\left[\frac{S_e}{h(t; \beta)}; \kappa\right] \frac{\partial}{\partial t} \left[\frac{S_e}{h(t; \beta)}\right] \\
&= \psi\left[\frac{S_e}{h(t; \beta)}; \kappa\right] \left[\frac{S_e}{h^2(t; \beta)}\right] \left|\frac{\partial h(t; \beta)}{\partial t}\right|,
\end{aligned}$$

where  $\psi(z; \kappa) = d\Psi(z; \kappa)/dz$ .

### D.3.3 The induced fatigue-life model when $\log[h(N; \beta)]$ has a horizontal asymptote

When  $h(N; \beta)$  has a horizontal asymptote,  $\lim_{t \rightarrow \infty} h(N; \beta) = \exp(E) > 0$ . Then

$$\begin{aligned}
\lim_{t \rightarrow \infty} F_N(t; S_e) &= \lim_{t \rightarrow \infty} \Psi\left[\frac{S_e}{h(t; \beta)}; \kappa\right] \\
&= \Psi\left[\frac{S_e}{\exp(E)}; \kappa\right] < 1,
\end{aligned}$$

which implies that the cdf  $F_N(t; S_e)$  has a discrete atom of probability at  $\infty$ . The size of the discrete atom is

$$1 - \Psi\left(\frac{S_e}{\exp(E)}; \kappa\right).$$

### D.3.4 The induced fatigue-life model when $\log[h(N; \beta)]$ has a vertical asymptote

When there is a vertical asymptote, as  $t$  decreases toward  $\exp(B)$ ,  $h(t; \beta)$  is unbounded. Thus

$$\lim_{t \downarrow \exp(B)} F_N(t; S_e) = 0.$$

Consequently,  $\exp(B)$  is a threshold parameter.

#### D.4 Some History and an Alternative Way to View the Relationship among Fatigue-Strength cdfs, Fatigue-Life cdfs, and their Respective Quantile Functions

Early researchers studying and developing statistical modeling and methods for experimental fatigue data recognized the existence of and relationships among fatigue-strength cdfs, fatigue-life cdfs, and their respective quantile functions. As mentioned in Section 1.6 of the main paper, examples include [Freudenthal and Gumbel \(1956\)](#); [Weibull \(1956\)](#); [Armitage \(1961\)](#); [Bastenaire et al. \(1961\)](#), and [Castillo and Galambos \(1987\)](#). It appears, from the examples that they present in their publications, that much of the knowledge that early researchers obtained about proper methods for modeling fatigue data came from relatively large fatigue-life data sets that were obtained across numerous research projects (some of which are presented in Figure 15 and Figures 18–20). They made extensive use of  $N$  versus  $S$  scatter plots and probability plots (both Weibull and lognormal) based on nonparametric estimates of the fatigue-life distribution cdf (sometimes called plotting positions) at each level of stress used in the experiments. Observations about special features like curvature in  $S$ - $N$  plots and changes in distribution spread as a function of stress in probability plots were noted. However, the early work used notation and terminology somewhat different from what is in common use today.

The purpose of this section is to review some of those early ideas and link them to the more modern presentation in our paper. [Armitage \(1961\)](#) and [Bastenaire et al. \(1961\)](#) provide a nice summary of the work done in the 1950s and we will introduce some notation from the latter to help establish the links. [Bastenaire et al. \(1961\)](#), for example, say

$$\text{Probability of fracture} = F(S, N) \tag{65}$$

and in other works, the function is written as  $P(S, N)$  and has been called the “PSN function” or the “PSN field.” One difficulty with the  $P(S, N)$  and similar notation is that it can lead to confusion about what is random and what is fixed in the statistical model (although many of the early papers, e.g., [Weibull, 1956](#), did explicitly define notation for fatigue-life and fatigue-strength cdfs or corresponding survival functions).

To link this older notation to the more precisely specified parametric probability model and technical material in our paper and this appendix, suppose that  $P(u, v)$  is a function determined by the  $S$ - $N$  regression relationship and specified probability model for fatigue life (when the fatigue-life model is specified as in Section 2) or fatigue strength (when the fatigue-strength model is specified as in Section 3.2). The dummy argument  $u$  is associated with strain, stress or strength, depending on the context, and  $v$  is associated time (number of cycles).

For concreteness, we define  $P(u, v)$  according to the particular rather general probability model introduced in Section D.3.1 where  $S = h(N; \beta)$  is, for fixed  $\beta$ , a positive monotonically decreasing function of  $N$  that serves as an  $S$ - $N$  regression relationship and a scale parameter for the fatigue-strength random variable  $X$  while  $\Psi(z; \kappa)$  is the cdf of a random variable with a scale parameter equal to 1 and one or more constant shape parameters in  $\kappa$ . The idea behind this model is that the explanatory variable  $N_e$  changes the scale but not the shape of the strength distributions. One reason for this formulation is that all of the sometimes-desirable compatibility conditions (e.g., that quantile lines are decreasing and do not cross) will always hold. To simplify the presentation in the rest of this section we suppress the dependency of  $h(N; \beta)$  on  $\beta$  and the dependency of  $\Psi(z; \kappa)$  on  $\kappa$ .

Then the *specified* fatigue-strength cdf (56) can be written as

$$F_X(x; N_e) = \Pr(X \leq x; N_e) = P(x, N_e) = \Psi\left(\frac{x}{h(N_e)}\right), \quad x > 0, N_e > 0.$$

As in (61), the  $p$  quantile of the fatigue-strength random variable  $X$  is

$$x_p(N_e) = P_X^{-1}(p, N_e) = h(N_e) \Psi^{-1}(p), \quad 0 < p < 1, N_e > 0. \quad (66)$$

where  $P_X^{-1}(p, N_e)$  is the inverse of  $P(u, v)$  for the  $u$  argument.

By changing the names of the arguments in  $P(x, N_e)$ , as in Section D.3.2, the *induced* cdf of fatigue life  $N$  is

$$F_N(t; S_e) = \Pr(N \leq t; S_e) = P(S_e, t) = \Psi\left(\frac{S_e}{h(t)}\right), \quad t > 0, S_e > 0.$$

It is important to note that  $h(t)$  in this cdf is *not* a scale parameter for  $N$ ; instead it controls the shape and spread of the distribution of  $N$ . As in (64), the  $p$  quantile of the fatigue-life random variable  $N$  is

$$t_p(S_e) = P_N^{-1}(p, S_e) = h^{-1}\left(\frac{S_e}{\Psi^{-1}(p)}\right), \quad 0 < p < 1, S_e > 0. \quad (67)$$

where  $P_N^{-1}(p, S_e)$  is the inverse of  $P(u, v)$  for the  $v$  argument.

Now if one equates  $S_e$  to (66) and solves for  $N_e$ , the result is the same as (67). This establishes that the quantile curves for the fatigue-strength distribution are the same as those for the fatigue-life distribution.

Besides being technically interesting, the results in this section have practical value for the implementation of statistical methods for the analysis of fatigue data. In particular

- Once one has an algorithm to compute the fatigue-strength cdf (fatigue-life cdf), that same algorithm can be used to compute the fatigue-life cdf (fatigue-strength cdf) by just changing the definition of the arguments of the function.
- Corresponding pdfs will not have the same form, but can be obtained by differentiating the cdf by the appropriate argument (depending on which pdf is needed).
- The existence of closed-form expressions for the quantile functions depends whether closed-form expressions for the needed inverse functions are available or not. To make a plot of quantile curves, only one algorithm is required and if quantile estimates (and confidence/credible intervals) are needed and no close-for expression is available, simple root-finding methods can be used.

## E A Comparison of $S$ - $N$ Relationship Shapes and How to Choose the Best One

The existence of coordinate asymptotes is an important distinguishing characteristic for the  $S$ - $N$  relationships. Figure 16 shows the  $S$ - $N$  relationships for four of the models considered in the main paper for all four combinations of the existence of coordinate asymptotes.



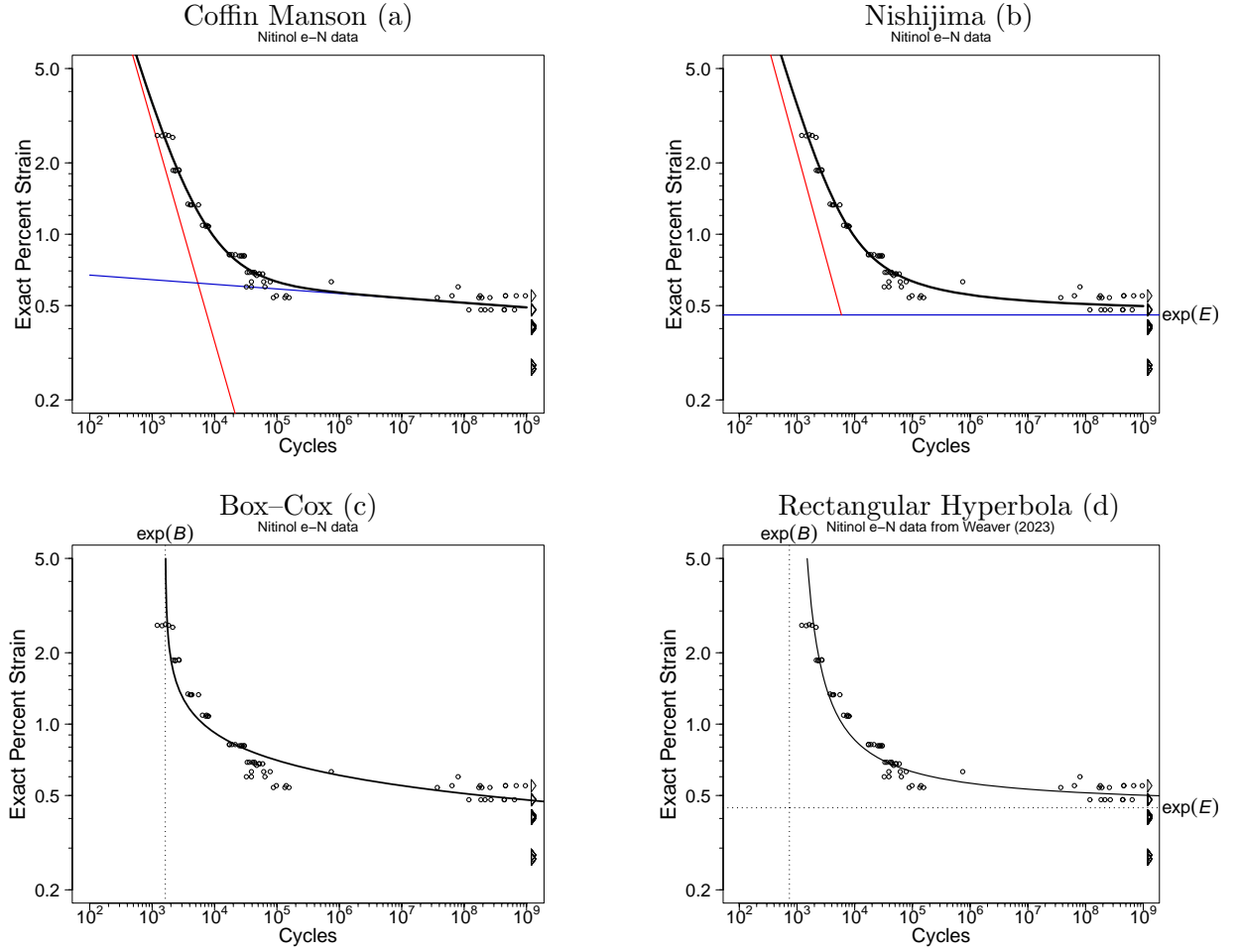


Figure 16: Median  $S-N$  estimates for models fit to the complete nitinol data for the Coffin–Manson relationship with *no coordinate asymptotes* (a); Nishijima relationship with a *horizontal asymptote* (b); Box–Cox relationship with a *vertical asymptote* (c); and a rectangular hyperbola relationship with *both horizontal and vertical asymptotes* (d).

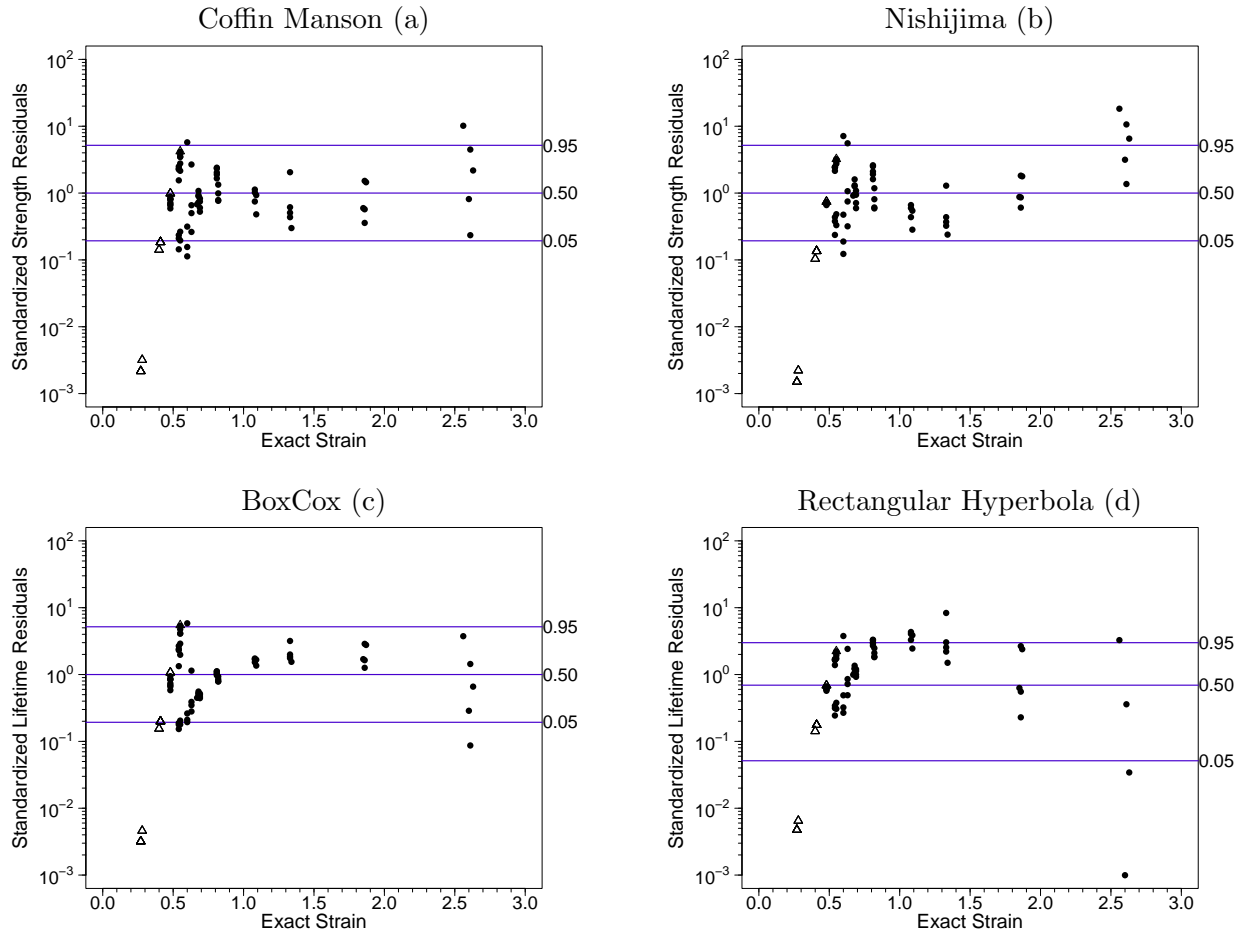


Figure 17: Residuals versus strain plots for models fit to the complete nitinol data: Coffin–Manson (a); Nishijima (b); Box–Cox (c); and rectangular hyperbola (d).

As described and illustrated in Section 4.3 and Examples 5.1 and 5.2 of the main paper, residual analysis is an important tool for statistical model building. Providing further compelling support for the use of residual analysis, Figure 16 shows the fitted median curve for four different  $S$ - $N$  models, fit to nitinol data used in Weaver et al. (2023) (including additional data taken at a different laboratory). There is some evidence of lack of fit for the Box–Cox model and to a lesser degree for the rectangular hyperbola model. The residuals versus strain plots in Figure 17 provide more complete and accurate information about the adequacy of the different models. In particular, there appears to be an upside-down-U pattern for the Box–Cox and to a lesser degree for the rectangular hyperbola models, perhaps caused by the steeply increasing (due to the vertical asymptote)  $S$ - $N$  curve in the high-strain region. The residual plots highlight the more subtle differences between the Coffin–Manson and Nishijima  $S$ - $N$  relationships. Taking into account the runouts, across different values of stress/strain the distribution of the residuals for the Coffin–Manson have empirical distributions that are more constant than those for the Nishijima model.

## F Examples Comparing Lognormal and Weibull Distributions Fit to $S$ - $N$ Data from Different Materials and Specimen Types

Figure 2 in the main paper compared the lognormal and Weibull multiple probability plots for the laminate panel  $S$ - $N$  data, showing that the lognormal distribution fit much better, as would be suggested by the cumulative damage failure mechanism (Section 2.5). Figures 18, 19, and 20 provide side-by-side comparisons of lognormal and Weibull multiple probability plots for nine additional  $S$ - $N$  data sets of various different materials and specimen types.

The three wire data sets in Figure 18 came from Freudenthal (1952). In Figure 19, the aluminum 6061-T6 data were used in Birnbaum and Saunders (1969). For this data set, the failure times larger than 1800 thousand cycles were converted to right censored observations at that point because the fit in the upper tail was bad (interest is focused on the lower tail and those upper-tail observation could bias lower-tail estimates). The C35 steel data came from tests of slightly notched specimens and were given in Maennig (1968). These data were subsequently analyzed in Castillo and Galambos (1987) and Castillo et al. (2019). The concrete  $S$ - $N$  data came from Holmen (1979, 1982) and were subsequently analyzed in Castillo and Hadi (1995), the rejoinder of Pascual and Meeker (1999), and Castillo et al. (2007).

In Figure 20, the 0.02 inch diameter nitinol wire rotating bend  $S$ - $N$  data are a subset of the data presented in Weaver et al. (2023) that were generated in the FDA laboratories. The  $S$ - $N$  data based on sharply notched specimens of 2024-T4 aluminum alloy specimens were given in Shimokawa and Hamaguchi (1979) but also analyzed in Shen (1994). The Ti64 data (same as used in Examples 1.2 and 5.1) have not appeared in any previous publication.

Among all nine comparisons, the Weibull distribution fit better or just as well as the lognormal only for the four tests on wire specimens. This is not surprising given the weakest-link nature of the fatigue-to-fracture mechanism in a wire. For the other five examples, the lognormal distribution generally provided a better fit across the different levels of stress or strain.

Note that these kinds of comparisons are convenient when fatigue tests are (as they often are) conducted by allocating a substantial number of test units to particular levels of stress so that separate nonparametric (and parametric) estimates can be computed at those levels of stress. In experiments where there is a large number of unique level of stress with few repeats such probability plots are not possible and distributional assessment has to be made on the basis of residual probability plots after finding a regression relationship that fits the data well, as described in Section 4.3 of the main paper and illustrated in Figures 10b, 12b, and 14b.

In Section 3.2.1 of the main paper and Section C.2 of this appendix, we provided strong motivation for and recommendations to specify the fatigue-strength model instead of the fatigue-life model. One might then question the value of probability plots of the fatigue-life distributions at the different test levels of stress, especially because the form of the induced life distributions will differ from the distributions of the specified fatigue-strength model when the  $S$ - $N$  relationship is nonlinear when plotted on log-log axes. As illustrated in Figures 11a and Figure 4a, especially at the higher levels of stress or strain (because the  $S$ - $N$  relationship is approximately linear when plotted on log-log axes), the shapes/spreads of the fatigue-strength and the fatigue-life distributions are similar.

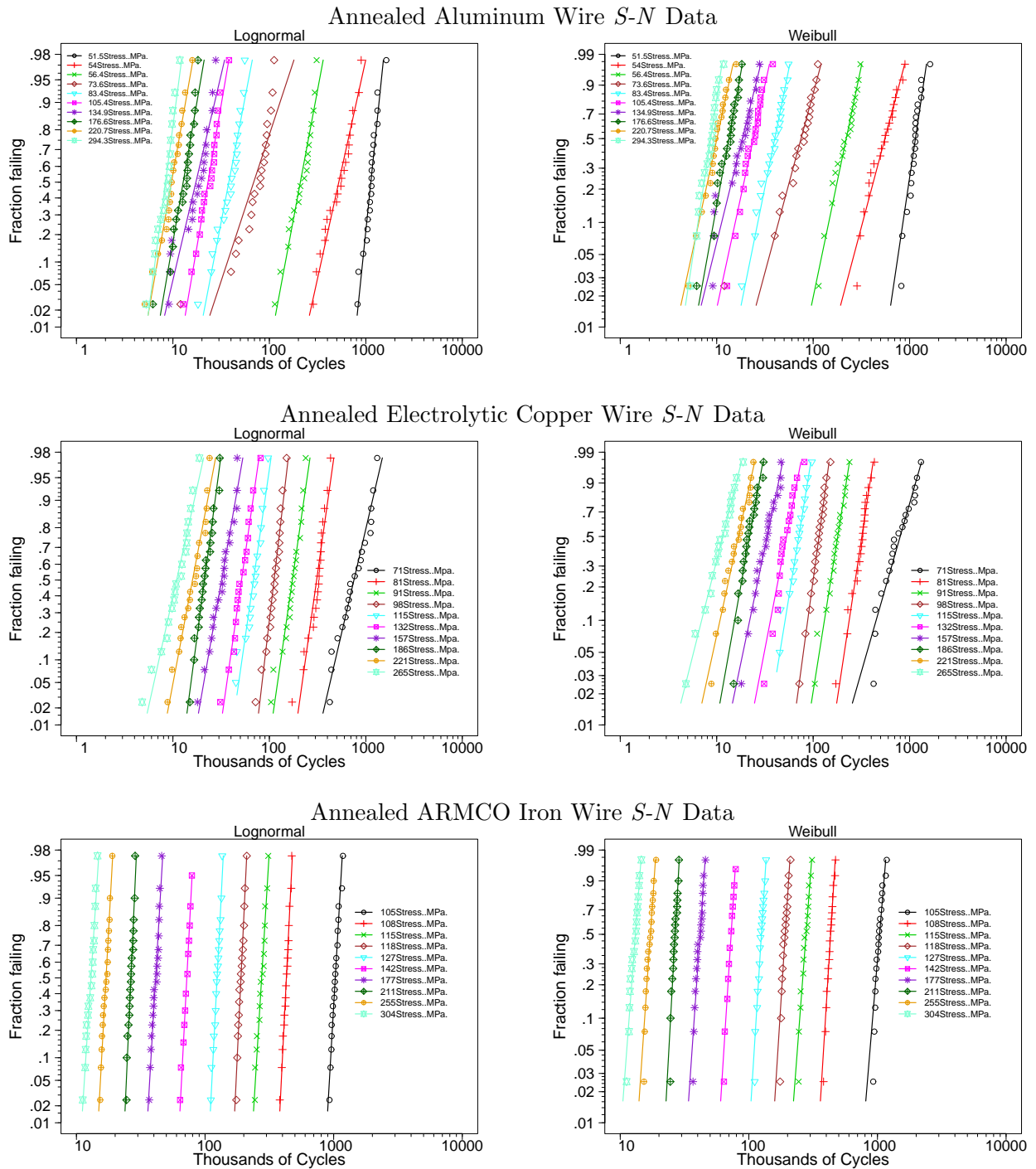


Figure 18: Comparison of lognormal (left) and Weibull (right) distribution probability plots for the annealed aluminum wire, annealed electrolytic copper wire, and annealed ARMCO iron wire  $S-N$  data.

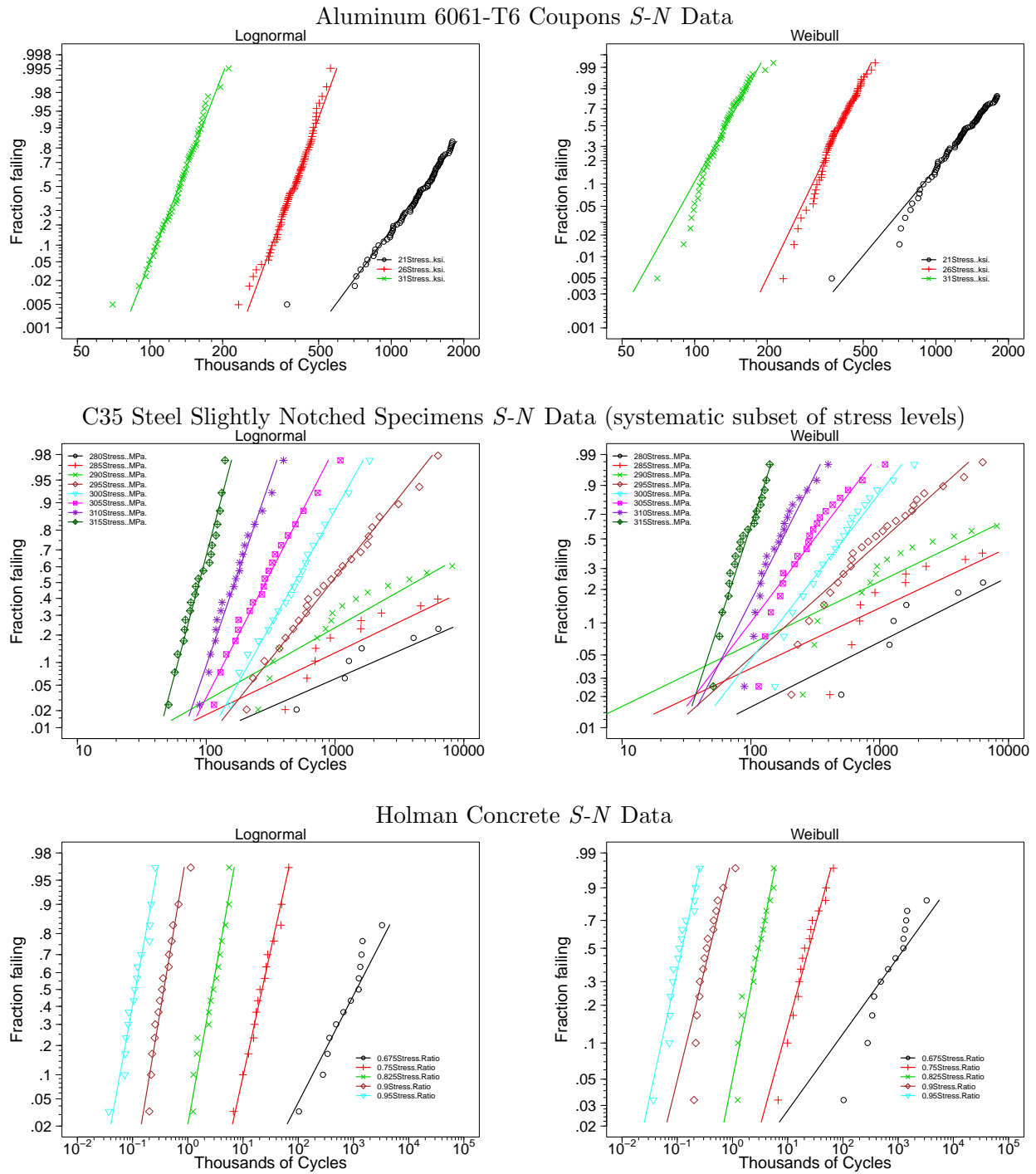


Figure 19: Comparison of lognormal (left) and Weibull (right) distribution probability plots for the aluminum 6061-T6 coupons, slightly notched C35 steel specimens, and the Holman concrete  $S-N$  data.

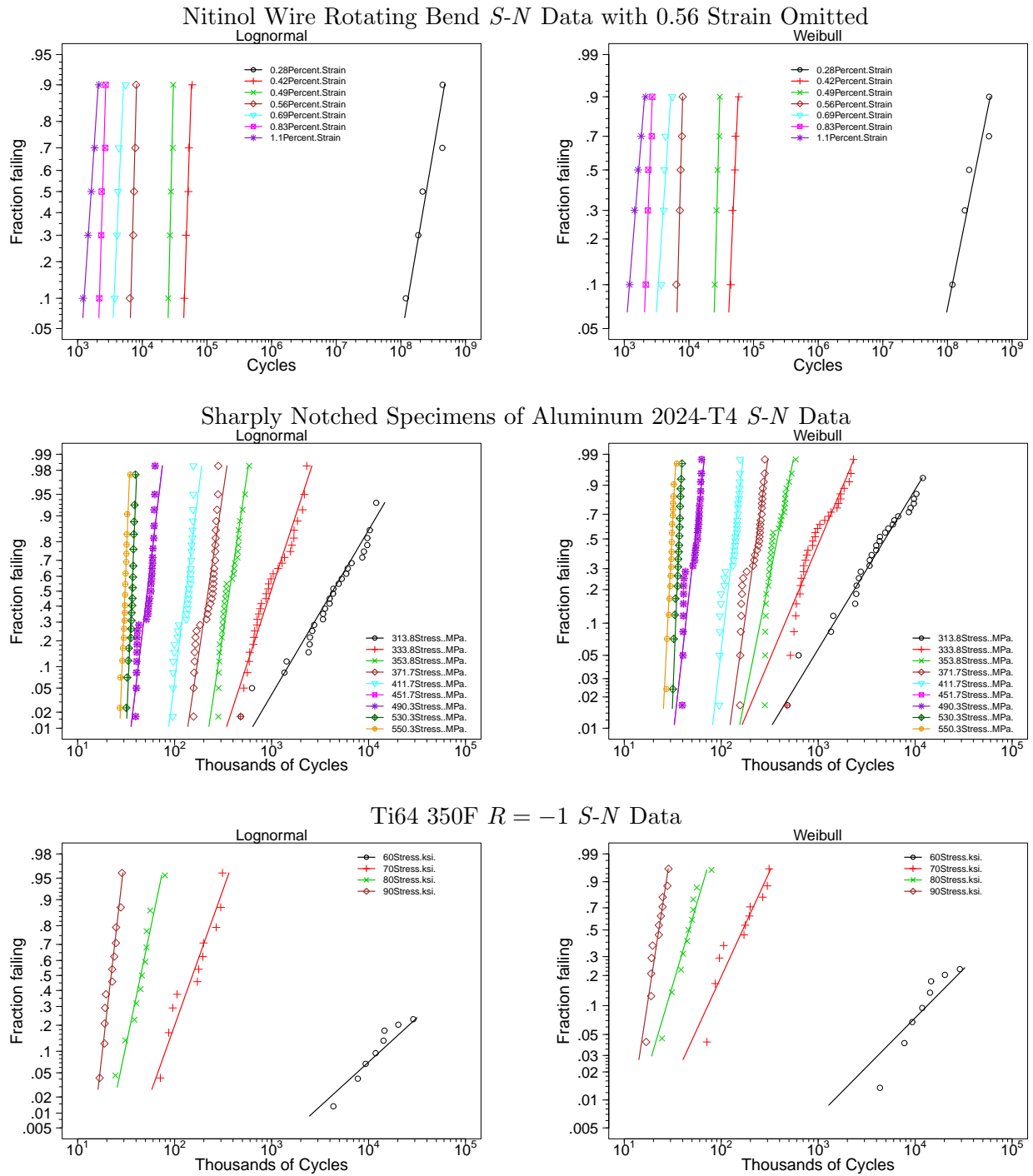


Figure 20: Comparison of lognormal (left) and Weibull (right) distribution probability plots for the nitinol wire rotating bend, sharply notched aluminum 2024-T4 Specimens, and the Ti64 350F  $R = -1$   $S-N$  data.

## G Further Explanation of the Castillo et al. $S$ - $N$ Model

This section provides additional technical details for the Castillo et al. model given in (28) and described in Section 5.7 of the main paper. In particular, we provide explicit expressions for the Weibull parameters and quantile functions for the fatigue life  $N$  and fatigue strength  $X$  random variables.

### G.1 The Distribution of Fatigue Life

In the main paper, we stated that by starting with (28) one can replace  $x$  with  $S_e$  and the result can be interpreted as the cdf for fatigue life  $N$  at a given level of stress  $S_e$ :

$$\begin{aligned} F_N(t; S_e) &= \Pr(N \leq t; S_e) = F(t, S_e) \\ &= 1 - \exp\left\{-\left[\frac{\log(t) - \gamma_N}{\eta_N}\right]^\beta\right\}, \quad t > \exp(\gamma_N), S_e > \exp(E) \end{aligned} \quad (68)$$

where  $\gamma_N = B + \gamma/[\log(S_e) - E]$  and  $\eta_N = \eta/[\log(S_e) - E]$ . Also, it can be shown that  $Y_N = \log(N)$  given  $S_e$  has a three-parameter Weibull distribution with scale parameter  $\eta_N$ , threshold parameter  $\gamma_N$ , and shape parameter  $\beta$ . Also,

$$W = \left(\frac{Y_N - \gamma_N}{\eta_N}\right)^\beta = \left(\frac{\log(N) - \gamma_N}{\eta_N}\right)^\beta$$

at a given  $S_e$  has an exponential distribution with scale parameter 1 or, equivalently, a two-parameter Weibull distribution with scale and shape parameters both equal to 1. Then

$$\epsilon = \log(W) = \log\left[\left(\frac{Y_N - \gamma_N}{\eta_N}\right)^\beta\right] = \log\left[\left(\frac{\log(N) - \gamma_N}{\eta_N}\right)^\beta\right] \quad (69)$$

has a smallest extreme value (Gumbel) distribution with location parameter  $\mu = 0$  and scale parameter  $\sigma = 1$ . Solving for  $N$  in (69) gives

$$N = \exp\left[\gamma_N + \eta_N[\exp(\epsilon)]^{1/\beta}\right] = \exp\left[\left(B + \frac{\gamma}{\log(S_e) - E}\right) + \left(\frac{\eta}{\log(S_e) - E}\right)[\exp(\epsilon)]^{1/\beta}\right]. \quad (70)$$

### G.2 Distribution of Fatigue Strength

In the main paper, we stated that by starting with (28) one can replace  $t$  with  $N_e$  and the result can be interpreted as the cdf for fatigue strength  $X$  at a given number of cycles  $N_e$ :

$$\begin{aligned} F_X(x; N_e) &= \Pr(X \leq x; N_e) = F(N_e, x) \\ &= 1 - \exp\left\{-\left[\frac{\log(x) - \gamma_X}{\eta_X}\right]^\beta\right\}, \quad x > \exp(\gamma_X), N_e > \exp(B) \end{aligned} \quad (71)$$

where  $\gamma_X = E + \gamma/[\log(N_e) - B]$  and  $\eta_X = \eta/[\log(N_e) - B]$ . Also, it can be shown that  $Y_X = \log(X)$ , the logarithm of fatigue strength given  $N_e$  has a three-parameter Weibull distribution with scale



parameter  $\eta_X$ , threshold parameter  $\gamma_X$ , and shape parameter  $\beta$ . Then, parallel to (69),

$$\epsilon = \log \left[ \left( \frac{Y_X - \gamma_X}{\eta_X} \right)^\beta \right] = \log \left[ \left( \frac{\log(X) - \gamma_X}{\eta_X} \right)^\beta \right] \quad (72)$$

has a standard smallest extreme value (Gumbel) distribution. Solving for  $X$  in (72) gives

$$X = \exp \left[ \gamma_X + \eta_X [\exp(\epsilon)]^{1/\beta} \right] = \exp \left[ \left( E + \frac{\gamma}{\log(N_e) - B} \right) + \left( \frac{\eta}{\log(N_e) - B} \right) [\exp(\epsilon)]^{1/\beta} \right]. \quad (73)$$

### G.3 Quantiles of the Fatigue-life and the Fatigue-Strength Distributions

The fatigue-life  $p$  quantile curve is obtained by setting  $p = F_N[t_p(S_e); S_e]$  in (68). Solving for  $t_p(S_e)$  gives

$$\begin{aligned} t_p(S_e) &= \exp \left[ \gamma_N + \eta_N [-\log(1-p)]^{1/\beta} \right] \\ &= \exp \left[ \left( B + \frac{\gamma}{\log(S_e) - E} \right) + \left( \frac{\eta}{\log(S_e) - E} \right) [-\log(1-p)]^{1/\beta} \right], \quad 0 < p < 1, S_e > \exp(E). \end{aligned}$$

Similarly, the fatigue-strength  $p$  quantile is obtained by setting  $p = F_X[x_p(N_e); N_e]$  in (71), from which  $x_p(N_e)$  is derived as

$$\begin{aligned} x_p(N_e) &= \exp \left[ \gamma_X + \eta_X [-\log(1-p)]^{1/\beta} \right] \\ &= \exp \left[ \left( E + \frac{\gamma}{\log(N_e) - B} \right) + \left( \frac{\eta}{\log(N_e) - B} \right) [-\log(1-p)]^{1/\beta} \right], \quad 0 < p < 1, N_e > \exp(B). \end{aligned}$$

### G.4 Comments

Observe that

- The error terms  $\epsilon$  for the random variables  $N$  in (70) and  $X$  in (73) have the same distribution and that either of these equations leads back to the cdfs derived from (28) in the main paper.
- Setting  $p = F[t_p(S_e), S_e]$  in (28) in the main paper leads to

$$[\log(t_p(S_e)) - B][\log(S_e) - E] = \gamma + \eta[-\log(1-p)]^{1/\beta}. \quad (74)$$

Analogously, setting  $p = F[N_e, x_p(N_e)]$  in (28) in the main paper leads to

$$[\log(N_e) - B][\log(x_p(N_e)) - E] = \gamma + \eta[-\log(1-p)]^{1/\beta}. \quad (75)$$

Equations (74) and (75) correspond to Equation (18) of Castillo et al. (1985) and the Castillo et al. (1985) model in Table A.21 on page 195 and Equation (A.26) on page 204 of Castillo and Fernández-Canteli (2009).

- The respective  $p$  quantiles of  $N$  and  $S$  coincide as illustrated in Figure 21. The right-hand side of (74) and (75) decreases as  $\gamma \rightarrow 0$  which implies that the  $p$  quantile curve moves closer to the vertical asymptote  $\exp(B)$  and horizontal asymptote  $\exp(E)$ .

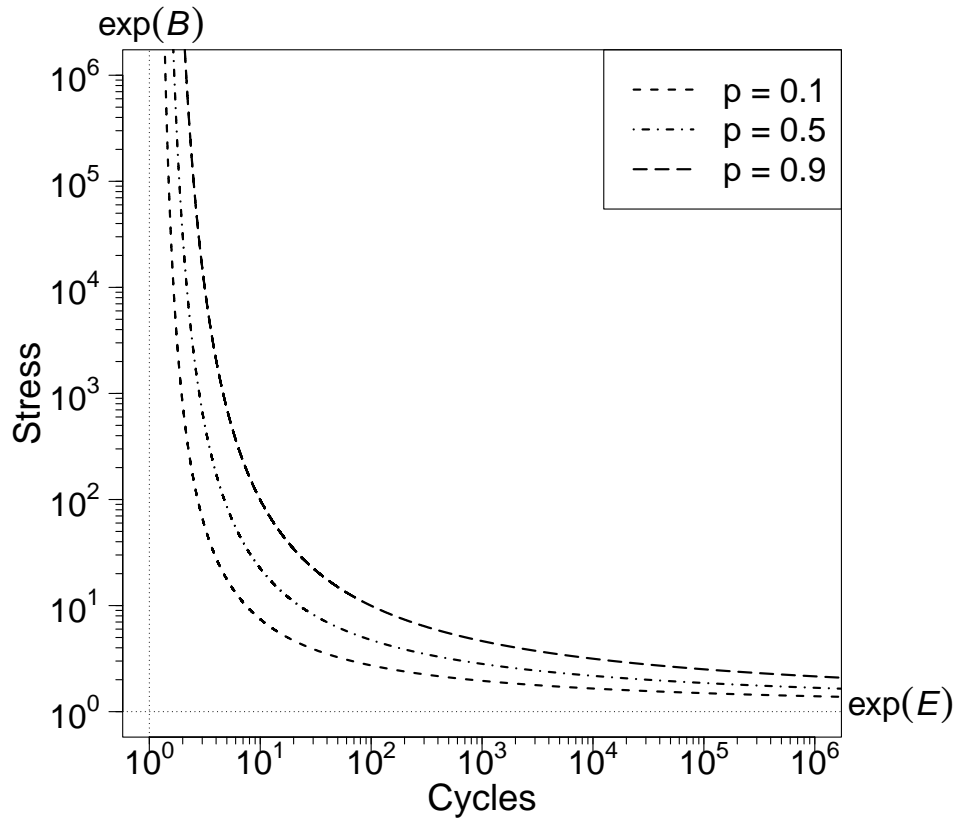


Figure 21: The 0.10, 0.50, and 0.90 quantile curves for the Castillo et al. rectangular-hyperbola Weibull  $S$ - $N$  model with  $\exp(E) = \exp(B) = 1$ ,  $\gamma = 3$ ,  $\beta = 2$ , and  $\eta = 5$ .

## H More Details from the Data Analysis/Modeling Examples

The data analysis/modeling examples in the main paper focus on the main features of the fitted models. To save space, less interesting, but potentially useful details are presented in this section.

### H.1 More Details for the Box–Cox/Loglinear- $\sigma_N$ $S$ - $N$ Model Fit to the Laminate Panel Data

Example 2.2 in the main paper gives a summary of the results of fitting the Box–Cox/loglinear- $\sigma_N$   $S$ - $N$  model to the laminate panel data. Note that in this example, the fatigue-life model is specified and the fatigue-strength model is induced.

#### H.1.1 Model and prior distributions

The lognormal distribution regression model fit to the laminate panel data was

$$\log(N/N_{\max}) = \mu(S) + \sigma(S)\epsilon,$$

where

$$\begin{aligned}\mu(S) &= \beta_0 + \beta_1 \nu(S/S_{\max}; \lambda) \\ \sigma(S) &= \beta_0^{[\sigma]} + \beta_1^{[\sigma]} \log(S/S_{\max}).\end{aligned}$$

$$\nu(S; \lambda) = \begin{cases} \frac{S^\lambda - 1}{\lambda} & \text{if } \lambda \neq 0 \\ \log(S) & \text{if } \lambda = 0, \end{cases}$$

is the Box–Cox power transformation, and  $\epsilon \sim \text{NORM}(0, 1)$ . Here stress  $S$  and number of cycles  $N$  were scaled for numerical reasons (as described in [Liu and Meeker, 2024](#)). The unknown traditional parameters (TPs) to be estimated from the data are  $\beta_0$ ,  $\beta_1$ ,  $\lambda$ ,  $\beta_0^{[\sigma]}$ , and  $\beta_1^{[\sigma]}$ .

As suggested in [Liu and Meeker \(2024, Section 6.2\)](#), the MCMC algorithm was run to generate posterior draws of the unrestricted stable parameters (USPs). The USPs are  $\lambda$  and

$$\begin{aligned}\log(\sigma_{\text{Low}}) &= \beta_0^{[\sigma]} + \beta_1^{[\sigma]} \log(S_{\text{High}}) \\ \log(\sigma_{\text{High}}) &= \beta_0^{[\sigma]} + \beta_1^{[\sigma]} \log(S_{\text{Low}}) \\ \log(t_{\text{Low}}) &= \beta_0 + \beta_1 \nu(S_{\text{High}}; \lambda) + \Phi^{-1}(0.50)\sigma_{\text{Low}} \\ \log(t_{\text{High}}) &= \beta_0 + \beta_1 \nu(S_{\text{Low}}; \lambda) + \Phi^{-1}(0.50)\sigma_{\text{High}}\end{aligned}$$

where  $S_{\text{Low}}$  and  $S_{\text{High}}$  are, respectively, the smallest and the largest levels of stress in the data where failures were observed.

The marginal prior distributions for the USPs  $\log(\sigma_{\text{Low}})$ ,  $\log(\sigma_{\text{High}})$ ,  $\lambda$ ,  $\log(t_{\text{Low}})$ , and  $\log(t_{\text{High}})$  were chosen to be flat. The resulting noninformative joint prior for the USPs results in Bayesian posterior estimates that are close to the ML estimates.

### H.1.2 Posterior draws and parameter estimates

The following table is a summary of the posterior draws for the USPs.

Inference for Stan model: BoxCoxLogLinSigma.

4 chains, each with iter=30000; warmup=5000; thin=5;

post-warmup draws per chain=5000, total post-warmup draws=20000.

	mean	se_mean	sd	2.5%	25%	50%	75%	97.5%	n_eff	Rhat
log_SigmaLow	-1.02	0	0.12	-1.25	-1.11	-1.03	-0.94	-0.77	19655	1
log_SigmaHigh	-0.48	0	0.11	-0.68	-0.55	-0.48	-0.41	-0.26	19668	1
lambda	-2.18	0	0.48	-3.14	-2.50	-2.17	-1.85	-1.24	19766	1
log_tLow	-5.73	0	0.07	-5.86	-5.77	-5.73	-5.68	-5.59	19385	1
log_tHigh	-0.20	0	0.11	-0.41	-0.28	-0.21	-0.13	0.01	19507	1

Figure 22a shows trace plots for the parameters (indicating good mixing) and Figure 22b the corresponding pairs plot.

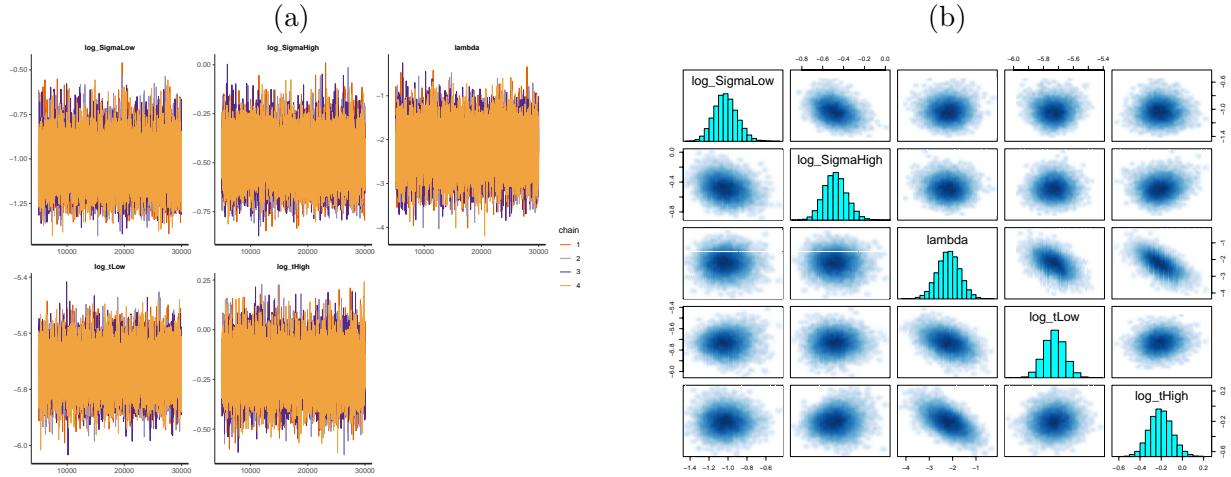


Figure 22: Trace plots (a) and a pairs plot (b) of the posterior draws for the Box-Cox/loglinear- $\sigma_N$  model fit to the laminate panel data.

The following table is a summary of the marginal posterior draws for the Traditional Parameters based on UnScaled data (TPUSs), computed as described in Liu and Meeker (2024, Sections 4.4 and 4.5).

Laminate Panel Test Data Lognormal distribution BoxCoxLogLinSigma model

Summary of the marginal posteriors for the

Traditional Parameters based on UnScaled data (TPUSs)

based on 20000 Stan draws

	2.5%	25%	50%	75%	97.5%
Beta0	7.09e+03	1.86e+05	1.12e+06	6.61e+06	2.12e+08
Beta1	-6.62e+08	-1.66e+07	-2.44e+06	-3.45e+05	-8.73e+03
lambda	-3.12e+00	-2.50e+00	-2.18e+00	-1.85e+00	-1.23e+00
Beta0.log.Sigma	2.18e+00	6.36e+00	8.48e+00	1.05e+01	1.46e+01
Beta1.log.Sigma	-2.67e+00	-1.96e+00	-1.60e+00	-1.23e+00	-5.03e-01

## H.2 More Details for the Nishijima/Lognormal $S$ - $N$ Model Fit to the Ti64 Data

### H.2.1 Comparison of lognormal and Weibull distributions

Figure 23 uses lognormal and Weibull probability plots to compare the two distributions fit to the Ti64 data. The lognormal distribution fits better. Although this example uses a specified fatigue-strength

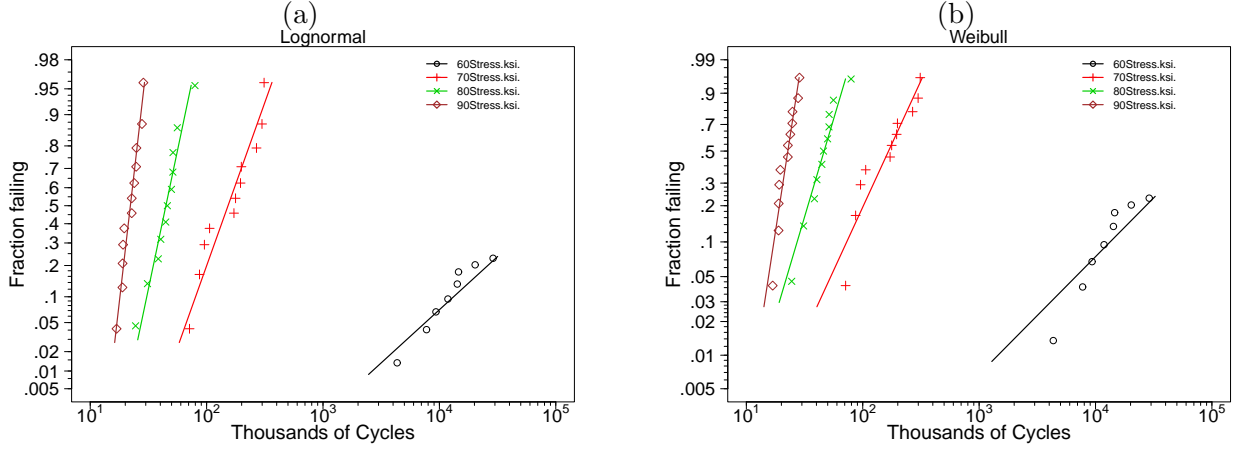


Figure 23: A comparison of lognormal (a) and Weibull (b) probability plots for the Ti64 data.

model, probability plots of the fatigue-life distributions are useful because the fatigue-life and fatigue-strength distributions have similar shapes along parts of the  $S$ - $N$  relationship that are approximately linear. The  $S$ - $N$  relationship is often approximately linear where stress levels are higher.

### H.2.2 Model and prior distributions

Example 5.1 in the main paper gives a summary of the results of fitting the Nishijima  $S$ - $N$  model to the Ti64 data. Note that in this example, the fatigue-strength model is specified and the fatigue-life model (providing the basis for the likelihood function) is induced. The lognormal distribution regression model for fatigue-strength  $X$  was

$$X = \log[h(N; \beta)] + \sigma_X \epsilon$$

where stress  $S$  and number of cycles  $N$  were scaled for numerical reasons (as described in Liu and Meeker (2024)), and  $\epsilon \sim \text{NORM}(0, 1)$ . Specifically,  $S/S_{\max}$  was substituted for  $S$  and  $N/N_{\max}$  was substituted for  $N$ . The Nishijima  $S$ - $N$  relationship is

$$S = h(N; \beta) = \exp\left(\frac{-A \log(N) + B + E + \sqrt{[A \log(N) - (B - E)]^2 + 4C}}{2}\right),$$

The unknown traditional parameters (TPs) to be estimated from the data are  $A$ ,  $B$ ,  $C$ ,  $E$ , and  $\sigma_X$ .

As suggested in Liu and Meeker (2024, Section 5.2), the MCMC algorithm was run to generate posterior draws of the unrestricted stable parameters (USPs). First we define three points on the  $S$ - $N$

curve

$$\begin{aligned} S_{\text{Low}} &= h(N_{\text{High}}; \beta) \\ S_{\text{Mid}} &= h(N_{\text{Mid}}; \beta) \\ S_{\text{High}} &= h(N_{\text{Low}}; \beta), \end{aligned}$$

where  $N_{\text{Low}}$  is the smallest value of  $N$  in the data,  $N_{\text{High}}$  is the largest value of  $N$  in the data that is a failure, and  $N_{\text{Mid}} = \exp[(\log(N_{\text{Low}}) + \log(N_{\text{High}}))/2]$ . Also,

$$\begin{aligned} \log(S_{\text{Mid-U}}) &= [\log(S_{\text{High}}) + \log(S_{\text{Low}})]/2 \\ \log(S_{\text{Mid-L}}) &= 2 \frac{[\log(S_{\text{Low}}) - E][\log(S_{\text{High}}) - E]}{\log(S_{\text{Low}}) + \log(S_{\text{High}}) - 2E} + E. \end{aligned}$$

Then, following [Liu and Meeker \(2024\)](#), the USPs are defined as

$$\begin{aligned} \log S_{\text{Low}} &= \log(S_{\text{Low}}) \\ \log \Delta_{\text{SHighSLow}} &= \log[\log(S_{\text{High}}) - \log(S_{\text{Low}})] \\ \text{qlogisp} &= \text{qlogis}(p) \\ \log \Delta_{\text{SLowE}} &= \log[\log(S_{\text{Low}}) - E] \\ \log \sigma_X &= \log(\sigma_X), \end{aligned}$$

where  $\text{qlogis} = \log[p/(1-p)]$  is the logit transformation and

$$p = \frac{\log(S_{\text{Mid-U}}) - \log(S_{\text{Mid}})}{\log(S_{\text{Mid-U}}) - \log(S_{\text{Mid-L}})}.$$

Marginal priors for the USPs  $\log S_{\text{Low}}$ ,  $\log \Delta_{\text{SHighSLow}}$ ,  $\log \Delta_{\text{SLowE}}$ , and  $\log \sigma_X$  were specified as flat. Attempting to use a flat prior on  $\text{qlogisp}$ , in addition, resulted in an improper posterior distribution. Figure 24 is a relative profile likelihood for  $\text{qlogisp}$ . The improper posterior results from the flatness of the relative profile likelihood for large values of  $\text{qlogisp}$ . As shown in [Liu and Meeker \(2024, Section 5.6\)](#) when  $\text{qlogisp} \rightarrow \infty$ , the Nishijima model approaches a rectangular hyperbola model and the relative profile likelihood indicates that the rectangular hyperbola model is also consistent with the data. This and the relative profile likelihood for  $\text{qlogisp}$  in Figure 24 suggest two alternative priors for  $\text{qlogisp}$  that will result in a proper posterior distribution:

- A weakly informative prior that does not allow  $\text{qlogisp}$  to be too large (large values of  $\text{qlogisp}$  cause numerical instability), effectively fitting the Nishijima model. The exact specification of the prior location is not critical (because inferences about distribution probabilities and quantiles will not be affected) as long as the lower tail covers small values of  $\text{qlogisp}$  where the profile relative likelihood is very close to zero and upper tail of the prior distribution is on the flat part of the profile relative likelihood for  $\text{qlogisp}$  so that  $\text{qlogisp}$  cannot be too large. We used a normal distribution with a 0.005 quantile of -10 and a 0.995 quantile of 10.
- An informative prior that constrains  $\text{qlogisp}$  to be a somewhat large value so that the fitted model is, essentially, a rectangular hyperbola model. Again, the exact values are not critical as long as the prior distribution is almost entirely on the flat part of the profile relative likelihood

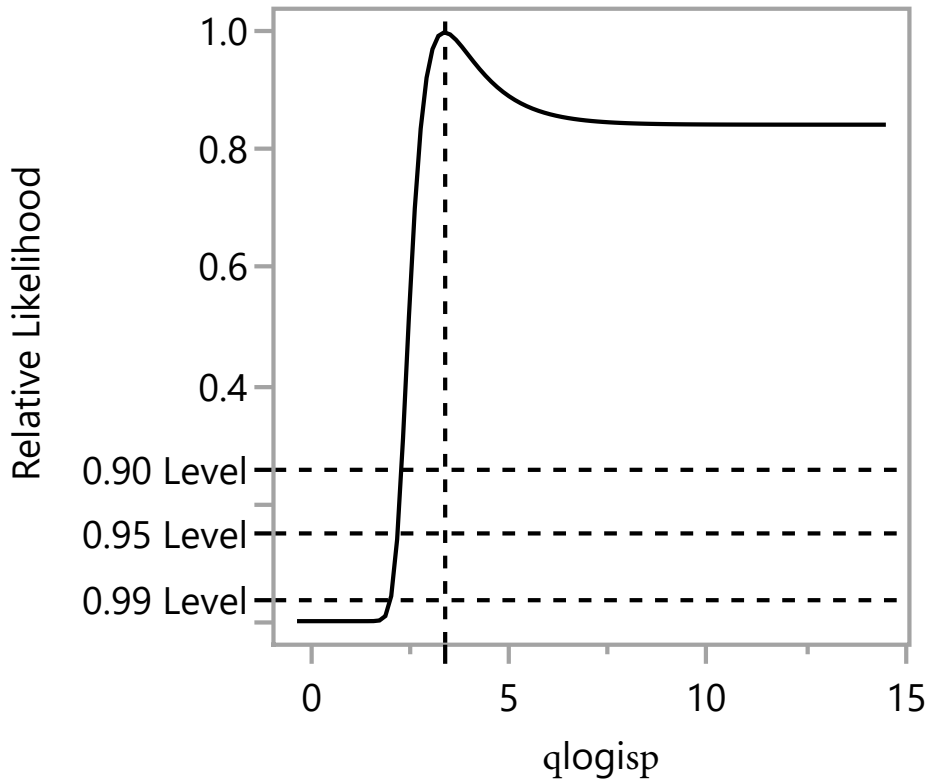


Figure 24: Relative profile likelihood for  $qlogisp$  for the Nishijima/Lognormal model fit to the Ti64 data.

for  $qlogisp$ . We used a normal distribution with a 0.005 quantile of 10 and a 0.995 quantile of 11.

We experimented with both alternatives and present summaries of both in the following two subsections. For estimation of lower-tail quantiles of the fatigue-life or the fatigue-strength distributions at lower levels of stress, the Nishijima model is conservative, relative to the Rectangular Hyperbola model. For this reason, the results we present in the main paper use the weakly informative prior that constrains  $qlogisp$  to effectively fit the Nishijima model.

### H.2.3 Posterior draws and parameter estimates for the weakly informative prior for $qlogisp$ (Nishijima model)

The following table is a summary of the posterior draws for the USPs.

Inference for Stan model: Nishijima.

4 chains, each with iter=30000; warmup=5000; thin=5;

post-warmup draws per chain=5000, total post-warmup draws=20000.

	mean	se_mean	sd	2.5%	25%	50%	75%	97.5%	n_eff	Rhat
log_SLow	-0.38	0.00	0.01	-0.39	-0.39	-0.38	-0.37	-0.36	19737	1
log_DeltaSHighSLow	-0.81	0.00	0.04	-0.89	-0.84	-0.81	-0.79	-0.74	19593	1
qlogisp	4.89	0.01	1.74	2.35	3.50	4.64	6.02	8.76	18714	1
log_DeltaSLowEhyp	-2.36	0.00	0.22	-2.93	-2.46	-2.32	-2.21	-2.03	17796	1

log_sigma_error	-3.31	0.00	0.11	-3.52	-3.39	-3.32	-3.24	-3.08	19478	1
sigma_error	0.04	0.00	0.00	0.03	0.03	0.04	0.04	0.05	19456	1
lp__	215.28	0.01	1.61	211.28	214.47	215.62	216.47	217.37	19426	1

Figure 25a shows trace plots for the parameters (indicating good mixing) and Figure 25b the corresponding pairs plot.

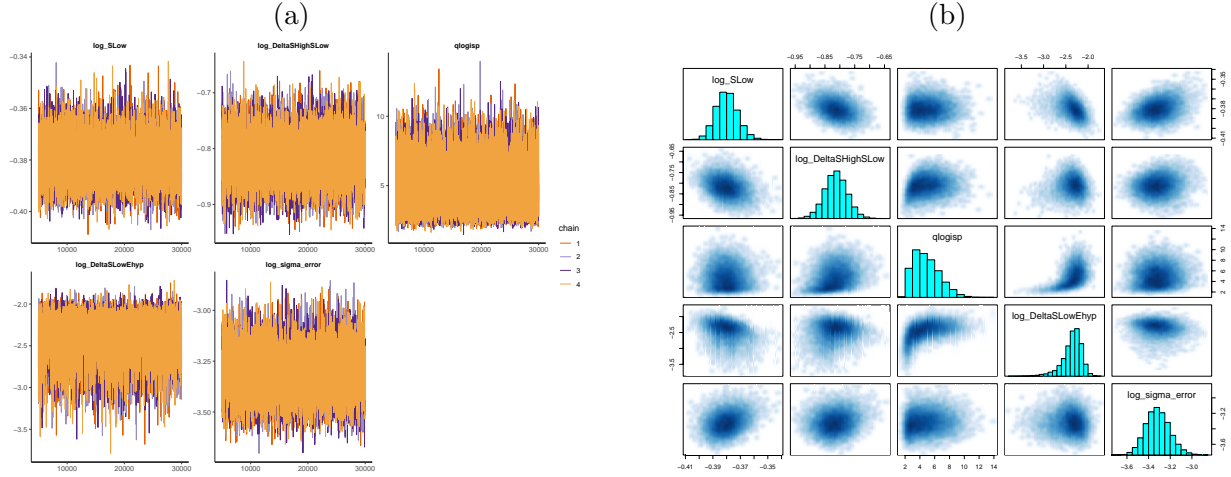


Figure 25: Trace plots (a) and a pairs plot (b) of the posterior draws for the Nishijima model fit to the Ti64 data.

The following table is a summary of the marginal posterior draws for the TPUSs, computed as described in [Liu and Meeker \(2024, Sections 4.4 and 4.5\)](#).

Ti64 350F R=-1 Lognormal distribution Nishijima model

Summary of the marginal posteriors for the

Traditional Parameters based on UnScaled data (TPUSs)

based on 20000 Stan draws

	2.5%	25%	50%	75%	97.5%
Ahyp	0.3200	1.0600	3.3800	13.4000	208.0000
Bhyp	5.1600	5.9700	8.2800	18.3000	215.0000
Chyp	0.1230	0.8030	3.1000	13.0000	211.0000
Ehyp	3.9800	4.0100	4.0200	4.0400	4.0700
sigma.X	0.0295	0.0337	0.0362	0.0391	0.0457

## H.2.4 Posterior draws and parameter estimates for the informative prior for qlogisp (rectangular hyperbola model)

The following table is a summary of the posterior draws for the USPs.

Inference for Stan model: Nishijima.

4 chains, each with iter=30000; warmup=5000; thin=5;

post-warmup draws per chain=5000, total post-warmup draws=20000.

	mean	se_mean	sd	2.5%	25%	50%	75%	97.5%	n_eff	Rhat
log_SLow	-0.38	0	0.01	-0.40	-0.39	-0.38	-0.37	-0.36	19994	1



log_DeltaSHighSlow	-0.80	0	0.04	-0.88	-0.83	-0.80	-0.78	-0.73	19513	1
qlogisp	10.50	0	0.19	10.12	10.37	10.50	10.63	10.89	19534	1
log_DeltaSlowEhyp	-2.24	0	0.13	-2.50	-2.32	-2.24	-2.15	-1.99	19599	1
log_sigma_error	-3.30	0	0.11	-3.51	-3.38	-3.31	-3.23	-3.08	19175	1

Figure 26a shows trace plots for the parameters (indicating good mixing) and Figure 26b the corresponding pairs plot. Note that the marginal posterior distribution of `qlogisp` matches the informative

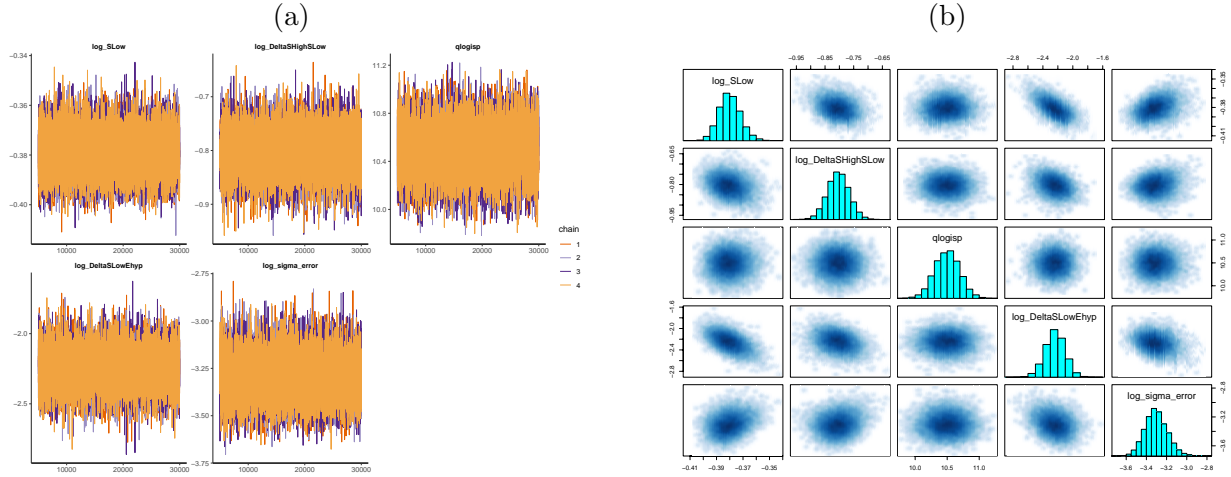


Figure 26: Trace plots (a) and a pairs plot (b) of the posterior draws for the Rectangular Hyperbola model fit to the Ti64 data.

prior described above. This is because the relative profile likelihood for `qlogisp` is flat over the range of the specified informative prior.

The following table is a summary of the marginal posterior draws for the TPUSs, computed as described in [Liu and Meeker \(2024, Sections 4.4 and 4.5\)](#).

Ti64 350F R=-1 Lognormal distribution Nishijima model

Summary of the marginal posteriors for the

Traditional Parameters based on UnScaled data (TPUSs)

based on 20000 Stan draws

	2.5%	25%	50%	75%	97.5%
Ahyp	781.0000	1.02e+03	1.18e+03	1.35e+03	1.75e+03
Bhyp	564.0000	9.91e+02	1.21e+03	1.44e+03	1.95e+03
Chyp	640.0000	9.43e+02	1.17e+03	1.42e+03	2.06e+03
Ehyp	3.9700	4.00e+00	4.01e+00	4.03e+00	4.05e+00
sigma.X	0.0299	3.41e-02	3.66e-02	3.95e-02	4.65e-02

## H.2.5 Additional residual analyses

Figure 27 shows plots of the standardized strength residuals based on the fit of the Nishijima model fit to the Ti64 data versus lifetime (a) and strength (b) fitted values. In the residuals versus lifetime fitted values plot, each column of residuals corresponds to one of the four stress levels that were used in the experiment. Taking into account the 28 out of 37 runouts at 60 ksi, there is no evidence of any departure from the assumed model.

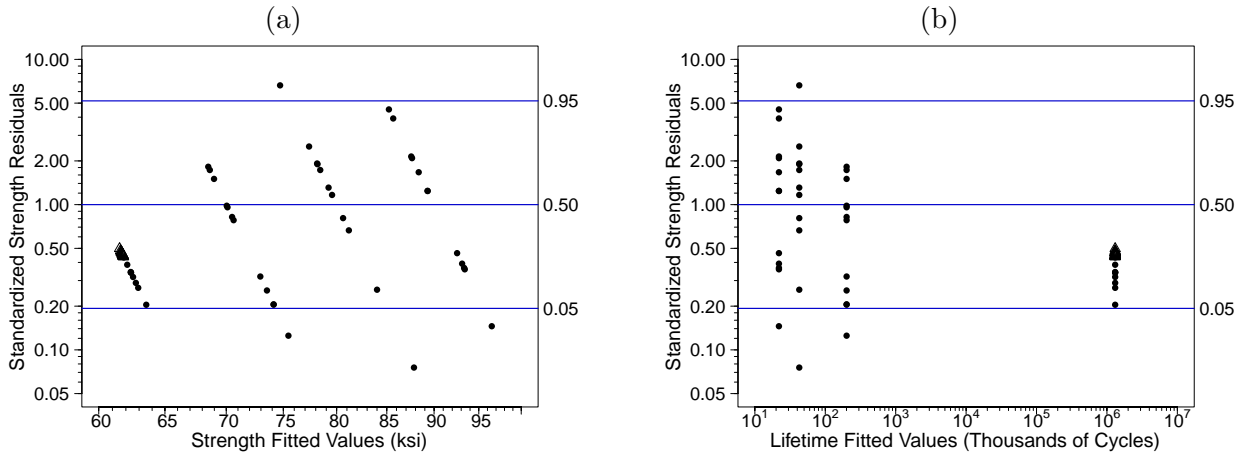


Figure 27: Residuals from the Nishijima model fit to the Ti64 data versus lifetime fitted values (a) and strength fitted values (b).

In the residuals versus strength fitted values plot, again, each group corresponds to a level of stress used in the experiment. The plot of residuals versus strength fitted values is, however, harder to interpret because the fitted values also depend on the number of cycles for each data point.

### H.3 More Details for the Coffin–Manson/Lognormal $S$ - $N$ Model Fit to the Superelastic Nitinol Data

#### H.3.1 Comparison of lognormal and Weibull distributions

Figure 28 uses lognormal and Weibull probability plots to compare the two distributions fit to the nitinol data. Both distributions fit well.

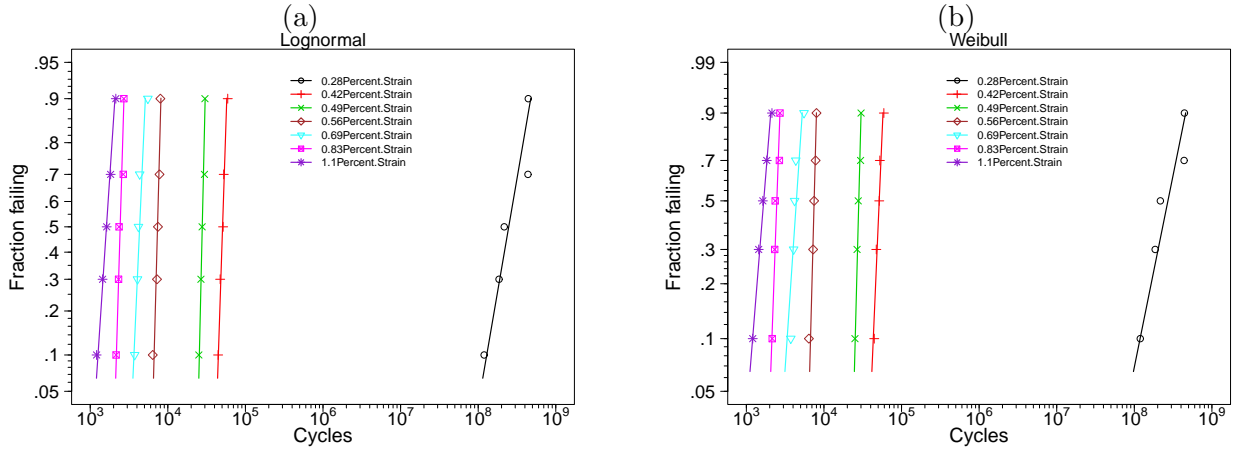


Figure 28: A comparison of lognormal (a) and Weibull (b) probability plots for the nitinol data with the bimodal data at 0.56% strain removed.

#### H.3.2 Model and prior distributions

Example 5.2 in the main paper gives a summary of the results of fitting the Coffin–Manson model to the superelastic nitinol  $S$ - $N$  data.

Note that in this example, the fatigue-strength model is specified and the fatigue-life model (providing the basis for the likelihood function) is induced. The lognormal distribution regression model for fatigue-strength  $X$  was

$$X = \log[h(N; \beta)] + \sigma_X \epsilon$$

where stress  $S$  and number of cycles  $N$  were scaled for numerical reasons (as described in [Liu and Meeker \(2024\)](#)), and  $\epsilon \sim \text{NORM}(0, 1)$ . Specifically,  $S/S_{\max}$  was substituted for  $S$  and  $N/N_{\max}$  was substituted for  $N$ . The Coffin–Manson  $S$ - $N$  relationship is

$$S = h(N; \beta) = A_{\text{el}}(2N)^b + A_{\text{pl}}(2N)^c,$$

The unknown parameters to be estimated from the data are  $A_{\text{el}} > 0$ ,  $A_{\text{pl}} \geq 0$ ,  $b \leq 0$ ,  $c < 0$ , with the constraint  $|c| > |b|$ .

As suggested in [Liu and Meeker \(2024, Section 4.2\)](#), the MCMC algorithm was run to generate posterior draws of the unrestricted stable parameters (USPs). First we define two points on the  $S$ - $N$  curve

$$\begin{aligned} S_{\text{Low}} &= A_{\text{el}}(2N_{\text{High}})^b + A_{\text{pl}}(2N_{\text{High}})^c \\ S_{\text{High}} &= A_{\text{el}}(2N_{\text{Low}})^b + A_{\text{pl}}(2N_{\text{Low}})^c, \end{aligned}$$

where  $N_{\text{Low}}$  is the smallest value of  $N$  in the data and  $N_{\text{High}}$  is the largest value of  $N$  in the data that is a failure. Then, following [Liu and Meeker \(2024\)](#), the USPs are defined as

$$\begin{aligned} \log S_{\text{Low}} &= \log(S_{\text{Low}}) \\ \log \Delta_{\text{SHighSLow}} &= \log[\log(S_{\text{High}}) - \log(S_{\text{Low}})] \\ \text{qlogisp} &= \text{qlogis}(b/\kappa) \\ \log \Delta_{\text{Slopes}} &= \log(\kappa - c), \text{ and} \\ \log \sigma_X &= \log(\sigma_X), \end{aligned}$$

where  $\text{qlogis} = \log[p/(1-p)]$  is the logit transformation and

$$\kappa = \frac{\log(S_{\text{Low}}) - \log(S_{\text{High}})}{\log(N_{\text{High}}) - \log(N_{\text{Low}})}.$$

The marginal prior distributions for the USPs  $\log S_{\text{Low}}$ ,  $\log \Delta_{\text{SHighSLow}}$ ,  $\text{qlogisp}$ ,  $\log \Delta_{\text{Slopes}}$ , and  $\log \sigma_X$ , were chosen to be flat. The resulting noninformative joint prior for the USPs results in Bayesian posterior estimates that are close to the ML estimates.

### H.3.3 Posterior draws and parameter estimates

The following table is a summary of the posterior draws for the USPs.

Inference for Stan model: CoffinManson.

4 chains, each with iter=30000; warmup=5000; thin=5;

post-warmup draws per chain=5000, total post-warmup draws=20000.

	mean	se_mean	sd	2.5%	25%	50%	75%	97.5%	n_eff	Rhat
log_SLow	-1.68	0	0.02	-1.73	-1.70	-1.68	-1.67	-1.63	19137	1
log_DeltaHighLow	0.61	0	0.03	0.56	0.59	0.61	0.63	0.66	17993	1
qlogisp	-1.67	0	0.25	-2.20	-1.82	-1.65	-1.50	-1.23	17819	1
log_DeltaSlopes	-0.27	0	0.08	-0.42	-0.33	-0.27	-0.22	-0.11	18460	1
log_sigma_error	-2.43	0	0.11	-2.64	-2.51	-2.43	-2.36	-2.20	19169	1

Figure 29a shows trace plots for the parameters (indicating good mixing) and Figure 29b the corresponding pairs plot.

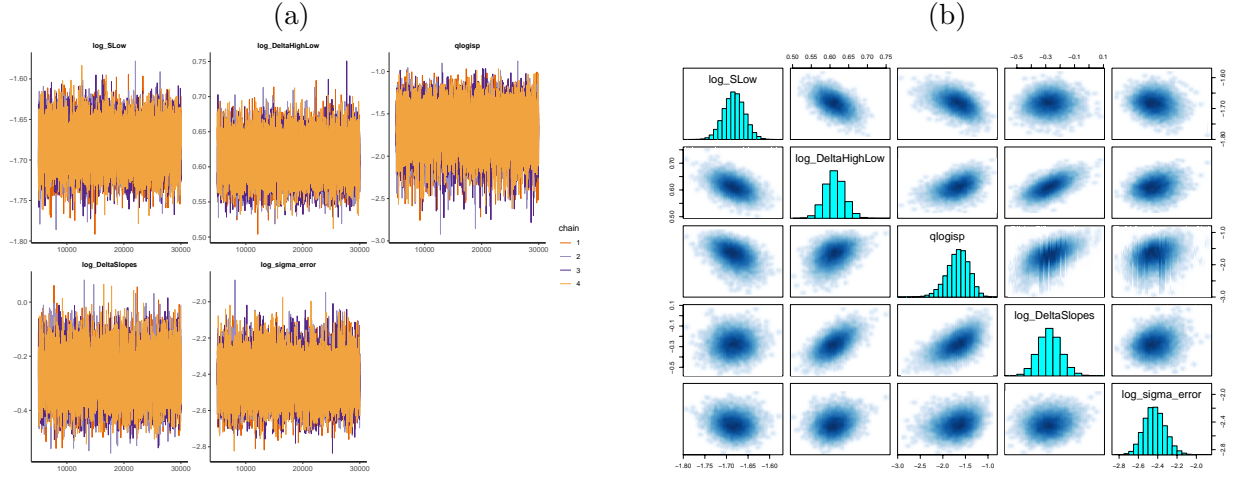


Figure 29: Trace plots (a) and a pairs plot (b) of the posterior draws for the Coffin–Manson model fit to the nitinol data.

The following table is a summary of the marginal posterior draws for the TPUSs, computed as described in [Liu and Meeker \(2024, Sections 4.4 and 4.5\)](#).

Nitinol e-N data from Falk (2019) Lognormal distribution CoffinManson model

Summary of the marginal posteriors for the

Traditional Parameters based on UnScaled data (TPUSs)

based on 20000 Stan draws

	2.5%	25%	50%	75%	97.5%
Ae1	0.6700	0.7500	0.7970	0.8500	0.962
Ap1	1130.0000	2020.0000	2850.0000	4060.0000	8750.000
be1	-0.0332	-0.0265	-0.0231	-0.0198	-0.014
cp1	-1.0400	-0.9480	-0.9050	-0.8640	-0.794
sigmaX	0.0718	0.0814	0.0877	0.0944	0.110

### H.3.4 Additional residual analyses

Figure 30 shows plots of the standardized strength residuals based on the fit of the Coffin Manson model to the nitinol data versus lifetime (a) and strength (b) fitted values.

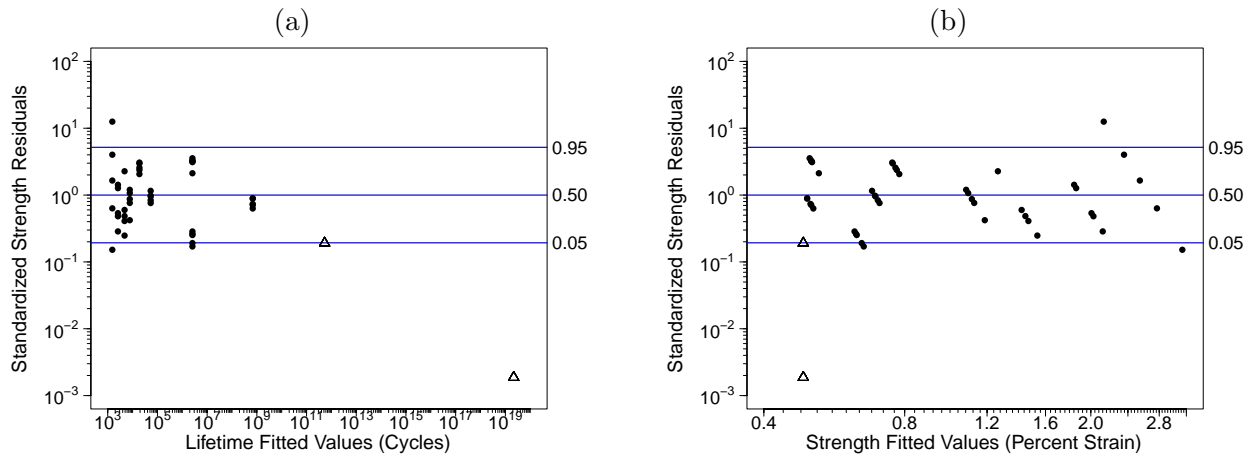


Figure 30: Residuals from the Coffin–Manson model fit to the nitinol data versus lifetime fitted values (a) and strength fitted values (b).

## References

- Armitage, P. H. (1961). Statistical aspects of fatigue. *Metallurgical Reviews* 6, 353–387. [56]
- ASTM (2015). *E739-10 Standard Practice for Statistical Analysis of Linear or Linearized Stress-Life (S-N) and Strain-Life ( $\epsilon$ -N) Fatigue Data*. ASTM International. [6]
- ASTM (2017). *F3211-17 Standard Guide for Fatigue-to-Fracture (FtF) Methodology for Cardiovascular Medical Devices*. ASTM International. [12]
- Awad, M., M. DeJack, and V. Krivtsov (2004). Evaluation of fatigue life regression models. Technical report, SAE Technical Paper 2004-01-0625. [22]
- Babuška, I., Z. Sawlan, M. Scavino, B. Szabó, and R. Tempone (2016). Bayesian inference and model comparison for metallic fatigue data. *Computer Methods in Applied Mechanics and Engineering* 304, 171–196. [13]
- Basquin, O. H. (1910). The exponential law of endurance tests. In *Proceedings of the American Society for Testing and Materials*, Volume 10, pp. 625–630. [15]
- Bastenaire, F., M. Bastien, and G. Pomey (1961). Statistical analysis of fatigue test results and its application to new series of data. *Acta Technica Academiae Scientiarum Hungaricae* 35–36, 7–26. [12, 13, 56]
- Bastenaire, F. A. (1972). New method for the statistical evaluation of constant stress amplitude fatigue-test results. In *Probabilistic Aspects of Fatigue*. American Society for Testing and Materials International. [22, 32]
- Bathias, C. (1999). There is no infinite fatigue life in metallic materials. *Fatigue & Fracture of Engineering Materials & Structures* 22, 559–565. [16]
- Birnbaum, Z. W. and S. C. Saunders (1969). Estimation for a family of life distributions with applications to fatigue. *Journal of Applied Probability* 6, 328–347. [60]

- Carroll, R. J. and D. Ruppert (1988). *Transformation and weighting in regression*. Chapman and Hall/CRC. [16]
- Castillo, E. and A. Fernández-Canteli (2009). *A Unified Statistical Methodology for Modeling Fatigue Damage*. Springer. [12, 20, 22, 37, 65]
- Castillo, E., A. Fernández-Canteli, V. Esslinger, and B. Thürlimann (1985). Statistical model for fatigue analysis of wires, strands and cables. In *IABSE Proceedings*, pp. 1–40. [37, 65]
- Castillo, E., A. Fernández-Canteli, A. Hadi, and M. López-Aenlle (2007). A fatigue model with local sensitivity analysis. *Fatigue & Fracture of Engineering Materials & Structures* 30, 149–168. [60]
- Castillo, E., A. Fernández-Canteli, H. Pinto, and M. López-Aenlle (2008). A general regression model for statistical analysis of strain–life fatigue data. *Materials Letters* 62, 3639–3642. [37]
- Castillo, E. and J. Galambos (1987). Lifetime regression models based on a functional equation of physical nature. *Journal of Applied Probability* 24, 160–169. [13, 37, 56, 60]
- Castillo, E. and A. S. Hadi (1995). Modeling lifetime data with application to fatigue models. *Journal of the American Statistical Association* 90, 1041–1054. [60]
- Castillo, E., M. Muniz-Calvente, A. Fernández-Canteli, and S. Blasón (2019). Fatigue assessment strategy using Bayesian techniques. *Materials* 12, 3239. [13, 37, 60]
- Crowder, M. J., A. C. Kimber, R. L. Smith, and T. J. Sweeting (1994). *Statistical Analysis of Reliability Data* (Paperback ed.). Chapman & Hall. [20]
- Dowling, N. (2013). *Mechanical Behavior of Materials: Engineering Methods for Deformation, Fracture, and Fatigue* (Fourth ed.). Pearson. [6, 34, 40]
- EASA (2018). AMC E 510 European Union Aviation Safety Agency Certification Specifications and Acceptable Means of Compliance for Engines CS-E. <https://www.easa.europa.eu/en/downloads/67945/en>. Accessed: 12 March 2024. [11]
- Efron, B. and R. J. Tibshirani (1993). *An Introduction to the Bootstrap*. Chapman & Hall. [27]
- FAA (2009a). U.S. Federal Aviation Administration Advisory Circular AC 33.70-1: Guidance Material for Aircraft Engine Life-Limited Parts Requirements. [https://www.faa.gov/documentLibrary/media/Advisory\\_Circular/AC\\_33\\_70-1\\_Chg\\_1.pdf](https://www.faa.gov/documentLibrary/media/Advisory_Circular/AC_33_70-1_Chg_1.pdf). Accessed: 12 March 2024. [11]
- FAA (2009b). U.S. Federal Aviation Administration Advisory Circular AC 33.70-2: Damage Tolerance of Hole Features in High-Energy Turbine Engine Rotors. [http://www.faa.gov/documentLibrary/media/Advisory\\_Circular/AC\\_33\\_70-2.pdf](http://www.faa.gov/documentLibrary/media/Advisory_Circular/AC_33_70-2.pdf). Accessed: 12 March 2024. [11]
- Falk, W. (2019). A statistically rigorous fatigue strength analysis approach applied to medical devices. In *Fourth Symposium on Fatigue and Fracture of Metallic Medical Materials and Devices*. ASTM International. [13, 23, 38]
- FDA (2010). U.S. Food and Drug Administration Non-clinical engineering tests and recommended labeling for intravascular stents and associated delivery systems.”. <https://www.fda.gov/media/71639/download>. Accessed: 12 March 2024. [11]

- Freudenthal, A. (1952). Planning and interpretation of fatigue tests. In *Symposium on Statistical Aspects of Fatigue*. ASTM International. [60]
- Freudenthal, A. M. and E. J. Gumbel (1953). On the statistical interpretation of fatigue tests. *Proceedings of the Royal Society of London. Series A. Mathematical and Physical Sciences* 216, 309–332. [12]
- Freudenthal, A. M. and E. J. Gumbel (1954). Minimum life in fatigue. *Journal of the American Statistical Association* 49, 575–597. [12]
- Freudenthal, A. M. and E. J. Gumbel (1956). Physical and statistical aspects of fatigue. *Advances in Applied Mechanics* 4, 117–158. [12, 13, 56]
- Gelman, A., D. Simpson, and M. Betancourt (2017). The prior can often only be understood in the context of the likelihood. *Entropy* 19, 555. [28]
- Gnedenko, B. V., Y. K. Belyayev, and A. D. Solov'yev (1969). *Mathematical Methods of Reliability Theory*. Academic Press. [20]
- Grove, D. and F. Campean (2008). A comparison of two methods of analysing staircase fatigue test data. *Quality and Reliability Engineering International* 24, 485–497. [18, 22]
- Haddad, T., A. Himes, and M. Campbell (2014). Fracture prediction of cardiac lead medical devices using bayesian networks. *Reliability engineering & system safety* 123, 145–157. [12]
- Hanaki, S., Y. Iwao, M. Yamashita, H. Uchida, M. Zako, and T. Kurashiki (2003). On a decision method of the S-N curve based on fatigue strength distribution (in Japanese). *Journal-Society of Materials Science Japan* 52, 23–27. [23]
- Hanaki, S., M. Yamashita, H. Uchida, and M. Zako (2010). On stochastic evaluation of S–N data based on fatigue strength distribution. *International Journal of Fatigue* 32, 605–609. [23]
- Hauteville, R., X. Hermite, and F. Lefebvre (2022). A new generic method to analyse fatigue results. *Procedia Structural Integrity* 38, 507–518. [32]
- Holmen, J. O. (1979). *Fatigue of concrete by constant and variable amplitude loading*. Ph. D. thesis, Norwegian Institute of Technology, University of Trondheim. [60]
- Holmen, J. O. (1982). Fatigue of concrete by constant and variable amplitude loading. In S. P. Shah (Ed.), *Fatigue of Concrete Structures*, Volume 75, pp. 71–110. American Concrete Institute. [60]
- Hong, Y., W. Q. Meeker, and L. A. Escobar (2008). The relationship between confidence intervals for failure probabilities and life time quantiles. *IEEE Transactions on Reliability* 57, 260–266. [28]
- ISO (2012). *ISO 12107: Metallic Materials-Fatigue Testing-Statistical Planning and Analysis of Data* (Second ed.). ISO. [6, 32]
- ISO (2017). *ISO 5840 Cardiovascular implants – Cardiac valve prostheses*. International Organization for Standardization. [11]



- Johnson, V. E., M. Fitzgerald, and H. F. Martz (1999). Estimating fatigue curves with the random fatigue-limit model: Discussion. *Technometrics* 41, 294–296. [28]
- King, C. B., Y. Hong, S. P. Dehart, P. A. Defeo, and R. Pan (2016). Planning fatigue tests for polymer composites. *Journal of Quality Technology* 48, 227–245. [40]
- Koenker, R. (2005). *Quantile Regression*, Volume 38. Cambridge university press. [40]
- Little, R. E. and E. H. Jebe (1975). *Statistical Design of Fatigue Experiments*. Halsted Press. [22]
- Liu, P., Y. Hong, L. A. Escobar, and W. Q. Meeker (2024). On equivalence of likelihood-based confidence bands for fatigue-life and fatigue-strength distributions. <https://arxiv.org/abs/2403.12757>. Accessed: 20 March 2024. [27, 28]
- Liu, P. and W. Q. Meeker (2024). Robust numerical methods for nonlinear regression. <https://arxiv.org/abs/2403.12759>. Accessed: 20 March 2024. [27, 28, 29, 34, 67, 68, 69, 70, 72, 73, 75, 76]
- Maennig, W. W. (1968). Calculation of the fatigue strength values of steel using an arctan transformation according to R. Müller. *Materials Testing* 10, 191–199. [60]
- Mann, N. R., R. E. Schafer, and N. D. Singpurwalla (1974). *Methods for Statistical Analysis of Reliability and Life Data*. Wiley. [20]
- Mattingly, J. D., W. H. Heiser, and D. T. Pratt (2002). *Aircraft Engine Design*. AIAA. [11]
- Meeker, W. Q. and L. A. Escobar (1995). Teaching about approximate confidence regions based on maximum likelihood estimation. *The American Statistician* 49, 48–53. [27]
- Meeker, W. Q., L. A. Escobar, and F. G. Pascual (2022). *Statistical Methods for Reliability Data* (Second ed.). Wiley. [7, 12, 15, 16, 20, 38, 40, 54]
- Meeker, W. Q., L. A. Escobar, and S. Zayac (2003). Use of sensitivity analysis to assess the effect of model uncertainty in analyzing accelerated life test data. In W. R. Blischke and D. N. P. Murthy (Eds.), *Case Studies in Reliability and Maintenance*, Chapter 12, pp. 269–292. Wiley. Accessed: 12 January 2024. [16]
- Meeker, W. Q., G. J. Hahn, and L. A. Escobar (2017). *Statistical Intervals: A Guide for Practitioners and Researchers*. Wiley. [31]
- MMPDS (2021). *Metallic Materials Properties Development and Standardization (MMPDS-16): Chapters 1-9*, Volume 2. Battelle Memorial Institute. [6, 40]
- Müller, C., M. Wächter, R. Masendorf, and A. Esderts (2017). Accuracy of fatigue limits estimated by the staircase method using different evaluation techniques. *International Journal of Fatigue* 100, 296–307. [23]
- Nelson, W. B. (1973). Analysis of residuals from censored data. *Technometrics* 15, 697–715. [29]
- Nelson, W. B. (1984). Fitting of fatigue curves with nonconstant standard deviation to data with runouts. *Journal of Testing and Evaluation* 12, 69–77. [12, 17, 22, 40]



- Nelson, W. B. (2004). *Accelerated Testing: Statistical Models, Test Plans, and Data Analyses* (Paperback ed.). Wiley. [12, 16, 22, 40]
- Nishijima, S. (1980). Statistical analysis of small sample fatigue data (in Japanese). *Transactions of Japanese Society Mechanical Engineering Series A* 46, 1303–1313. [32]
- Nishijima, S. (1985). Statistical analysis of small sample fatigue data. *Transactions of National Research Institute for Metals* 27, 234–245. [32]
- Pascual, F. G. (2003). The random fatigue-limit model in multi-factor experiments. *Journal of Statistical Computation and Simulation* 73, 733–752. [40]
- Pascual, F. G. and W. Q. Meeker (1997). Regression analysis of fatigue data with runouts based on a model with nonconstant standard deviation and a fatigue limit parameter. *Journal of Testing and Evaluation* 25, 292–301. [17]
- Pascual, F. G. and W. Q. Meeker (1999). Estimating fatigue curves with the random fatigue-limit model (with discussion). *Technometrics* 41, 277–302. [7, 27, 36, 60]
- Pawitan, Y. (2013). *In All Likelihood: Statistical Modelling and Inference Using Likelihood* (Paperback ed.). Oxford University Press. [27]
- Pollak, R., A. Palazotto, and T. Nicholas (2006). A simulation-based investigation of the staircase method for fatigue strength testing. *Mechanics of Materials* 38, 1170–1181. [23]
- R Core Team (2022). *R: A Language and Environment for Statistical Computing*. R Foundation for Statistical Computing. [28]
- Severini, T. A. (2000). *Likelihood Methods in Statistics*. Oxford University Press. [27]
- Shanmugam, V., T. Zhao, W. Krams, A. Joshi, H. Cao, and P. Schmidt (2019). Fatigue reliability analysis framework for medical devices based on a probabilistic finite element approach. In *Fourth Symposium on Fatigue and Fracture of Metallic Medical Materials and Devices*, pp. 132–147. ASTM International. [12]
- Shen, C.-L. (1994). *The Statistical Analysis of Fatigue Data*. Ph. D. thesis, The University of Arizona. [60]
- Shimokawa, T. and Y. Hamaguchi (1979). Relationship between fatigue life distributions and S-N curve of sharply notched specimens of 2024-T4 aluminum alloy. *Japan Society for Aeronautical and Space Sciences* 21, 225–237. [60]
- Shimokawa, T. and Y. Hamaguchi (1987). Statistical evaluation of fatigue life and fatigue strength in circular-hole notched specimens of a carbon eight-harness-satin/epoxy laminate. In T. Tanaka, S. Nishijima, and M. Ichikawa (Eds.), *Statistical Research on Fatigue and Fracture*, pp. 159–176. Elsevier Science. [7]
- Smith, R. L. (1985). Maximum likelihood estimation in a class of nonregular cases. *Biometrika* 72, 67–90. [19]

- Spindel, J. and E. Haibach (1979). The method of maximum likelihood applied to the statistical analysis of fatigue data. *International Journal of Fatigue* 1, 81–88. [12]
- Stan Development Team (2022a). *RStan: The R Interface to Stan*. R Package Version 2.30. [28]
- Stan Development Team (2022b). *Stan User’s Guide, Version 2.30*. [28]
- Stromeyer, C. (1914). The determination of fatigue limits under alternating stress conditions. *Proceedings of the Royal Society of London. Series A, Containing Papers of a Mathematical and Physical Character* 90, 411–425. [16]
- Tian, Q., C. Lewis-Beck, J. B. Niemi, and W. Q. Meeker (2024). Specifying prior distributions in reliability applications (with discussion). *Applied Stochastic Models in Business and Industry* 44, 5–62. [28]
- Toasa Caiza, P. D. and T. Ummenhofer (2018). A probabilistic Stüssi function for modelling the SN curves and its application on specimens made of steel S355J2+N. *International Journal of Fatigue* 117, 121–134. [39]
- Weaver, J., G. Sena, K. Aycock, A. Roiko, W. Falk, S. Sivan, and B. Berg (2023). Rotary bend fatigue of nitinol to one billion cycles. *Shape Memory and Superelasticity* 9, 50–73. [8, 35, 40, 59, 60]
- Weibull, W. (1956). Scatter of fatigue life and fatigue strength in aircraft structural materials and parts. In A. Freudenthal (Ed.), *Fatigue in Aircraft Structures*, pp. 126–145. Academic Press. [12, 13, 23, 56]
- Woo, S. (2020). *Reliability Design of Mechanical Systems* (Second ed.). Springer. [12]
- Wu, C. J. and Y. Tian (2014). Three-phase optimal design of sensitivity experiments. *Journal of Statistical Planning and Inference* 149, 1–15. [23]